

## University of Southampton Research Repository ePrints Soton

Copyright © and Moral Rights for this thesis are retained by the author and/or other copyright owners. A copy can be downloaded for personal non-commercial research or study, without prior permission or charge. This thesis cannot be reproduced or quoted extensively from without first obtaining permission in writing from the copyright holder/s. The content must not be changed in any way or sold commercially in any format or medium without the formal permission of the copyright holders.

When referring to this work, full bibliographic details including the author, title, awarding institution and date of the thesis must be given e.g.

AUTHOR (year of submission) "Full thesis title", University of Southampton, name of the University School or Department, PhD Thesis, pagination

**UNIVERSITY OF SOUTHAMPTON**

Faculty of Engineering, Science and Mathematics

School of Mathematics

**Superfluid Neutron Star Dynamics,  
Mutual Friction and Turbulence**

by

**Trevor Lloyd Sidery**

Submitted for the degree of Doctor of Philosophy

March 2008

UNIVERSITY OF SOUTHAMPTON  
Faculty of Engineering, Science and Mathematics  
School of Mathematics

Doctor of Philosophy

ABSTRACT

**Superfluid Neutron Star Dynamics,  
Mutual Friction and Turbulence**

by Trevor Lloyd Sidery

This thesis investigates the role of superfluidity in neutron stars and associated phenomena. We model the internal fluid of a neutron star as a two-component system: one of charged particles and one of superfluid neutrons. We derive a set of multi-constituent hydrodynamic equations that allows for a mutual friction between the constituents. We show that when a velocity difference exists between the two constituents the momentum of each constituent is modified by an entrainment parameter. Throughout all of this work we take direction from both theoretical and experimental work on superfluid Helium. This suggests that a force due to vortex lines in the superfluid acts between the two constituents. The hydrodynamic equations are on a scale at which the effect of vortices can be averaged over. The form of the mutual friction between the two constituents depends on the configuration of the vortices. Firstly, we concentrate on an array of vortices. The mutual friction is calculated both for a straight array, and then extended to a ‘moderately’ curved array. We also investigate a turbulent model for the superfluid neutrons in which the vortices are in a tangle. To include rotation in our model we use a phenomenological approach to construct the mutual friction for a polarised tangle. The hydrodynamic equations are used to investigate how entrainment and mutual friction affect plane waves. We show that there are conditions in which the waves are unstable and discuss how this may lead to turbulence. As a first step in considering the neutron star crust we consider how oscillations in the fluid are

dissipated on a boundary. As before, we concentrate on the effects of entrainment and mutual friction. Finally, we consider a simple global model of the glitch phenomenon seen in neutron stars in which the important process is a reconfiguration of the vortex array. We use this model to consider how the observational data may constrain parameters.

# Contents

List of Figures . . . . .	i
Declaration of Authorship . . . . .	v
Acknowledgements . . . . .	vii
<b>1 Introduction</b>	<b>1</b>
<b>2 Neutron Stars</b>	<b>4</b>
2.1 Birth of a Neutron Star . . . . .	4
2.2 Structure . . . . .	6
2.2.1 The Crust . . . . .	7
2.2.2 The Core . . . . .	8
2.2.3 The Star Exterior . . . . .	9
2.3 Observing Neutron Stars . . . . .	10
2.4 Phenomena . . . . .	11
2.4.1 Glitches . . . . .	11
2.4.2 Free precession . . . . .	13
2.4.3 Timing noise . . . . .	14
<b>3 Superfluids</b>	<b>15</b>
3.1 Helium ( $^4\text{He}$ ) . . . . .	15

3.2	The Two-fluid Model . . . . .	18
3.2.1	Irrotationality . . . . .	19
3.3	Hydrodynamic equations . . . . .	20
3.4	A few extra properties . . . . .	23
3.5	Neutron-Proton fluid . . . . .	24
<b>4</b>	<b>Formulation of multifluid hydrodynamic equations</b>	<b>26</b>
4.1	Methods of Modelling . . . . .	27
4.2	Lagrangian variation . . . . .	28
4.3	The Principle of least Action . . . . .	32
4.4	Equations of Motion . . . . .	35
4.5	The Hydrodynamic Lagrangian . . . . .	35
4.6	Rewriting the Hydrodynamic Force . . . . .	36
4.7	A Single fluid . . . . .	37
4.8	The two fluid equations . . . . .	38
<b>5</b>	<b>Mutual Friction</b>	<b>42</b>
5.1	Vortices and circulation . . . . .	42
5.2	The mutual friction in Neutron stars . . . . .	44
5.3	Magnus Force . . . . .	45
5.4	Mutual Friction . . . . .	50
5.5	Estimating the coefficients . . . . .	53
5.6	Curved Vortices . . . . .	55
5.6.1	Biot-Savart . . . . .	56
5.7	Induced Velocities . . . . .	59

5.8	Mutual Friction for Curved Vortices . . . . .	61
5.9	Conservation of vorticity . . . . .	63
5.10	Summary . . . . .	65
<b>6</b>	<b>Turbulence</b>	<b>67</b>
6.1	Conditions for turbulent flows . . . . .	67
6.2	Isotropic Turbulence . . . . .	69
6.2.1	Vinen . . . . .	69
6.2.2	Schwarz . . . . .	71
6.3	Digression . . . . .	73
6.4	Polarised Turbulence . . . . .	75
6.4.1	Applying this to Neutron Stars . . . . .	84
6.5	Summary . . . . .	85
<b>7</b>	<b>Plane Waves</b>	<b>87</b>
7.1	Time Derivative of a Vector . . . . .	88
7.2	Equations of Motion in a Slowly Rotating Frame . . . . .	90
7.3	Single Fluid . . . . .	91
7.3.1	Finding the frequencies . . . . .	92
7.4	Two Fluids . . . . .	94
7.5	Solutions . . . . .	101
7.5.1	No rotation, coupling, or friction . . . . .	102
7.5.2	Entrainment . . . . .	102
7.5.3	Chemical coupling . . . . .	103
7.5.4	Slow rotation . . . . .	104

7.5.5	Mutual friction with slow rotation . . . . .	105
7.5.6	A More Detailed Look at the Waves . . . . .	109
7.6	Hall modes . . . . .	111
7.7	The Donnelly-Glaberson Instability . . . . .	115
7.8	Turbulence . . . . .	119
7.9	Summary . . . . .	121
<b>8</b>	<b>Boundary Effects</b>	<b>122</b>
8.1	One Fluid . . . . .	123
8.2	Two Fluids . . . . .	127
8.2.1	No Mutual Friction . . . . .	127
8.2.2	Mutual Friction . . . . .	130
8.3	Dissipation . . . . .	133
8.3.1	Single Fluid . . . . .	133
8.3.2	Two Fluids . . . . .	135
8.4	Summary . . . . .	138
<b>9</b>	<b>Glitches</b>	<b>140</b>
9.1	Conservation of energy and angular momentum . . . . .	140
9.1.1	Single fluid . . . . .	141
9.1.2	Two constituents . . . . .	142
9.2	Simple spin down model . . . . .	144
9.3	Modelling a Glitch . . . . .	147
9.3.1	Pre-glitch . . . . .	148
9.3.2	The glitch . . . . .	149



9.3.3 Relaxation . . . . .	153
9.4 Matching Data . . . . .	155
9.5 Summary . . . . .	157
<b>10 Summary</b>	<b>158</b>

# List of Figures

2.1	A sketch of the structure of a neutron star. . . . .	7
2.2	An illustration of the pasta phases at the base of the crust. There is a transition from a lattice of nuclei to uniform matter. The dark areas signify the nuclei, while the lighter areas contain free nucleons. . . . .	8
2.3	A sketch of the dipole model of the external magnetic field field of a neutron star. Also shown is the radius from the star at which field lines would be traveling at the speed of light if they follow the rotation of the star. . . . .	9
2.4	A sketch of a typical glitch. The angular velocity $\Omega$ of the crust is plotted against time. The jump in rotation is of magnitude $\Delta\Omega$ . . . . .	12
3.1	An experiment to measure viscosity. The level of the fluid in the manometers shows the pressure of the fluid. The piston force fluid from the left container to the right through the thin connecting tube. The more viscous the fluid is, the greater force is need to push the fluid and hence there will be a pressure difference between the fluid in each container . . . . .	16
3.2	An experiment to measure angular momentum. A container full of rotating superfluid is tilted with respect to the axis of superfluid rotation. The rate of precession of the container shows the angular momentum of the superfluid. . . . .	17

3.3	A sketch of an array of superfluid vortices. The macroscopic rotation of the superfluid is due to averaging over the effect of the vortex array. . . . .	22
3.4	A sketch of a pair of vortices crossing (a) and reconnecting (b). The reconnection produces Kelvin waves along the vortex. . . . .	24
4.1	This diagram shows how we define the Lagrangian variation. To vary a quantity we displace the underlying flow lines $x_i(\mathbf{a}, t)$ by an active displacement $\xi_i(\mathbf{x}, t)$ . . . . .	28
5.1	To find the force acting on the vortex we integrate the change in momentum of the surrounding fluid over a volume that encloses the vortex line. For a straight vortex we choose a cylindrical volume with the vortex line at it's centre. $\delta V$ is a small segment of this volume, while $C$ is a closed line encircling the vortex line. $\hat{\kappa}$ is the direction of vortex circulation and $n_k$ is a unit vector that points out of the volume of integration. . . . .	47
5.2	The figure shows how we parametrise the vortex. We define $s$ as the position vector of the vortex with parameter $\xi$ that denotes distance along the vortex from an arbitrary, but fixed, point. The tangent vector $\mathbf{s}' = \frac{d\mathbf{s}}{d\xi}$ is also the direction of circulation of the vortex $\hat{\kappa}$ . The normal vector is defined by $\mathbf{s}'' = \frac{d^2\mathbf{s}}{d^2\xi}$ and the binormal by $\mathbf{s}' \times \mathbf{s}''$ . . . . .	57
6.1	The setup of the Swanson et. al. [75] rotating counterflow experiment. A square tube filled with superfluid $^4\text{He}$ is set into rotation with angular velocity $\Omega$ . A heat flux $\dot{Q}$ is applied from the heater below the tube. This induces a normal fluid flow $v_n$ and a superfluid counterflow $v_s$ . . . . .	76

6.2	Swanson et. al. [75] results. For various fixed slow rotation rates the relation between the vortex line density and the constituent velocity difference are plotted. . . . .	77
6.3	Swanson et. al. 1983 [75] results. For various fixed constituent velocity differences the relation between vortex line density and rotation is plotted. The vortex density shown is the measured density minus the expected vortex density of a turbulent flow for a particular velocity difference. The numbers to the right of the graph are $V_{ns}^2$ in $\text{cm}^2 \text{ s}^{-2}$ calculated from the heat flux. . . . .	78
6.4	The results from Swanson et. al. [75] used to plot $L/L_R$ vs $V_{ns}^2/\kappa\Omega$ . Also shown are the apparent critical points at which the behaviour of the fluid changes. . . . .	79
7.1	The vector $\mathbf{A}$ is being rotated by $\mathbf{\Omega}$ , this is shown at time $t$ and $t+\delta t$ . $\mathbf{A}$ is at an angle $\gamma$ to the axis of rotation. In time $\delta t$ the vector has rotated by angle $\delta\theta$ , which is a change of $\delta\mathbf{A}$ in the vector $\mathbf{A}$ . .	88
8.1	The velocity field of the rotating boundary problem at time $t = 0$ . The boundary is at $z = 0$ . We can see that the field is only significantly modified from the non-rotating case when the rotation is large. . . . .	125
8.2	The $x$ -direction velocity field of the two constituent rotating boundary problem at time $t = 0$ . The boundary is at $z = 0$ . . . . .	130
9.1	A typical glitch profile . . . . .	147
9.2	Simulated results for the pre-glitch and glitch regions using initial fluid rotations suggested by data from PSR B1737-30. The angular velocities of the two constituents in the first 50 seconds are not parallel but the effect of the magnetic spindown torque is smaller than the resolution of the graph. . . . .	153

- 9.3 The rate of change in angular velocity ( $d\Omega_p/dt$ ) is plotted with respect to time. Note that parameters that were used to plot this graph were not realistic, but chosen to emphasise the overall features.155

# Declaration of Authorship

I, Trevor Lloyd Sidery, declare that the thesis entitled “Superfluid Neutron Star Dynamics, Mutual friction and Turbulence” and the work presented in the thesis are both my own, and have been generated by me as the result of my own original research. I confirm that:

- this work was done wholly or mainly while in candidature for a degree at this university
- where any part of this thesis has previously been submitted for a degree or any other qualification at this university or any other institution, this has clearly been stated;
- where I have consulted the published work of others, this is always clearly stated;
- where I have quoted from the work of others, the source is always given. With exception of such quotations, the thesis is entirely my own work;
- I have acknowledged all main sources of help;
- where the thesis is based on work done by myself jointly with others I have made clear exactly what was done by others and what I have contributed myself;
- parts of this work have been published as:  
Andersson, N., Sidery, T., Comer, G.L., Mon.Not.Roy.Astron.Soc. **368** 162 (2006),

Andersson, N., Sidery, T., Comer, G.L., Mon.Not.Roy.Astron.Soc. **381** 747  
(2007)

and

Sidery, T., Andersson, N., Comer, G.L., arXiv0706.0672 (2007)

has been accepted for publication in MNRAS.

**Signed:**

**Date:**

# Acknowledgements

I am indebted to my supervisor Nils Andersson for his support and guidance throughout my PhD, in particular for his help and patience while I was writing up this thesis. I would also like to thank the rest of the Southampton relativity group for their willingness to help with my questions. I am grateful to Greg Comer for his collaborative input into this work. There have been many people that have kept me from going insane; for this I would like to thank, in no particular order, Brynmor Haskell, David Hilditch, Charlotte Hague and Michael Maynard-Smith. Also, Will and Judi Clark have made the period of writing up a great deal easier by providing a place to stay, cooked meals and friendship. Finally, I would like to thank my parents for their support and my brothers for being a constant source of competition.



# Chapter 1

## Introduction

The study of physics is a process of observing nature, creating hypotheses, and then testing the consequences of our theory by again observing nature. To rigorously test our hypotheses it is important to look at situations in which the physical parameters are extreme, for example at high and low temperatures or densities. There is, of course, a limit to how far we can push these conditions in a laboratory. To overcome this problem we may have to go back to observing nature directly.

Neutron stars provide an exciting test bed for extreme physics [33] [40]. They are hotter, denser and have stronger magnetic and gravitational fields than anything we can hope to create on earth. Any denser and a neutron star would collapse to a black hole in which the properties of the matter are hidden from us. Of course, unlike in the laboratory, neutron stars are not a controlled environment and so to test our hypotheses a large amount of modelling is required. Less important effects must often be neglected so that we can try and piece together what is happening in the star and check if this agrees with current theories.

Our current knowledge of neutron stars is derived from observation of their electromagnetic spectrum [54]. This has given information that, along with the currently accepted laws of physics, has helped create a model for the structure of the star. Still, there are observations that are as yet not explained. It is the responsibility of theorists to try provide useful models that can be tested against the available

---

data. An important area of research is the study of the internal fluid dynamics of the star. The properties of the fluid will affect the way a star oscillates and the various timescales involved.

By looking at the electromagnetic spectrum we can only ever gain information on how the internal structure affects the surface of the star rather than observing the fluid directly. However, at some point in the future we should be able to detect gravitational radiation from neutron stars. A gravitational wave is generated when a body is accelerated. This includes non-uniform rotation and internal density changes. Because of this, gravitational waves carry information about the mass as a whole rather than just the surface. They also are not affected much by passing through matter and so give a less distorted signal than electromagnetic radiation which is strongly affected by intergalactic dust. The downside is that they are difficult to detect as the gravitational perturbation is small. A typical wave from a nearby binary star system will displace two particles 1 meter apart by  $10^{-21}$  meters.

It is important for theorists to model the expected signature of the gravitational radiation emitted from neutron stars for a few reasons. Experimenters building the detectors need to know if there are any particular frequencies at which it is worth making sure that one has a good sensitivity. Also when gravitational waves are detected template waveforms will be needed to help pick out the separate sources. If there is to be any hope that these templates are helpful then good models are needed. One important part of this will be modelling the fluid in the star.

This thesis starts with a brief introduction to the structure of neutron stars and the superfluid nature of the internal neutron fluid. We then introduce some of the properties of laboratory superfluids so that we have a grasp of some necessary concepts. The equations of motion for a multi-constituent fluid, as suggested by Prix [62], will be derived and extended by comparing with results found for superfluid helium. Next we concentrate on the mutual friction between the superfluid neutrons and other fluid constituents via vortex lines. Chapter 5 provides a detailed derivation of mutual friction for an array of straight vortices, and has

---

already been published in MNRAS [10]. We then extend this analysis to a curved array of vortices (work that has appeared in MNRAS as the appendix of [11]). Chapter 6 provides a discussion of the mutual friction that should be considered when the neutron fluid is turbulent. Most of the results can also be found in [11]. Chapter 7 (also published in MNRAS [74]) considers plane-wave propagation and various dispersion relations. The aim is to understand how the properties of our multi-constituent fluid affect oscillations. We also investigate instabilities in the fluid that could lead to turbulent flow. Chapter 8 investigates the role of mutual friction in two-constituent oscillations at a boundary. This is a first step in calculating the energy dissipated at the core-crust interface in a neutron star. Finally, in Chapter 9 we apply the two-constituent model to the glitch phenomenon that is seen in neutron star observations.

## Chapter 2

# Neutron Stars

To fully understand the processes in neutron stars many areas of physics are important. More than this, the conditions inside and around a neutron star are unlike anything that can be measured directly in a laboratory. This complexity is the reason that these objects are so interesting to investigate. It is also the reason that extracting physics from any data gathered is so difficult. Any model that is used to compare with observations must be highly complex and still may not account for all the processes involved. It is important to start from a simpler model and compare with data that might involve fewer of the stars processes. To do this we need to understand what is expected from currently known physics and previous observations.

### 2.1 Birth of a Neutron Star

For billions of years stars like our sun are in a state of equilibrium. In their cores atoms collide and create heavier atoms. This process, known as fusion, releases large amounts of thermal energy which stabilises the star from collapsing under the force of its own gravity. For most of a star's life hydrogen is the fuel and helium is created. When the core of the star has used up a certain amount of hydrogen, the star begins to collapse. This increases the temperature to the point at which helium can undergo fusion. With a new source of fuel the energy created increases

the thermal pressure and once again stabilises the star. Finally there comes a point at which this process is no longer sufficient to balance gravity. The way in which this happens depends upon the size of the star. For a larger star the atoms combine until they are producing iron. This is the largest atom for which fusion produces energy. This means that there are fewer atoms involved in useful collisions. For smaller stars the temperature never increases enough to start fusion processes with the larger atoms. In both cases the star collapses. For the larger stars this results in a supernova. The core of the star collapses to what is known as the remnant. The rest of the star also collapses, but there are extra processes occurring which release a large amount of energy in the form of neutrinos. Neutrinos have a very weak interaction with normal matter and so escape the star. With all this energy being released the collapse happens even faster. The core reaches a critical density at which point in-falling material crashes into the core, creating an outgoing shock wave. This is known as core bounce. After only 200 km the shock wave stalls. There will then be some process which continues to eject the matter, but the details of this are not yet known. One suggestion is that the denser matter will become opaque to the neutrinos. The matter is then blown out by the energy contained in large amounts of neutrinos. This process of mass ejection is the supernova.

After this catastrophic event, the remnant is left with a halo of gas. The mass of the remnant depends on the mass of the original star. This in turn dictates the nature of the remnant. For larger remnants a black hole will be formed in which gravity has overcome all other forces. If the remnant has a mass of approximately 1.4 solar masses then a neutron star will be formed. For this type of nova it is unlikely that any other types of objects will be formed. Various theoretical models have given the possible range of neutron star masses between 0.2 and 2 solar masses [54]. A lower bound of 1 solar mass is more likely from the nature of the processes involved in producing the star. For a 1.4 solar mass star the possible range of diameter is between 20 and 30 km [54]. In a neutron star the force of gravity is balanced by neutron degeneracy pressure.

There is also thought to be a second way in which neutron stars may be formed. A large proportion (40 %) of stars are in binary systems. That is, systems in which

two stars orbit each other. One of the stars may at some point go nova and form a white dwarf. As long as this event does not eject the star from the orbit it will start accreting matter from its companion. This means that the material in the atmosphere of the normal star will spiral into the white dwarf. If the white dwarf accretes enough matter it may push the mass of the star to the point at which the force of gravity exceeds electron degeneracy pressure. The star will then collapse to a neutron star [42].

Between going supernova and becoming a stable neutron star there is an intermediary stage where the star is known as a proto-neutron star. This is a very short stage in which more neutrinos escape, which both contracts and cools the star. It is only about 50 seconds after the supernova before the mean free path of the neutrinos becomes larger than the radius of the star [17]. It also becomes energetically favourable for the protons and electrons to combine and form neutrons, releasing more neutrinos. The final star is now very dense, cooling quickly and may have a significant rotation and very large magnetic field. These last two properties are the result of conservation of angular momentum and magnetic flux. As the star collapses it is easy to see that a relatively small initial spin will translate into a large rotation for the final small object. The period of rotation is thought to be between 1s and 1ms. We can also see that as the star collapses the density of magnetic flux lines will greatly increase. The field is thought to get larger than  $10^{13}$  Gauss in some cases.

## 2.2 Structure

The structure of a neutron star is something which we have only limited information about. From observations of the stars exterior some progress has been made in probing the interior of the star. From figure 2.1 we can see the regions that we tend to split the star into. The outer kilometer of the star is the crustal region. We also have the inner core and the outer core, though the designation of their interface is less clear.

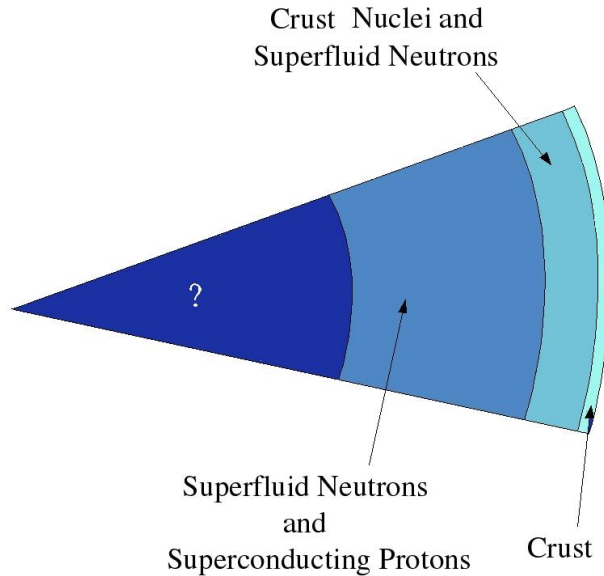


Figure 2.1: A sketch of the structure of a neutron star.

### 2.2.1 The Crust

The density of the crust ranges from  $10^6 \text{ g cm}^{-3}$  at the surface to near nucleonic densities at the crust-core boundary. At the very surface we would expect the crust to be comprised of a lattice of iron nuclei. As the density increases the nuclei become more rich with neutrons such that near the inner boundary of the crust the number of nucleons in a nucleus is about 200 but with a proton fraction of about 0.1. These nuclei have never been seen in a laboratory, so even at these relatively low densities the nature of the matter has had to be extrapolated from current physical models. At a density of  $4 \times 10^{11} \text{ g cm}^{-3}$  it becomes energetically favourable for the neutrons in the nuclei to become free flowing. This is known as neutron drip. We now have a flow of free neutrons in a lattice of nuclei. There is a transition from this lattice to homogeneous matter as the nuclei become closer together at increasing density (fig. 2.2). Moving from the less dense region towards the crust-core boundary there are several stages to this transition (known as the pasta phases) [40]. At first there is the array of nuclei in a sea of neutrons. As the density increases, the form of these nuclei becomes distorted and closer together until they become cylindrical tubes of nucleonic matter (spaghetti). These then

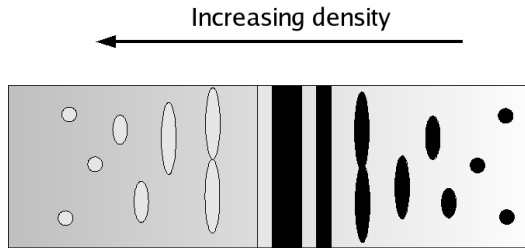


Figure 2.2: An illustration of the pasta phases at the base of the crust. There is a transition from a lattice of nuclei to uniform matter. The dark areas signify the nuclei, while the lighter areas contain free nucleons.

join to become sheets of matter between which is a flow of neutrons (lasagna). As these sheets become thicker towards the boundary it makes less sense to think of them as nuclei as there is no longer a confinement of nucleons. There are just alternating layers of both protons and neutrons and layers of just neutrons. Finally there are pockets of neutrons (Swiss cheese) before there is a sea of nucleonic matter and the crust has become core material (sauce). The free neutrons in the crust will be in a superfluid phase if the temperature is less than about  $10^9$  K. The next chapter will discuss the properties of superfluids. When thinking about how the crust interacts with the core we can see that there is no sharp transition but the boundary between the two regions is blurred.

### 2.2.2 The Core

At the temperatures and densities involved in the core we start to lose our intuition about the nature of the matter. In the outer core we expect that the neutron will be in a superfluid state, while the protons will be in a superconducting state. There will also be electrons in the mix. We expect that the ratio of protons to electrons to neutrons will be roughly 1:1:20. As we cannot see the inside of the star or recreate the environment in a laboratory the process of modelling the dynamics of the core fluid and investigating how this might interact with the exterior of the star is necessary in furthering our understanding. By the time we reach the center of the star we would expect densities of  $10^{15} \text{g cm}^{-3}$ . At this point, various



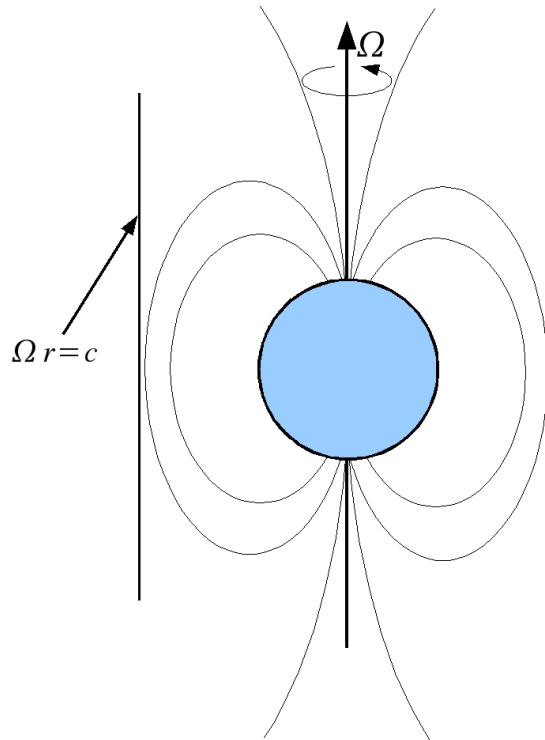


Figure 2.3: A sketch of the dipole model of the external magnetic field of a neutron star. Also shown is the radius from the star at which field lines would be traveling at the speed of light if they follow the rotation of the star.

reasonable theoretical models give very different predictions. We may expect to find more exotic matter, for example hyperons or a quark soup, which may also have superfluid properties.

### 2.2.3 The Star Exterior

There are many situations in which the exterior of the star can look different [54]. For stars in binary systems matter can be accreted on to the surface. There are various phenomena and oscillations associated with this. When studying the interior of the star we must look for clues on the surface. For this reason we will concentrate on a particular class of neutron star called a pulsar. A pulsar is seen as a pulsating beacon of radiation, like a lighthouse. The beam is due to the stars enormous magnetic field. As seen in figure 2.3 we would expect a dipolar field. In

reality we do not expect the magnetic poles of the star to coincide with the axis of rotation though they will be attached to the crust. There will be some distance from the star at which the magnetic field lines that are dragged around with the crust would be travelling at the speed of light. Any field lines that are outside this radius become open field lines. It is these open field lines which contribute to producing the beacon of radiation. The exact mechanism that produces the radiation is a current area of research, but it is thought that these open field lines are a vital part. As the star is rotating the magnetic pole will move around with the same period as the star. For an observer these will lead to pulses like a lighthouse. These pulses therefore give us a direct measure of the period of rotation of the magnetic field, and hence the rotation of the crust.

## 2.3 Observing Neutron Stars

Currently all observations are made by detecting electromagnetic radiation. This gives us a great deal of information about the surface of the star, but none directly about the core. Observations of a neutron stars spectrum give clues as to the temperature of the star. If the neutron star is in a binary system then we gain information about its mass. It is through properties like these that we can apply our models to try to infer the stars structure. Observations of an accreting star may give insight into it's surface properties, in particular it's magnetic structure. Pulsars are a very useful source as we can gain a lot of information from the lighthouse like pulses of radiation. Apart from information about the radiating magnetic poles themselves this effect can give a clue to the internal structure of the star. As we would expect the magnetic field to be bound to the crust of the star, the frequency of the pulses should coincide with the period of rotation. There are observed phenomena in which the pulses are not as regular as would be expected from a stably rotating object. If we stick with the assumption that the pulses give us the angular velocity of the surface then these phenomena could be due to internal physics. It is in this indirect way that we can gain clues about the structure of the star. Due to the nature of electromagnetism, currently, it is only

through this seismological approach that we can gather data about the core of neutron stars. As mentioned in the introduction, detection of gravitational waves would be a way of observing the star as a whole. As the core of the star contains the majority of the mass we would hope that there are internal processes that would be observable.

## 2.4 Phenomena

When modelling the structure of a neutron star it is necessary to have the observed phenomenon in the back of your mind. We concentrate on those phenomena that are thought to be due to the internal structure of the star.

### 2.4.1 Glitches

The frequency of pulses from a neutron star is thought to give us the rotational period of the neutron star. We would expect that, in the absence of a companion star, the stars period will increase slowly over time. The increase in period will be due to magnetic torque and possibly gravitational radiation. Observations show that occasionally the period of a neutron star suddenly decreases [55] [49]. After this so called 'glitch', there are several time scales over which the star relaxes back to towards its original behaviour. The final period and rate of decrease in period may not exactly match those expected if the glitch had not occurred. There are a two main categories that glitch observations can be divided into. The most common has a sharp rise in frequency and then a longer relaxation (see fig 2.4). These are often split into another two categories. We call the size of the glitch the ratio of the change in angular velocity of the glitch  $\Delta\Omega$  against the initial frequency  $\Omega_0$ . For neutron stars that glitch there often seems to be two separate amplitudes of glitch. Large glitches have a 'size'  $(\Delta\Omega/\Omega_0) \approx 10^{-6}$  while smaller glitches have a relative change in frequency of  $\approx 10^{-9}$ . The size of detected glitches covers the range  $10^{-9} - 10^{-6}$  but seems to show more prevalence for the extremes. A second class of glitch has only been observed in one pulsar [71] [72]. In this type of glitch

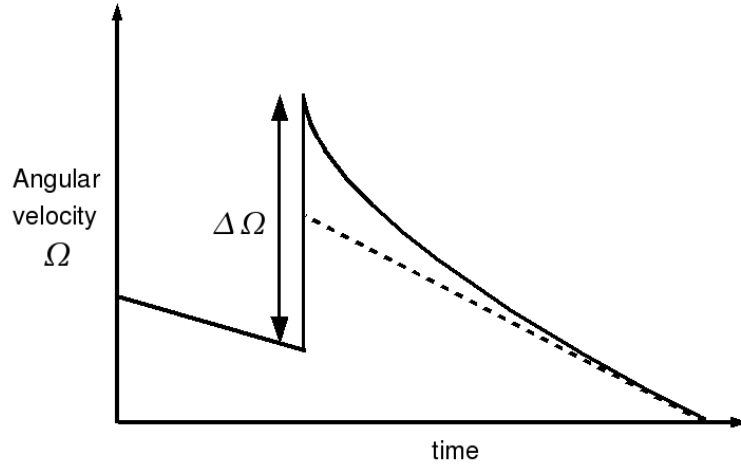


Figure 2.4: A sketch of a typical glitch. The angular velocity  $\Omega$  of the crust is plotted against time. The jump in rotation is of magnitude  $\Delta\Omega$ .

the rise in frequency occurs on a time scale of 100's of days. For the more common glitch this rise is less than 40 seconds and cannot currently be resolved. From this point on we concentrate on the fast glitches, of which there are a larger number of observations. There have been several models as to the processes that cause these glitches. Two popular proposals for the process that causes this phenomenon are the crust cracking and superfluid vortex unpinning models.

### Crust cracking

When a neutron star first forms it may be rapidly spinning. The crust that forms will be slightly elliptical due to the centrifugal force. Over time the stars angular velocity will decay. The natural shape of the internal fluid of the star will become more spherical. This causes stresses in the crust which is still elliptical [15]. At some point the crust will crack and become more spherical. This shifts the distribution of matter and so to conserve angular momentum the star spins up. The relaxation would be the time that it takes for the star to stabilise after the crust cracking. It has been found that this model as it stands cannot account for the rate at which larger glitches occur in some pulsars [2].

### Superfluid vortex unpinning

In the core of the star we expect to find superconducting protons, superfluid neutrons and electrons. If all the charged components of the star are coupled then the crust will be locked to the protons and electrons. The crusts angular velocity will be linked to the angular velocity of the internal fluid. There will be a magnetic torque acting on the charged components that causes their angular velocities to decay. On the other hand the superfluid neutrons angular momentum is determined by the configuration of superfluid vortices. If the vortices are pinned to the crust the angular momentum of the neutron fluid will be fixed. There will be a growing velocity difference between the neutrons and the protons. If, at some point, there is a way to unpin the vortices then there can be an exchange of angular momentum [6]. This will increase the angular velocity of the protons which we would see as the glitch. We will discuss a mechanism that may cause glitches in more detail in chapter 9 after we have looked at the properties of superfluids more thoroughly in chapter 3. The neutron fluid moment of inertia could be up to an order of magnitude larger than that of the proton fluid and so a small decrease in the neutron fluid velocity will mean a larger increase in the crust. If glitches are a result of internal dynamics then we have a way to probe the internal structure of a neutron star [53].

#### 2.4.2 Free precession

The precession of a star occurs when the principal axis of inertia is not aligned with the rotation axis. In this situation the axis of rotation rotates around a second axis. As the rate of precession depends on the distribution of the inertia this phenomenon is a good probe of the neutron star core as the core contains most of the matter in the star [43]. We will not discuss free precession in detail here, but work done in this thesis will be relevant for it [32].

### 2.4.3 Timing noise

Timing noise is a variation in the pulse data to which no phenomenon has been assigned. It is not, as the name suggests, always a seemingly random signal. The signal can be quite coherent but with no obvious label to attach to it, or not quite clear enough to say with the necessary confidence that a known phenomenon like free precession is occurring.

## Chapter 3

# Superfluids

As described in the previous chapter, the fluid in neutron star outer cores is a mixture of superfluid neutrons, superconducting protons, and free electrons. As we can't test properties of this fluid in a laboratory it is useful to look at fluids which are expected to have similar behaviour. We can hope to gather data and expertise from those who have studied such systems. Such a fluid with a superfluid phase is helium ( $^4\text{He}$ ). The superfluid phase of  $^4\text{He}$  is known as He II.  $^3\text{He}$  also has a superfluid phase, but only at millikelvin temperatures and so there have been less experiments done with this fluid than with  $^4\text{He}$ . We therefore concentrate on He II.

### 3.1 Helium ( $^4\text{He}$ )

Before describing the model for liquid helium we will look at some of its observed properties. As a liquid is cooled down it is usually expected that at some point the molecules in the fluid will form a solid as the entropy goes towards zero. Rather than solidifying, helium goes into a superfluid state at approximately 2.17K and stays in this state down to 0K. The fact that it is still fluid with no entropy shows that something different to a conventional liquid must be happening. To cool helium down to these temperatures the vapour is pumped away from the vigorously boiling liquid surface. At the phase transition temperature (known as

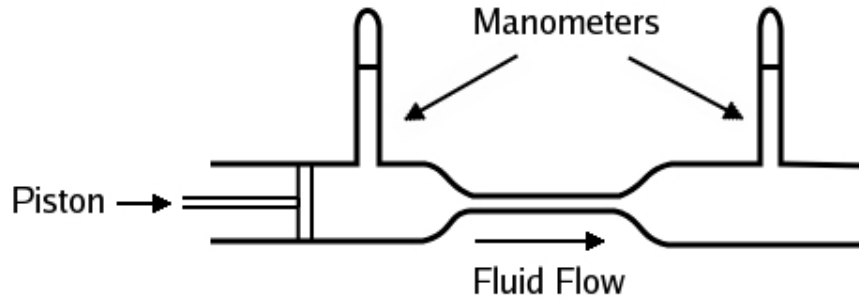


Figure 3.1: An experiment to measure viscosity. The level of the fluid in the manometers shows the pressure of the fluid. The piston forces fluid from the left container to the right through the thin connecting tube. The more viscous the fluid is, the greater force is needed to push the fluid and hence there will be a pressure difference between the fluid in each container.

the 'lambda point') the surface suddenly becomes completely calm. This is a result of super heat conductivity. The superfluid is such a good conductor of heat that hot spots cannot form and rise to the surface. It is not true to say that helium is never solid, but the fluid needs to be under pressure. Experimenters even have evidence of a supersolid state in helium [47].

The property of superfluidity that gives its name is that it can appear to have zero viscosity. One can measure a fluid's viscosity experimentally by forcing it through a small tube as in figure 3.1 [34]. The fluid is pushed from one container into the other by using a piston. For a normal fluid the friction between the tube and the fluid will cause an increase in pressure in the first container. This will be measured as a rise in the level on the manometer. When this is done with a superfluid, such that the velocity of the fluid going through the tube is less than some critical value, no pressure difference is measured. This would suggest that the fluid is inviscid.

Another way of measuring viscosity is to vibrate a musical string inside the fluid [34]. By comparing the damping time with that of the string in a vacuum the viscosity can be found. It would seem that these two experiments should give the same result as they are measuring the same quantity. In the first case the



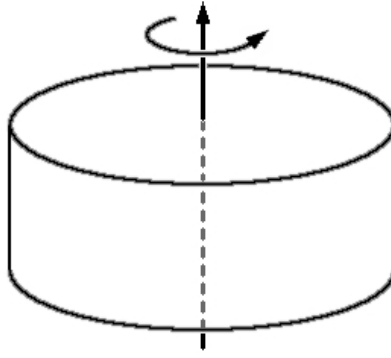


Figure 3.2: An experiment to measure angular momentum. A container full of rotating superfluid is tilted with respect to the axis of superfluid rotation. The rate of precession of the container shows the angular momentum of the superfluid.

fluid is being pushed past an object, whereas the second experiment is pushing an object through the liquid. However, the string in the superfluid helium has a faster damping time than in vacuum. Contrary to the previous experiment, this would suggest that the fluid is viscous.

We now consider some rotational properties of superfluids. Taking a cylindrical container filled with helium with a temperature above the lambda point, we rotate the cylinder (fig. 3.2) [34]. This will spin up the fluid by viscous effects. Now we lower the temperature below the lambda point and then stop the spin of the container. If the superfluid stores angular momentum then it will act as a gyroscope and tilting the container will cause it to precess around its original orientation. We find that the rate of precession is proportional to the angular momentum stored, which in turn can be found to have a relation to the temperature. This may not seem surprising at first sight. We have seen situations in which there appears to be no viscous effects in the fluid. No energy will be taken out of the superfluid and so we expect the angular momentum to be conserved in the fluid. What is unusual is that once the experiment is set up the rate of precession is still related to the temperature. As the temperature is lowered the rate of precession increases.

## 3.2 The Two-fluid Model

To describe these phenomena we must look more closely at the nature of helium itself. Most molecules have a sufficient attraction to each other that they form crystalline structures as they cool down. This is because the attractive forces between the molecules are no longer overcome by energetic movement. The fluid as a whole can have a range of temperatures but the separate molecules have a minimum amount of allowable energy. If a fluid is cooled then there will be some point at which some of the molecules will be in their ground (lowest energy) state. By the time this occurs most fluids will already have frozen into a solid state. This is not true of helium as interactions between the atoms are extremely weak. The point at which some of the helium atoms go into their ground state is the lambda point. As the temperature is still non-zero we will have a fluid in which some particles are in the ground state and some in excited states.

To understand why He II might have unusual properties we need to look at the consequences of an atom being in its ground state. If an atom has the minimum energy it is impossible for it to lose any energy to its environment. The amount of energy that the atom can store is not a continuous spectrum. There are discrete amounts of energy that the atom can have. This means that a atom will only receive energy from its environment if the amount of energy exchanged is above a threshold. For a slow moving cool system there will be few interactions between the fluid and its surroundings. This is how the fluid can seem inviscid as no energy exchange means no viscous effects. It is often taken that the energetic atoms form the 'normal' component, while the atoms in their ground state are the 'superfluid' component. There will always be a normal component until the temperature reaches zero as for the fluid to have a positive temperature some of the molecules must be in excited states. It is, however, a little misleading to say that there are two separate fluid components as any excited atom may have enough energy to excite an atom in the superfluid component. This may in turn lower the energetic atom to its ground state. On the other hand we could describe the second fluid component as the flow of energy (or entropy). When it comes to

modeling the dynamics of the superfluid helium, the usual approach is to describe the two components separately with some coupling.

We are now in a position to explain the results of the viscosity experiments. In the second experiment, in which a string was oscillating in the fluid, the superfluid was shown to have a non-zero viscosity. It can now be seen that this will come from the normal component as the temperature will be above absolute zero. Why then did the first experiment show zero viscosity? In this experiment the fluid was forced through a small tube. The normal component may not be able to get through due to its viscosity, but the superfluid component can still flow freely. Hence it is only the viscosity of the superfluid component that is measured. It should be noted that a non-zero viscosity is measured once the velocity of the fluid traveling through the tube exceeds some critical value. At this point the walls of the tube can excite some of the helium molecules out of their ground state.

### 3.2.1 Irrotationality

When all the particles are in the same quantum state we can describe the whole fluid with a single wave function [5]. This is true for a superfluid in which all the particles are in their ground state. Denoting  $\Psi$  as the wave function of all the superfluid particles in the system we have

$$\Psi_0(r) = \sqrt{n_0(r)} e^{i\phi(r)} \quad (3.2.1)$$

What is the definition of  $n_0$ ? The wave function of a single particle describes the probability of finding the particle within a region. There is no way of distinguishing between the particles in a superfluid in which all the atoms are in a single quantum state. The wave function  $\Psi$  is the sum of all the identical wave functions and therefore describes the expected number density of particles. This gives that for a system with  $N_0$  particles in a volume  $V$

$$N_0 = V n_0 = \int_V |\Psi_0|^2 dr^3 \quad (3.2.2)$$

This gives us that  $n_0$  is the particle number density. The mass current ( $j_i$ ) is given by

$$\begin{aligned}
 j_i &= \frac{\hbar}{2i} [\Psi_0^* \nabla_i \Psi_0 - \Psi_0 \nabla_i \Psi_0^*] \\
 &= \frac{\hbar}{2i} \left[ \Psi_0^* \left( e^{i\phi} \nabla_i \sqrt{n_0} + i e^{i\phi} \sqrt{n_0} \nabla_i \phi \right) - \Psi_0 \left( e^{-i\phi} \nabla_i \sqrt{n_0} - i e^{-i\phi} \sqrt{n_0} \nabla_i \phi \right) \right] \\
 &= \frac{\hbar}{2i} [\sqrt{n_0} \nabla_i \sqrt{n_0} + i n_0 \nabla_i \phi - \sqrt{n_0} \nabla_i \sqrt{n_0} + i n_0 \nabla_i \phi] \\
 &= \hbar [n_0 \nabla_i \phi]
 \end{aligned} \tag{3.2.3}$$

Using that  $n_0$  is the particle number density and  $j_i = \rho v_i$  we get

$$v_i = \frac{\hbar}{m} \nabla_i \phi \tag{3.2.4}$$

where  $m$  is the mass of a particle. We should note that the definition of the mass current  $j_i$  defines  $v_i$ . We would expect that  $v_i$  is the conventional velocity, but we will see later that this is not necessarily the case for multi-constituent fluids. Taking the curl of this equation gives

$$\epsilon_{ijk} \nabla^j v^k = 0 \tag{3.2.5}$$

This means a superfluid is irrotational. We will return to this in more detail later.

### 3.3 Hydrodynamic equations

The first equations that were used to describe the motion of a superfluid were derived by Landau [52]. In essence the derivation is based on conservation laws (mass, momentum and energy) and the irrotational behaviour of the superfluid component. The final equations are similar to the continuity and Navier-Stokes equations for a conventional fluid. Given in tensor notation they are

$$\frac{\partial \rho}{\partial t} + \nabla^j j_j = 0 \tag{3.3.1}$$

$$\frac{\partial \rho s}{\partial t} + \nabla^j (\rho s v_j^n) = 0 \tag{3.3.2}$$

$$\frac{\partial v_i^n}{\partial t} + v_n^j \nabla_j v_i^n = -\frac{1}{\rho_n} \nabla_i P_n + \frac{\eta}{\rho_n} \nabla^2 v_i^n \tag{3.3.3}$$

$$\frac{\partial v_i^s}{\partial t} + \nabla_i \left( \frac{1}{2} v_s^2 + \mu \right) = 0 \tag{3.3.4}$$

where  $v_i$ ,  $\rho$ ,  $s$  and  $j_i$  are velocity, density, entropy and current density, respectively. The subscript/superscripts  $s$  and  $n$  denote the superfluid and normal fluid part, while no label denotes total.  $P$  is the pressure, while  $\mu$  is the chemical potential and  $\eta$  is the normal fluids viscosity coefficient. The equations (3.3.1) and (3.3.2) follow from the conservation of total mass and entropy. Note that it would be slightly misleading to conserve superfluid and normal components separately as there is a constant exchange of population between the two. When we are writing equations of motion we are concerned with average properties. When considering average properties these two expressions can be rewritten as the conservation of the two constituents as at the scale of observation there is no change in any fluid property due to particle exchange eg. momentum, energy, etc... Equations (3.3.3) and (3.3.4) follow from the conservation of each fluid constituent momentum. Note that the viscous term is zero in the superfluid momentum equation as expected.

In showing the derivation for the irrotationality of the superfluid constituent a vital detail was missed out. When integrating the circulation over a circular area, it can be found that the circulation is non-zero. In fact we know it must be, otherwise the superfluid cannot rotate at all. In the rotation experiment the precession of the container showed some evidence of angular momentum being retained in the superfluid part. Noting that the phase ( $\phi$ ) of the superfluid can be larger by any multiple of  $2\pi$  without changing the wave function of the system and using (3.2.4) we get,

$$\int_S \epsilon_{ijk} \nabla^j v_s^k dS^i = \oint_{\delta S} v_j^s dl^j \quad (3.3.5)$$

$$= \frac{\hbar}{m} \oint_{\delta S} \nabla_j \phi dl^j \quad (3.3.6)$$

$$= \frac{\hbar}{m} [\phi]_{a-}^{a+} \quad (3.3.7)$$

$$= \frac{h}{m} n \quad n \in \mathbb{Z} \quad (3.3.8)$$

Defining  $\kappa = \frac{h}{m}$  we get that

$$\int_S \epsilon_{ijk} \nabla^j v_s^k dS^i = \kappa n \quad (3.3.9)$$

We have already shown that  $\epsilon_{ijk} \nabla^j v_s^k = 0$  so how can we explain the above result that integrating this quantity over a surface can give a non-zero value? The

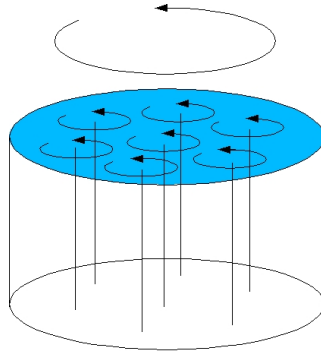


Figure 3.3: A sketch of an array of superfluid vortices. The macroscopic rotation of the superfluid is due to averaging over the effect of the vortex array.

quantisation of circulation of a superfluid was first noted by Onsager [59]. It was Feynman [22] who suggested that a superfluid could have a non-zero circulation via the existence of an array of vortices in the fluid (figure 3.3). These are lines along which the superfluidity breaks down and which have an inverse radial velocity distribution around them. At each point in the superfluid the circulation is zero, but taken over an area the circulation includes the vortex singularities. In fact it can be shown that on a larger scale, the angular velocity of a rotating fluid is given by  $n_v \kappa$  (where  $n_v$  is the vortex number density). Going back to the rotation experiment, once vortex lines have been created, it is hard for them to be destroyed. Vortex lines must end on a boundary and so to be destroyed their ends must join somehow. In fact there is often a force between a vortex line and the walls of the container that keeps the ends in place. This means that the circulation of a superfluid in the rotating system will be conserved. It is easy to see that the superfluid will retain its angular momentum and hence we see precession. Moreover, if the temperature changes there is a change in the proportion of molecules in their superfluid state. The number of vortices will stay constant, so the angular momentum of the superfluid will change. This in turn will cause a different rate of precession.

The inclusion of vortices in a model will modify the equations. This is because the vortices are part of the superfluid component, but are themselves 'normal' fluid. This means that they set up a coupling between the two components which we

see as a mutual friction, a dissipative force within the fluid. There is also a non-dissipative part to the force. Here are the HVBK equations, so named because they were found by Hall, Vinen, Bekharevich and Khalatnikov [39] [16]. They describe the motion of the superfluids as before, but also include the forces associated with curved vortices.

$$\left(\frac{\partial}{\partial t} + v_s^j \nabla_j\right) v_i^s + \frac{1}{\rho} \nabla_i P - S \nabla_i T - \frac{\rho_n}{2\rho} \nabla_i (v_n - v_s)^2 = \nu \omega^j \nabla_j \hat{\omega} - \frac{F_i^{ns}}{\rho_s} \quad (3.3.10)$$

$$\left(\frac{\partial}{\partial t} + v_n^j \nabla_j\right) v_i^n + \frac{1}{\rho} \nabla_i P + \frac{\rho_s}{\rho_n} S \nabla_i T + \frac{\rho_s}{2\rho} \nabla_i (v_n - v_s)^2 = \frac{\eta}{\rho_n} \nabla^2 v_i^n + \frac{F_i^{ns}}{\rho_n} \quad (3.3.11)$$

where

$$\begin{aligned} F_i^{ns} = & \rho_s \omega \alpha \left[ \epsilon_{ijk} \hat{\omega}^j \epsilon^{klm} \hat{\omega}_l (v_m^n - v_m^s) + \nu \epsilon_{ijk} \nabla^j \hat{\omega}^k \right] \\ & + \rho_s \omega \alpha' \left[ \epsilon_{ijk} \hat{\omega}^j (v_n^k - v_s^k) + \nu \hat{\omega}^j \nabla_j \hat{\omega}_i \right] \end{aligned} \quad (3.3.12)$$

$\alpha$  and  $\alpha'$  are coefficients relating to the mutual friction, while  $\nu$  relates to the curvature of the vortices.  $\omega_i$  is the vorticity (average circulation) of the superfluid given by

$$\omega_i = \frac{1}{S} \int_S \epsilon_{ijk} \nabla^j v_s^k dS \quad (3.3.13)$$

where  $S$  is an open surface.

### 3.4 A few extra properties

This section provides a brief overview of some other properties of superfluids that will be useful in later discussions. The first property is something known as second sound. In any fluid a wave of density perturbations can propagate. This is of course just sound waves. For a superfluid there is a type of sound wave known as second sound. As we now have a two-component fluid, we can get a wave in which the total density is constant but the component densities are perturbed. The temperature (or entropy) of the fluid will therefore be perturbed as it is carried with the normal fluid component. The dispersion relation for this wave depends on the vortex line

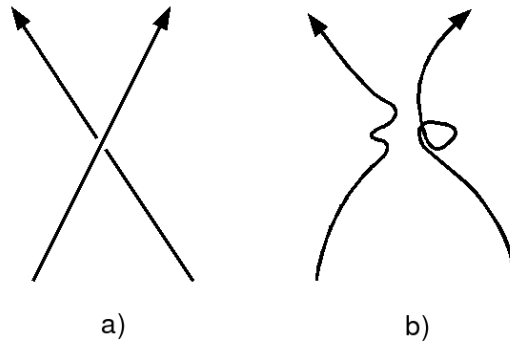


Figure 3.4: A sketch of a pair of vortices crossing (a) and reconnecting (b). The reconnection produces Kelvin waves along the vortex.

density. The detection of second sound is used as a way of determining the vortex line density in the superfluid.

We now consider vortex dynamics. As the large scale motion of superfluids are due to the vortices it is often useful to concentrate on the vortex dynamics before considering the macroscopic dynamics. It has been found that there are waves which are perturbations of the vortex lines. These are known as Kelvin waves and are helical in nature. The last property of vortices to mention is something known as reconnection. When two vortex lines cross they can change configuration (figure 3.4). Kelvin waves are excited when they reconnect. This can even cause more reconnections and loops of vortices to break off.

### 3.5 Neutron-Proton fluid

At first sight the situation in a neutron star looks very different. The temperature is of the order  $10^7 - 10^8 \text{K}$  which seems far removed from the helium lambda point at  $2.17 \text{K}$ . However, the densities in a neutron star raise the energy of the first excited state such that the equivalent to the lambda point is approximately  $10^9 \text{K}$ . In fact it is often taken as an approximation that the neutrons are all superfluid in the outer core. When modelling superfluids, this is the same as taking the zero temperature limit in the equations of motion. Because of this it is now accurate



to say that there is a mixture of two distinct fluids. The first fluid is the neutrons and the second is the charged particles (protons and electrons). The properties of the helium fluid arose from the energy gap between the ground state and first excited state. This is still true here but there will be subtle differences. For  ${}^4\text{He}$  the atoms are bosons and so can all be in the same state. Neutrons are fermions and so cannot all be in the same state. At the pressures and temperatures found in a neutron star the neutrons pair up, similar to cooper pairing found in  ${}^3\text{He}$ . The paired neutrons are now bosons and so can all be in the same quantum state. We also find that the momentum of the superfluid flow must be modified due to nuclear forces. This leads to extra terms in the equations of motion and is called entrainment.

## Chapter 4

# Formulation of multifluid hydrodynamic equations

Before deriving the equations that will help us to model the behaviour of the neutron star core fluid, it is important to consider the scales involved. Casual examination of a typical fluid, for example a cup of water, might suggest that it is calm. If the fluid is magnified such that we can distinguish the individual molecules our conclusions would be very different. We would observe a sea of molecules travelling in seemingly random directions and at different speeds. There would be collisions between the fluid particles which would exchange energy. How then are these two pictures of the fluid consistent? The particles are so small that a casual observer will only see the average velocities of the particles. If the motions of the particles are truly isotropic then the fluid would appear static. Even when a fluid flows, the particles will not all have the same velocity. If it was possible to know the positions and velocities of all the particles then in theory it might be possible to model the subsequent behaviour as seen by the casual observer. In reality this system would be too complicated to correctly model on even the fastest of supercomputers. A more realistic approach would be to find some way of describing the averaged behaviour directly. On the other hand, these equations will have lost the fine detail. If we want to model what the particles are doing then a different set of equations will be needed which describe directly the particle

interactions with its environment.

Superfluids are unusual in the fact that quantum effects impact on a large scale. The vortices are threaded throughout the fluid when it rotates. They may be as long as the superfluids container but only a few Fermi in radius. They directly impact on all scales. In this case we have three different important scales. The casual observer sees what is known as the macroscopic scale. There is the particle scale, known as the microscopic level. Lastly there is the mesoscopic. At this scale the particle flow appears averaged, but we can observe directly the interaction of vortices. Macroscopically the motion of the vortices is averaged as a changing rotation of the superfluid. When considering the macroscopic equations it will be necessary to include some averaged effect of the vortices. Again there may be situations where it is useful to consider the mesoscopic scale.

## 4.1 Methods of Modelling

Traditionally superfluids have been modelled as a two component fluid, split into the normal component and superfluid part. The flow of the two fluids have been modelled in many different ways. One common way to describe superfluid helium has been to start from conservation laws [46] [52]. Apart from the conservation of mass, momentum, energy and entropy another equation had to be found concerning the superfluid component of the fluid. This was found by assuming that superfluid flow is irrotational and that the momentum of a helium particle can be given as  $mv_i$ . The assumption of irrotational flow is well founded by looking at the physics of these quantum fluids, but the form of the momentum that needs to be used in a multifluid system is under contention. Another method is to derive the equations of motion from the Lagrangian of the system (see for example Prix 2004 [62]). This method involves minimising the Lagrangian integrated over some 4 dimensional (space + time) volume. This is done by making variations in this integral, due to changes in the Lagrangian, vanish. It is possible to derive the basic Euler equations by using this method and varying the Lagrangian with respect to velocity and momentum. The problem with this is that we also need to set extra

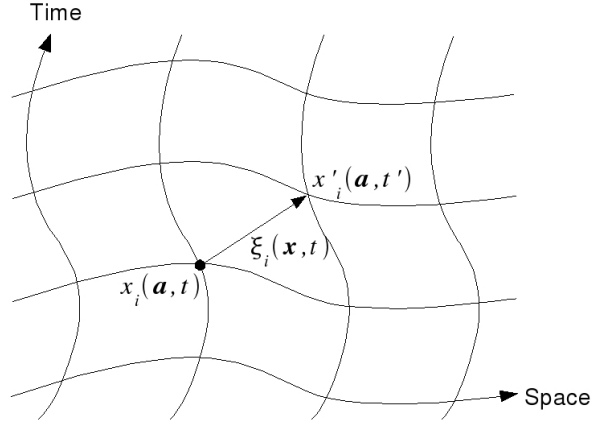


Figure 4.1: This diagram shows how we define the Lagrangian variation. To vary a quantity we displace the underlying flow lines  $x_i(\mathbf{a}, t)$  by an active displacement  $\xi_i(\mathbf{x}, t)$ .

conditions, like the conservation of mass, to complete the equations. To gain meaningful results without having to impose extra conditions, such as the conservation of mass, it must be the underlying flow lines that we vary. By constraining the variation in this way we find quantities that would normally be varied (current density and number density) in terms of variations in the flow lines. By using this method it is straightforward to see that no extra conditions need to be imposed. The following derivation of the hydrodynamic equations follows this method from Prix (2004) [62].

## 4.2 Lagrangian variation

To determine the equations of motion we use the principle of least action [50]. We need to vary the Lagrangian ( $\Lambda$ ) with respect to the flow lines. Following the work done by Prix [62] we define the flow lines by  $x_i = x_i(\mathbf{a}, t)$  and an active variation by  $\xi_i = \xi_i(\mathbf{x}, t)$ , see fig 4.1. Here  $\mathbf{a}$  is the position of a particle at time  $t = 0$ . Then the variation is

$$x'_i(\mathbf{a}, t') = x_i(\mathbf{a}, t) + \xi_i(\mathbf{x}, t) \quad \text{where} \quad t' = t + \tau(\mathbf{x}, t) \quad (4.2.1)$$

If we have a physical quantity  $Q$  an Eulerian variation ( $\delta$ ) will be a change in the quantity itself, e.g.

$$\delta Q = Q'(\mathbf{x}, t) - Q(\mathbf{x}, t) \quad (4.2.2)$$

A Lagrangian variation ( $\Delta$ ) on the other hand will be due to a displacement of the flow lines. eg.

$$\Delta Q = Q'(\mathbf{a}, t') - Q(\mathbf{a}, t) = Q'(\mathbf{x}', t') - Q(\mathbf{x}, t) \quad (4.2.3)$$

Expanding this to first order using (4.2.1) gives

$$\begin{aligned} \Delta Q &= Q'(\mathbf{x}, t) + \xi_j \nabla_j Q(\mathbf{x}, t) + \tau \frac{\partial}{\partial t} Q(\mathbf{x}, t) - Q(\mathbf{x}, t) \\ &= \delta Q + \xi_j \nabla_j Q(\mathbf{x}, t) + \tau \frac{\partial}{\partial t} Q(\mathbf{x}, t) \end{aligned} \quad (4.2.4)$$

We should note that this is not the only way to define the Lagrangian variation. This way of defining the variations is linked to parallel transport of the flow lines. We can see this if we rewrite the Lagrangian variation using the 4-vector form of  $\xi_\mu$  and  $\nabla_\mu$  as

$$\Delta Q = \delta Q + \xi^\mu \nabla_\mu Q(\mathbf{x}, t) \quad (4.2.5)$$

We could have defined the Lagrangian variation using Lie derivatives [8] so that for scalars

$$\begin{aligned} \Delta f &= \delta f + \mathcal{L}_\xi f \\ &= \delta f + \xi^j \nabla_j f \end{aligned} \quad (4.2.6)$$

For scalars the difference between the two approaches is that there is no time variation in the Lagrangian variation defined by the Lie derivative. Time variations are necessary for extracting an energy equation and including particle creation terms. For vectors the Lagrangian variation using a Lie derivative would be

$$\begin{aligned} \Delta f^i &= \delta f^i + \mathcal{L}_\xi f^i \\ &= \delta f^i + \xi^j \nabla_j f^i - f^j \nabla_j \xi^i \end{aligned} \quad (4.2.7)$$

which we can see has extra terms that include the spacial variation  $\xi^i$ . We could have even used a 4-dimensional Lie derivative to gain time variations as well. We

can see that the definition of the Lagrangian variation is a choice, though we will continue to follow the formulation in Prix (2004) [62]. Using the Lagrangian variation derived from the active displacement (4.2.1) and (4.2.4) we can show how a variation in the flow lines affects the velocity of the fluid. The velocity is defined by

$$v^i \equiv \frac{\partial}{\partial t} x^i(\mathbf{a}, t) \quad (4.2.8)$$

The varied velocity is

$$\begin{aligned} v'^i(\mathbf{a}, t') &= \left. \frac{\partial}{\partial t'} x'^i(\mathbf{a}, t') \right|_a = \left. \frac{\partial}{\partial t'} x^i(\mathbf{a}, t) + \frac{\partial}{\partial t'} \xi^i(\mathbf{x}, t) \right|_a \\ &= \left. \frac{\partial}{\partial t} x^i(\mathbf{a}, t) \frac{\partial t}{\partial t'} \right|_a + \left\{ \frac{\partial}{\partial t} \xi^i(\mathbf{x}, t) + \frac{\partial}{\partial \mathbf{x}} \xi^i(\mathbf{x}, t) \cdot \frac{d\mathbf{x}}{dt} \right\} \left. \frac{\partial t}{\partial t'} \right|_a \\ &= \frac{\partial}{\partial t} x^i(\mathbf{a}, t) \left(1 - \frac{\partial}{\partial t} \tau(\mathbf{a}, t)\right) + \frac{\partial}{\partial t} \xi^i(\mathbf{a}, t) \left(1 - \frac{\partial}{\partial t} \tau(\mathbf{a}, t)\right) \end{aligned} \quad (4.2.9)$$

To first order the varied velocity will be

$$v'^i(\mathbf{a}, t') = v^i(\mathbf{a}, t) - v^i \frac{\partial}{\partial t} \tau(\mathbf{a}, t) + \frac{\partial}{\partial t} \xi^i(\mathbf{a}, t) \quad (4.2.10)$$

This gives the Lagrangian variation of the velocity as

$$\Delta v^i = -v^i \frac{\partial}{\partial t} \tau(\mathbf{a}, t) + \frac{\partial}{\partial t} \xi^i(\mathbf{a}, t) \quad (4.2.11)$$

Equivalently, by putting  $\xi$  and  $\tau$  in terms of  $\mathbf{x}$  and  $t$

$$\Delta v^i = \left[ \frac{\partial}{\partial t} \xi^i + v^l \nabla_l \xi^i \right] - \left[ v^i \frac{\partial}{\partial t} \tau + v^i v^l \nabla_l \tau \right] \quad (4.2.12)$$

The Eulerian variation is therefore

$$\delta v^i = \left[ \frac{\partial}{\partial t} \xi^i + v^l \nabla_l \xi^i - \xi^l \nabla_l v^i \right] - \left[ \frac{\partial}{\partial t} (v^i \tau) + v^i v^l \nabla_l \tau \right] \quad (4.2.13)$$

Noting that a change in volume ( $V$ ) from the position of the particles at time  $t = 0$  to time  $t$  will be given by

$$V(\mathbf{x}, t) = V_0(\mathbf{a}) \det(\mathcal{J}) \quad (4.2.14)$$

where  $\mathcal{J}$  is the Jacobian denoting the map between the physical space ( $\mathbf{x}$ ) and material space ( $\mathbf{a}$ ).

$$\mathcal{J}_j^i = \left. \frac{\partial x^i}{\partial a^j} \right|_t \quad (4.2.15)$$

By conservation of mass

$$V(\mathbf{x}, t)n(\mathbf{x}, t) = V_0(\mathbf{a})n_0(\mathbf{a}) \quad (4.2.16)$$

Rearranging gives,

$$n(\mathbf{x}, t) = \frac{n_0(\mathbf{a})}{\det \mathcal{J}} \quad (4.2.17)$$

Also  $n_0(\mathbf{a}) = n(\mathbf{a}, 0)$ . Now the change in the Jacobian is found when the flow lines are varied

$$\mathcal{J}_j^i(\mathbf{a}, t') = \left. \frac{\partial x^i(\mathbf{a}, t')}{\partial a^j} \right|_{t'} = \left. \frac{\partial x^i(\mathbf{a}, t)}{\partial a^j} \right|_{t'} + \left. \frac{\partial \xi^i(\mathbf{x}, t)}{\partial a^j} \right|_{t'} \quad (4.2.18)$$

To first order this will be

$$\begin{aligned} \mathcal{J}_j^i(\mathbf{a}, t') &= \frac{\partial x^i(\mathbf{a}, t)}{\partial a^j} + \frac{\partial x^i(\mathbf{a}, t)}{\partial t} \frac{\partial t}{\partial a^j} \Big|_{t'} + \left\{ \frac{\partial \xi^i(\mathbf{x}, t)}{\partial x^k} \frac{\partial x^k}{\partial a^j} + \frac{\partial \xi^i(\mathbf{x}, t)}{\partial t} \frac{\partial t}{\partial a^j} \right\} \Big|_{t'} \\ &= \mathcal{J}_j^i(\mathbf{a}, t) - v^i \frac{\partial \tau}{\partial a^j} + \frac{\partial \xi^i(\mathbf{x}, t)}{\partial x^k} \left\{ \frac{\partial x^k}{\partial a^j} + \underbrace{\frac{\partial x^k}{\partial t} \frac{\partial t}{\partial a^j} \Big|_{t'}}_{\text{higher order}} \right\} - \underbrace{\frac{\partial \xi^i(\mathbf{x}, t)}{\partial t} \frac{\partial \tau}{\partial a^j}}_{\text{higher order}} \\ &= \mathcal{J}_j^i(\mathbf{a}, t) - \mathcal{J}_j^l v^i \nabla_l \tau + \mathcal{J}_j^l \nabla_l \xi^i \end{aligned} \quad (4.2.19)$$

so the Lagrangian variation of the Jacobian is

$$\Delta \mathcal{J}_j^i = \mathcal{J}_j^l (\nabla_l \xi^i - v^i \nabla_l \tau) \quad (4.2.20)$$

There is an identity that says that for some square matrix  $A_{ij}$

$$\frac{\partial \det A}{\partial A_{ij}} = \det(A) (A^{-1})^{ij} \quad (4.2.21)$$

As the Lagrangian variation is small we can therefore use

$$\Delta(\det \mathcal{J}) = \det(\mathcal{J}) (\mathcal{J}^{-1})^j_i \Delta \mathcal{J}_j^i \quad (4.2.22)$$

so that

$$\frac{\Delta(\det \mathcal{J})}{\det \mathcal{J}} = \nabla_l \xi^l - v^l \nabla_l \tau \quad (4.2.23)$$

According to Prix [62] we now use this with (4.2.17) to get

$$\Delta n = n'(x', t') - n(x, t) = -n \nabla_l \xi^l + n v^l \nabla_l \tau \quad (4.2.24)$$

This was done using (4.2.23) so that

$$n' - n = \frac{n_0(a)}{\det \mathcal{J}'} - \frac{n_0(a)}{\det \mathcal{J}} = \frac{\det \mathcal{J} - \det \mathcal{J}'}{\det \mathcal{J} \det \mathcal{J}'} n_0(a) = \frac{-\Delta(\det \mathcal{J})}{\det \mathcal{J}} \frac{n_0(a)}{\det \mathcal{J}'} \quad (4.2.25)$$

To first order this is

$$n' - n = \frac{-\Delta(\det \mathcal{J})}{\det \mathcal{J}} \frac{n_0(a)}{\det \mathcal{J}} \quad (4.2.26)$$

Using this result the Euler variation of the number density is

$$\begin{aligned} \delta n &= \Delta n - \xi^j \nabla_j n - \tau \frac{\partial}{\partial t} n \\ &= -n \nabla_l \xi^l - \xi^l \nabla_l n + n v^l \nabla_l \tau - \tau \frac{\partial}{\partial t} n \\ &= -\nabla_l (n \xi^l) + \left[ n v^l \nabla_l \tau - \tau \frac{\partial}{\partial t} n \right] \end{aligned} \quad (4.2.27)$$

Using this together with the result for a change in velocity gives the Lagrangian variation of the density flow  $n_i$  as

$$\begin{aligned} \Delta n^i &= \Delta(n v^i) = n \Delta v^i + v^i \Delta n \\ &= n \left[ \frac{\partial}{\partial t} \xi^i + v^l \nabla_l \xi^i \right] - n \left[ v^i \frac{\partial}{\partial t} \tau + v^i v^l \nabla_l \tau \right] - v^i n \nabla_l \xi^l + v^i n v^l \nabla_l \tau \\ &= \left[ n \frac{\partial}{\partial t} \xi^i + n^l \nabla_l \xi^i - n^i \nabla_l \xi^l \right] - n^i \frac{\partial}{\partial t} \tau \end{aligned} \quad (4.2.28)$$

The Eulerian variation of  $n^i$  is therefore,

$$\begin{aligned} \delta n^i &= \Delta n^i - \xi^j \nabla_j n^i - \tau \frac{\partial}{\partial t} n^i \\ &= \left[ n \frac{\partial}{\partial t} \xi^i + n^l \nabla_l \xi^i - n^i \nabla_l \xi^l \right] - n^i \frac{\partial}{\partial t} \tau - \xi^j \nabla_j n^i - \tau \frac{\partial}{\partial t} n^i \\ &= \left[ n \frac{\partial}{\partial t} \xi^i + n^l \nabla_l \xi^i - \nabla_l n^i \xi^l \right] - \frac{\partial}{\partial t} n^i \tau \end{aligned} \quad (4.2.29)$$

### 4.3 The Principle of least Action

Variations of the number density and the number current have now been found with respect to changes in flow lines. The action of the system is defined by,

$$\mathcal{I} = \int \Lambda_H dV dt \quad (4.3.1)$$

The hydrodynamic Lagrangian density  $\Lambda_H$  will depend on the densities ( $n_X$ ) and currents ( $n_i^X$ ) in the fluid. Note that  $X$  and  $Y$  will be from here on used as constituent labels, with  $X \neq Y$ . The principle of least action says that the Lagrangian



should be defined such that the mechanics of a system will be found by showing where the action is a local minimum. This can be shown to be the kinetic energy density of the system minus the potential energy density. It can also be shown that the momentum ( $p_i^X$ ) and energy ( $p_0^X$ ) per fluid particle are defined by

$$p_0^X = \frac{\partial \Lambda_H}{\partial n_X} \quad p_i^X = \frac{\partial \Lambda_H}{\partial n_i^X} \quad (4.3.2)$$

Therefore a variation in the Lagrangian is given by

$$d\Lambda_H = \sum (p_0^X dn_X + p_X^j dn_j^X) \quad (4.3.3)$$

where the summation ( $\sum$ ) is over the different constituents. Using (4.2.27) and (4.2.29) it is now possible to define the change in the Lagrangian by changes in the flow lines

$$\begin{aligned} d\Lambda_H = \sum \left\{ p_0^X \left[ -\nabla^j (n_X \xi_j^X) + \left( n_j^X \nabla^j \tau_X - \tau_X \frac{\partial}{\partial t} n_X \right) \right] \right. \\ \left. + p_X^j \left[ n_X \frac{\partial}{\partial t} \xi_j^X + (n_l^X \nabla^l) \xi_j^X - (\xi_l^X \nabla^l) n_j^X - n_j^X (\nabla^l \xi_l^X) - \frac{\partial}{\partial t} (n_j^X \tau_X) \right] \right\} \end{aligned} \quad (4.3.4)$$

Expanding this term by term we get

$$\begin{aligned} d\Lambda_H = \sum \left\{ -\nabla^j (\xi_j^X n_X p_0^X) + \xi_j^X n_X \nabla^j p_0^X + \nabla^j p_0^X n_j^X \tau_X - \tau_X n_j^X \nabla^j p_0^X \right. \\ - \tau_X p_0^X \nabla^j n_j^X - \tau_X p_0^X \frac{\partial}{\partial t} n_X + \frac{\partial}{\partial t} p_X^j n_X \xi_j^X - \xi_j^X n_X \frac{\partial}{\partial t} p_X^j - \xi_j^X p_X^j \frac{\partial}{\partial t} n_X \\ + \nabla^l n_l^X p_X^j \xi_j^X - \xi_j^X p_X^j \nabla^l n_l^X - \xi_j^X n_l^X \nabla^l p_X^j - \xi_j^X p_X^l \nabla^j n_l^X - \nabla^j \xi_j^X p_X^l n_l^X \\ \left. + \xi_j^X n_l^X \nabla^j p_X^l + \xi_j^X p_X^l \nabla^j n_l^X - \frac{\partial}{\partial t} p_X^j n_j^X \tau_X + \tau_X n_j^X \frac{\partial}{\partial t} p_X^j \right\} \end{aligned} \quad (4.3.5)$$

Any divergence terms and time differentials will not affect the integral and can be ignored. This is because at the boundaries of the action integral the variations of the Lagrangian are taken as zero. So for a divergence,

$$\int \nabla^j R_j dv dt = \int R_j n^j da dt \quad (4.3.6)$$

where  $n^j$  is a unit vector pointing out of the surface of integration. If all the terms in  $R_i$  include  $\xi_i$  or  $\tau$  then on the surface of integration  $R_i$  will vanish. Similarly, taking a function  $R$  with every term including  $\xi_i$  or  $\tau$  then

$$\int \frac{\partial R_i}{\partial t} dt dv = \int [R_i]_{t^-}^{t^+} dv \quad (4.3.7)$$

where  $[R_i]_{t^-}^{t^+}$  is the function  $\frac{\partial R_i}{\partial t}$  integrated over  $t$  between the bounds  $t^+$  and  $t^-$ . At the limits between which  $t$  is integrated, any variations are zero and the integral vanishes. Grouping the terms by type of variation ( $\xi_i$  or  $\tau$ ) gives

$$\begin{aligned} d\Lambda_H = \sum \left\{ \tau_X \left[ -n_j^X \nabla^j p_0^X + n_j^X \frac{\partial}{\partial t} p_X^j - p_0^X \left( \frac{\partial}{\partial t} n_X + \nabla^j n_j^X \right) \right] \right. \\ \left. - \xi_j^X \left[ n_X \frac{\partial}{\partial t} p_X^j - n_X \nabla^j p_0^X + p_X^j \left( \frac{\partial}{\partial t} n_X + \nabla^l n_l^X \right) \right] \right. \\ \left. + n_l^X \nabla^l p_X^j - n_l^X \nabla^j p_X^l + p_X^l \nabla^j n_l^X - p_X^l \nabla^j n_l^X \right\} \end{aligned} \quad (4.3.8)$$

If we take that in a fluid there may be particle creation, and designate the rate as  $\Gamma_X$ , then,

$$\Gamma_X \equiv \frac{\partial}{\partial t} n_X + \nabla^j n_j^X \quad (4.3.9)$$

Using  $\epsilon_{ijk} n_X^j \epsilon^{klm} \nabla_l p_m^X = n_X^j \nabla_i p_j^X - n_X^j \nabla_j p_i^X$ , (4.3.8) becomes

$$\begin{aligned} d\Lambda_H = \sum \left\{ \tau_X \left[ -n_j^X \nabla^j p_0^X + n_j^X \frac{\partial}{\partial t} p_X^j - p_0^X \Gamma_X \right] \right. \\ \left. - \xi_j^X \left[ n_X \left( \frac{\partial}{\partial t} p_X^j - \nabla^j p_0^X \right) + p_X^j \Gamma_X - \epsilon^{jkl} n_k^X \epsilon_{lmq} \nabla^m p_X^q \right] \right\} \end{aligned} \quad (4.3.10)$$

so that the varied action action can be shown in the form

$$\delta \mathcal{I} = \sum \int \left\{ \tau_X g_X - \xi_j^X f_X^j \right\} dV dt \quad (4.3.11)$$

where

$$f_X^i = n_X \left[ \frac{\partial}{\partial t} p_X^i - \nabla^i p_0^X \right] - \epsilon^{ijk} n_j^X \epsilon_{klm} \nabla^l p_X^m + p_X^j \Gamma_X \quad (4.3.12)$$

$$g_X = v_j^X (f_X^j - p_X^j \Gamma_X) - p_0^X \Gamma_X \quad (4.3.13)$$

It can be seen from looking at the dimensions of the terms that  $f_i^X$  is a force and  $g_X$  an energy. For convenience we define a hydrodynamic force which does not include the particle creation term.

$$f_{HX}^i = n_X \left[ \frac{\partial}{\partial t} p_X^i - \nabla^i p_0^X \right] - \epsilon^{ijk} n_j^X \epsilon_{klm} \nabla^l p_X^m \quad (4.3.14)$$

Then the force and energy can be shown as

$$f_X^i = f_{HX}^i + p_X^j \Gamma_X \quad (4.3.15)$$

$$g_X = v_j^X f_{HX}^j - p_0^X \Gamma_X \quad (4.3.16)$$

## 4.4 Equations of Motion

A general variation of the Lagrangian will give an action of the following form

$$\delta\mathcal{I} = \int \left( \frac{\delta\Lambda}{\delta t} \tau + \frac{\delta\Lambda}{\delta x_j} \xi_j \right) dV dt \quad (4.4.1)$$

where  $\xi_i$  and  $\tau$  are common variations in all the constituents. We also know that

$$\frac{\delta\Lambda}{\delta t} = -\frac{\delta H}{\delta t} \quad \text{and} \quad \frac{\delta\Lambda}{\delta x_j} = \frac{d}{dt} \frac{\delta\Lambda}{\delta \dot{x}_j} \quad (4.4.2)$$

where  $H$  is the Hamiltonian. From this we can redefine the variation in action using the external force ( $f_{ext}^i$ ) and energy rate ( $g_{ext}$ )

$$\delta\mathcal{I} = \int \left( g_{ext} \tau - f_{ext}^j \xi_j \right) dV dt \quad (4.4.3)$$

Comparing this with the form of the action calculated directly from variations (4.3.11) gives the equations of motion

$$\sum_X f_X^i = f_{ext}^i \quad \text{and} \quad \sum_X g_X = g_{ext} \quad (4.4.4)$$

## 4.5 The Hydrodynamic Lagrangian

Up until now the Lagrangian has been of a general form. To apply it to superfluidity we need to specify its form for fluids. We assume that the Lagrangian of a fluid constituent will depend on the fluids kinetic energy and its potential energy ( $E$ ). It is worth noting that the potential may depend upon other constituents.

$$\Lambda_H(n_X, n_i^X) \equiv \sum m^X \frac{n_i^X n_X^i}{2n_X} - E \quad (4.5.1)$$

As this point we make the assumption that the energy of the system depends only upon number densities and the velocity difference between fluid components. We choose these quantities as they do not depend on the inertial frame of the observer and they are scalar quantities.

$$E = E(n_X, w_{YX}^2) \quad (4.5.2)$$

where we have defined

$$w_i^{XY} = v_i^X - v_i^Y \quad \text{and} \quad w_{XY}^2 = w_{XY}^i w_i^{XY} \quad (4.5.3)$$

A variation in the energy is therefore found by

$$\delta E = \sum_X \underbrace{\left( \frac{\partial E}{\partial n_X} \right)}_{\mu_X} \delta n_X + \sum_{X,Y} \frac{1}{2} \underbrace{\left( \frac{\partial E}{\partial w_{XY}^2} \right)}_{\alpha} \delta w_{XY}^2 \quad (4.5.4)$$

It can be seen that  $\mu_X$  are the chemical potentials of the fluid constituents. From this the momentum and energy, defined in (4.3.2), are

$$\begin{aligned} p_i^X &= \frac{\partial}{\partial n_i^X} \left( m^X \frac{n_i^X n_X^i}{2n_X} \right) - \frac{\partial E}{\partial w_{XY}^2} \frac{\partial w_{XY}^2}{\partial v_i^X} \frac{\partial v_j^X}{\partial n_j^X} \\ &= m^X v_i^X - \sum_Y \frac{2\alpha_{XY}}{n_X} w_i^{XY} \end{aligned} \quad (4.5.5)$$

$$\begin{aligned} p_0^X &= \frac{\partial}{\partial n_X} \left( m^X \frac{n_i^X n_X^i}{2n_X} \right) - \frac{\partial E}{\partial n_X} - \frac{\partial E}{\partial w_{XY}^2} \frac{\partial w_{XY}^2}{\partial v_i^X} \frac{\partial v_j^X}{\partial n_j^X} \frac{\partial n_i^X}{\partial n_X} \\ &= -\mu_X + \frac{1}{2} m^X v_X^2 - v_X^j p_j^X \end{aligned} \quad (4.5.6)$$

## 4.6 Rewriting the Hydrodynamic Force

For the equations of motion we want the hydrodynamic force in terms of quantities such as the fluid velocities and chemical potentials. We substitute the form of the conjugate momenta (4.5.5) and (4.5.6) into the hydrodynamic force (4.3.14).

$$\begin{aligned} f_i^{HX} &= n_X \left\{ \frac{\partial}{\partial t} p_i^X + \nabla_i \mu^X - \nabla_i \left( m \frac{v_X^2}{2} \right) + \nabla_i (v_X^j p_j^X) - \epsilon_{ijk} v_X^j \epsilon^{klm} \nabla_l p_m^X \right\} \\ &= n_X \left( \frac{\partial}{\partial t} + v_X^j \nabla_j \right) p_i^X + n_X \nabla_i \mu^X \\ &\quad + \underbrace{n_X \left\{ -\nabla_i \left( m \frac{v_X^2}{2} \right) + \epsilon_{ijk} p_X^j \epsilon^{klm} \nabla_l v_m^X + p_X^j \nabla_j v_i^X \right\}}_{=0 \text{ by vector identity}} \end{aligned}$$

Taking the terms signified by the underbrace and substituting the conjugate momentum (4.5.5) they expand to become

$$\begin{aligned} &= n_X \left\{ -\nabla_i \left( m \frac{v_X^2}{2} \right) + m^X \epsilon_{ijk} v_X^j \epsilon^{klm} \nabla_l v_m^X + m_X v_X^j \nabla_j v_i^X \right\} \\ &\quad \underbrace{=0 \text{ by vector identity}} \\ &\quad - \sum_Y 2\alpha^{XY} [\epsilon_{ijk} w_{XY}^j \epsilon^{klm} \nabla_l v_m^X + w_{XY}^j \nabla_j v_i^X] \\ &= - \sum_Y 2\alpha^{XY} w_{XY}^j \nabla_i v_j^X \end{aligned} \quad (4.6.1)$$

We have found that the hydrodynamic force (4.3.14) can be written as

$$f_i^{XH} = n_X \left( \frac{\partial}{\partial t} + v_X^j \nabla_j \right) p_i^X + n_X \nabla \mu^X + \sum_Y 2\alpha^{XY} w_{YX}^j \nabla_i v_j^X \quad (4.6.2)$$

## 4.7 A Single fluid

We expect that for a single fluid ( $o$ ) the equations of motion should reduce to the usual Euler equations. To show this we consider a single fluid that is acted on by a gravitational potential. From (4.4.4) we have that

$$f_i^{oH} = f_i^{ext} = -\rho_o \nabla_i \Phi \quad (4.7.1)$$

where we set  $f_{ext}$  to be the force due to the gravitational potential  $\Phi$ . From (4.6.2) we find  $f_i^{oH}$  is given for a single fluid by

$$f_i^{oH} = n_o \left( \frac{\partial}{\partial t} + v_o^j \nabla_j \right) p_i^o + n_o \nabla \mu^o \quad (4.7.2)$$

where all of the constituent velocity difference terms are ignored as there is no separate constituent with which velocity differences can be set up. The result would have been the same if we had two constituents which we lock together with a ‘fast’ dissipative effect. From (4.5.5) we also have that

$$p_i^o = m_o v_i^o \quad (4.7.3)$$

Where  $m_o$  is the mass of a single particle. Finally we combine (4.7.1), (4.7.2) and (4.7.3) to get,

$$m_o n_o \left( \frac{\partial}{\partial t} + v_o^j \nabla_j \right) v_i^o + m_o n_o \nabla_i \left( \frac{\mu^o}{m_o} \right) = -\rho_o \nabla_i \Phi \quad (4.7.4)$$

Dropping the index as we only have a single fluid and noting that  $mn = \rho$  then we are left with

$$\left( \frac{\partial}{\partial t} + v^j \nabla_j \right) v_i + \nabla_i \left( \Phi + \frac{\mu}{m} \right) = 0 \quad (4.7.5)$$

which is the expected Euler equation except that the pressure is written using the chemical potential. From (4.3.9) and assuming no particle creation we also get the usual continuity equation.

## 4.8 The two fluid equations

Now that we have derived the multi-constituent fluid equations we need to specialise to the situation in a neutron star. The first decision we need to make is how many constituents we think are important. For a full description of a neutron star core we expect there to be neutrons, protons, electrons and possibly other strange matter like hyperons. These particles may be in several states throughout the star. For example, for temperatures less than  $10^9$  K some proportion of the neutrons will be superfluid and the rest will be ‘normal’. We can model the normal fluid by an entropy flow. If we apply similar ideas to the other types of particles we may end up with 8 or more fluids. For the remainder of this thesis we are concentrating on the outer core. In this region we expect that there will be protons  $p$ , neutrons  $n$ , and electrons  $e$ . The neutrons will be superfluid and paired. We also introduce an entropy fluid constituent  $s$  that acts as the neutron ‘normal’ fluid. We will assume that all of the protons are in the same state. Then we have 4 constituents. We now assume that on the macroscopic scale the electrons and protons are locked together. Depending upon the state of the protons there are different reasons to accept this assumption. For a normal proton flow the mean free path of an electron interacting with a proton is of the order of micrometers whereas we are concerned with a system which is kilometers in size. On the macroscopic scale the viscosity between the two components will make them flow together. For a neutron star core we would expect the protons to be superconducting. Then the viscosity argument no longer holds. For a neutron star with magnetic field  $B_i = 10^{12}\text{G}$ , proton density  $n_p$ , Maxwell’s equations give

$$\epsilon_{ijk}\nabla^j B^k = \frac{4\pi}{c}en_p w_i^{ep} \quad (4.8.1)$$

where  $c$  is the speed of light and  $e$  is the charge of an electron. If the magnetic field varies over 1 km scales then

$$w_{ep} \sim 10^{-12} \left( \frac{B}{10^{12}\text{G}} \right) \text{cm/s} \quad (4.8.2)$$

For the size of magnetic field that we expect in a neutron star we therefore expect a small velocity difference between the two constituents. Locking the two fluids

will still be a reasonable approximation. There has been some work done with the 3 constituent model [7] but this is still too complicated for a first step in understanding the properties of neutron star cores. For a neutron star that is more than a few minutes old the temperature will be less than the critical temperature at which the neutrons become superfluid. We expect that the temperature of the star will be at least an order of magnitude colder than this critical point. Below the critical point the proportion of superfluid neutrons to normal neutrons increases exponentially with time. There will be a very small proportion of normal neutrons. We therefore take the zero temperature limit and assume that there is no entropy flow for the neutrons. The fluid will then have two components, the first "c" will consist of the charged particles "p, e" and the second constituent "n" will consist of the neutrons. For simplicity we set the number of particles of each species to be constant.

$$\Gamma_X = 0 \quad (4.8.3)$$

This just assumes that the effect of nucleonic processes is negligible on the timescales at which other processes occur. We assume charge neutrality so that the number densities of the electrons and protons have the relation

$$n_e = n_p \quad (4.8.4)$$

This allows us to ignore magnetic effects. We also use

$$m^n = m^p + m^e = m \quad (4.8.5)$$

to give the fluid component densities as

$$\rho_n = mn_n \quad \text{and} \quad \rho_c = mn_p \quad (4.8.6)$$

From (4.5.4) we have that

$$dE = \mu^n dn_n + \mu^e dn_e + \mu^p dn_p + \alpha^{en} dw_{en}^2 + \alpha^{pn} dw_{pn}^2 \quad (4.8.7)$$

where the relative velocities are now related by

$$w_i^{cn} \equiv v_i^c - v_i^n = w_i^{en} = w_i^{pn} \quad (4.8.8)$$

The total entrainment is given as

$$\alpha \equiv \alpha^{en} + \alpha^{pn} \quad (4.8.9)$$

As we are trying to consider the protons and electrons as being combined into a single constituent we define the combined chemical potential using

$$\mu^p dn_p + \mu^e dn_e = \mu^c dn_c \quad (4.8.10)$$

This gives the form of the change in energy as

$$dE = \mu^n dn_n + \mu^c dn_c + \alpha dw_{cn}^2 \quad (4.8.11)$$

For the neutron star model there will be an external force due to the gravitational potential  $\Phi$  such that the minimal equations of motion(4.4.4) are

$$f_i^n + f_i^c = -\rho \nabla_i \Phi \quad \text{and} \quad g^n + g^c = -\rho^j \nabla_j \Phi \quad (4.8.12)$$

The total density  $\rho$  is the sum of the two constituent densities.  $\rho_i$  is the sum of the momentum densities. The force and energy rate of the  $c$ -fluid are given by

$$f_i^c = f_i^p + f_i^e \quad \text{and} \quad g^c = g^p + g^e \quad (4.8.13)$$

From equations (4.3.15) and (4.3.16) the forces are given by

$$f_i^n = f_i^{nH} \quad f_i^c = f_i^{cH} \quad (4.8.14)$$

The energy rates are

$$g^n = v_n^j f_j^{nH} \quad g^c = v_c^j f_j^{cH} \quad (4.8.15)$$

Using (4.8.14) we can rewrite (4.8.12) as

$$f_i^{nH} + \rho_n \nabla_i \Phi = -f_i^{cH} - \rho_c \nabla_i \Phi \quad (4.8.16)$$

We can then split this into two equations by introducing a mutual force.

$$f_i^{nH} + \rho_n \nabla_i \Phi = f_i^{Mut} \quad (4.8.17)$$

$$f_i^{cH} + \rho_c \nabla_i \Phi = -f_i^{Mut} \quad (4.8.18)$$

We call this force the mutual friction. As can be seen above it is a force between the two constituents. We now have a complete set of hydrodynamic equations. From



this point on we will use the constituent index  $p$  for the charged fluid component. This stands for proton, and the constituent will often be described as the proton fluid. The continuity equations come from (4.3.9) giving the expected

$$\frac{\partial \rho_n}{\partial t} + \nabla^j (\rho_n v_j^n) = 0 \quad (4.8.19)$$

$$\frac{\partial \rho_p}{\partial t} + \nabla^j (\rho_p v_j^p) = 0 \quad (4.8.20)$$

We define

$$\varepsilon_n \equiv \frac{2\alpha}{\rho_n} \quad \varepsilon_p \equiv \frac{2\alpha}{\rho_p} \quad (4.8.21)$$

It is these parameters that we will often refer to as the entrainment. (4.8.17) and (4.8.18) can therefore be written as

$$\begin{aligned} \left( \frac{\partial}{\partial t} + v_j^n \nabla^j \right) [v_i^n + \varepsilon_n (v_i^p - v_i^n)] + \nabla_i \left( \phi + \frac{\mu_n}{m_n} \right) + \varepsilon_n (v_j^p - v_j^n) \nabla_i v_n^j \\ = \frac{f_i^{mut}}{\rho_n} \end{aligned} \quad (4.8.22)$$

$$\begin{aligned} \left( \frac{\partial}{\partial t} + v_j^p \nabla^j \right) [v_i^p + \varepsilon_p (v_i^n - v_i^p)] + \nabla_i \left( \phi + \frac{\mu_p}{m_p} \right) + \varepsilon_p (v_j^n - v_j^p) \nabla_i v_p^j \\ = \nu \nabla^2 v_i^p - \frac{f_i^{mut}}{\rho_p} \end{aligned} \quad (4.8.23)$$

These are the change in momentum equations. They are essentially balance of force equations. At this point it is worthwhile noting the differences between these equations with two constituents and the single fluid equations. We now have a mutual friction between the two constituents. The exact form and possible origin of this force will be discussed in the next chapter. We also have the entrainment parameter that enters the equations as a modification of the momenta of the two constituents. The total momentum has not been changed (we would worry about the formulation if it had) but each constituents momentum now depends upon the velocity difference. We can think of the entrainment as representing a, non-dissipative, drag between the two fluids such that the momenta are now not necessarily aligned with the constituent velocities [12]. There has been some work to constrain the values that entrainment may take [19] [64]. These find  $\varepsilon_p$  to be of order unity and so it will be an important quantity to consider.

## Chapter 5

# Mutual Friction

When deriving the two-fluid equations of motion it was shown that the formalism allowed a mutual force between the constituents. To use these equations as a model for neutron star cores we need to find the form of this force. As we can't study the interaction of superfluid neutrons and protons in a laboratory we cannot know all of the forces that might come into play. Hence, we turn to the properties of superfluid helium to help us to include the effects that are most likely to be important. Remembering the helium equations of motion we had some mutual force terms due to vortices. In this chapter the mutual friction is calculated for a straight vortex array. This is then modified for an array of curved vortices which will be important when investigating turbulence in the fluid.

### 5.1 Vortices and circulation

To calculate the mutual friction it is necessary to understand where this force originates from. As a vortex moves through the neutron fluid the Magnus force will act on the vortex. This is the force that makes a spinning ball curve through the air. It is due to a pressure gradient over the vortex because of the effect known as Bernoulli's principle in which faster flow has a lower pressure. There will also be a force on the vortex due to the electrons in the charged fluid scattering off the vortex. It is the balance of these two forces on the vortex line that leads to

a mutual friction. In our discussions on helium there was no issue in saying that the normal fluid flow interacts with the normal fluid vortex core. For the neutrally charged neutrons this is not so clear. To understand the processes involved we have to return to the circulation of the superfluid component. For  $^4\text{He}$  it was shown that the circulation was zero throughout the superfluid except where there were vortices. Conventionally to find the circulation we integrate the curl of the velocity field. It is more correct to say that you integrate the curl of the momentum so that the circulation is

$$C_i = \frac{1}{m} \int_S \epsilon_{ijk} \nabla^j p^k dS \quad (5.1.1)$$

For a single fluid this is exactly equivalent to what was done before. However, for a two component system the momentum of each component is modified via the entrainment. The circulation of the neutron component is therefore given by

$$\begin{aligned} C_i &= \int_S \left\{ \epsilon_{ijk} \nabla^j \left[ v_n^k + \varepsilon_n (v_p^k - v_n^k) \right] \right\} dS \\ &= \oint [v_i^n + \varepsilon_n (v_i^p - v_i^n)] dr \end{aligned} \quad (5.1.2)$$

We know from (3.2.3) that the nature of a superfluid means that the momentum can be written as the gradient of the phase. The circulation is therefore

$$\frac{\hbar}{m} \oint \nabla_i \phi dr = \kappa_i n_v \quad (5.1.3)$$

$n_v$  is defined here as the number of vortices that intersect the integrated area and  $\phi$  is the phase. So it is the momentum of the neutron fluid that is quantised. To emphasise this point we take the curl of the neutron equation of motion found in the previous chapter.

$$\left( \frac{\partial}{\partial t} + \mathcal{L}_{v_n} \right) \epsilon_{ijk} \nabla^j \left[ v_n^k + \varepsilon_n (v_p^k - v_n^k) \right] = 0 \quad (5.1.4)$$

We have rewritten the equations using the Lie derivative because it is commutative with curl. We have ignored the mutual friction force. If there are no forces acting then the circulation will not change. In fact we can see that (5.1.4) shows the circulation is constant, but only when we define the circulation from the momentum. This means that the quantized vortices now involve the velocities from both constituents. We can consider entrainment like a drag effect that causes some

of the protons to be dragged around the vortices in the neutron fluid. This will create a magnetic field which the electrons scatter off. When modeling helium it is possible that entrainment should be included, but is not necessary for mutual friction. For the fluid inside neutron stars entrainment is crucial for the interaction between the two constituents.

## 5.2 The mutual friction in Neutron stars

Before launching into the derivation of the mutual friction we will take a closer look at the nature of the fluids involved. In our discussions in chapter 4 we split the important length scale into three definite categories. The microscopic, mesoscopic and macroscopic scales in which the characteristic length scales are respectively, particle mean free paths, inter vortex spacing, and observable quantities. There are some subtleties to this. When calculating the mutual friction we will want to consider the protons and neutrons as a fluid on the mesoscopic scale. We can then derive the forces acting on a single vortex and then average over many vortices to find the macroscopic force on the separate constituents. We would like to consider the electrons and protons locked together on the macroscopic scale, but on the mesoscopic scale we require them to flow separately so that a magnetic field can be set up around the vortex. We will now have to specify what type of state we expect the protons to be in. For a normal proton fluid the proton-proton and proton-electron mean free path is of the order of the inter-vortex spacing. This means that we would not be able to treat the protons as a fluid on the mesoscopic scale. For a neutron star we expect the protons to be superconducting. The important length scale then becomes the coherence length which is much smaller than the inter-vortex spacing so the protons will behave as a fluid on the mesoscopic scale. Similar arguments apply for the neutrons as they are superfluid. The electrons on the other hand are not a fluid and on the mesoscopic scale are not coupled to the proton fluid. We have shown in section 4.8 that the electrons will be coupled to the protons on the large scale. For the following calculations we are considering that the interaction between the vortices and the fluid constituents

is due to the magnetic field created by entrained protons. It should be noted that other mechanisms have been suggested. There have been calculations done with normal protons [21] which are relevant in the crust of a neutron star. There have also been some calculations in which the vortex core has been considered as the region in which protons scatter [65].

### 5.3 Magnus Force

To find the mutual friction force we will start by considering a single straight vortex line. This calculation is on the mesoscopic scale. We will then have to make some assumptions about how to average over many vortices to find the macroscopic forces. We will be assuming that on the mesoscopic scale both the protons and neutrons can be considered as fluids. As previously mentioned the Magnus force will be acting on the vortex. We calculate this by considering a single vortex traveling through a constant flow. To calculate the force on the vortex it is necessary to find the change in momentum of the surrounding fluid over the entirety of the vortex. The change in constituent momentum  $p_i^X$  will be given by.

$$\begin{aligned}\frac{\partial p_i^X}{\partial t} &= \frac{\partial}{\partial t} \{n_X [v_i^X + \varepsilon_X (v_i^Y - v_i^X)]\} \\ &= n_X \frac{\partial}{\partial t} [v_i^X + \varepsilon_X (v_i^Y - v_i^X)] + [v_i^X + \varepsilon_X (v_i^Y - v_i^X)] \frac{\partial n_X}{\partial t}\end{aligned}\quad (5.3.1)$$

The Euler equations for the two fluids are

$$\begin{aligned}\left(\frac{\partial}{\partial t} + v_j^X \nabla^j\right) [v_i^X + \varepsilon_X (v_i^Y - v_i^X)] + \varepsilon_X (v_j^Y - v_j^X) \nabla_i v_X^j \\ + \nabla_i \left(\phi + \frac{\mu_X}{m_X}\right) = 0\end{aligned}\quad (5.3.2)$$

The equations of continuity are

$$\frac{\partial n_X}{\partial t} + \nabla^k (n_X v_k^X) = 0\quad (5.3.3)$$

Combining (5.3.1), (5.3.2) and (5.3.3) gives

$$\begin{aligned}
 \frac{\partial p_i^n}{\partial t} &= -n_n \nabla_i \left( \phi + \frac{\mu_n}{m_n} \right) - n_n \varepsilon_n \left( v_j^p - v_j^n \right) \nabla_i v_n^j \\
 &\quad - n_n v_j^n \nabla^j [v_i^n + \varepsilon_n (v_i^p - v_i^n)] - [v_i^n + \varepsilon_n (v_i^p - v_i^n)] \nabla^k (n_n v_k^n) \\
 &= -n_n \nabla_i \left( \phi + \frac{\mu_n}{m_n} \right) - n_n \varepsilon_n \left( v_j^p - v_j^n \right) \nabla_i v_n^j \\
 &\quad - \nabla^j \{ n_n v_j^n [v_i^n + \varepsilon_n (v_i^p - v_i^n)] \}
 \end{aligned} \tag{5.3.4}$$

and

$$\begin{aligned}
 \frac{\partial p_i^p}{\partial t} &= -n_p \nabla_i \left( \phi + \frac{\mu_p}{m_p} \right) - n_p \varepsilon_p \left( v_j^n - v_j^p \right) \nabla_i v_p^j \\
 &\quad - \nabla^j \{ n_p v_j^p [v_i^p + \varepsilon_p (v_i^n - v_i^p)] \}
 \end{aligned} \tag{5.3.5}$$

Assuming that the entrainment is locally constant and combining these equations gives the total change in momentum. Defining  $w_i^{XY} = v_i^X - v_i^Y$  as in (4.5.3) this is

$$\begin{aligned}
 \frac{\partial}{\partial t} (p_i^n + p_i^p) &= - (n_n + n_p) \nabla_i \phi - n_n \nabla_i \left( \frac{\mu_n}{m_n} \right) - n_p \nabla_i \left( \frac{\mu_p}{m_p} \right) + \nabla_i (\alpha w_{np}^2) \\
 &\quad - \nabla_k \left[ (n_n - 2\alpha) v_n^k v_i^n + (n_p - 2\alpha) v_p^k v_i^p + 2\alpha (v_n^k v_i^p + v_p^k v_i^n) \right] \\
 &= - \nabla_k \Pi_i^k
 \end{aligned} \tag{5.3.6}$$

where in the frame moving with the vortex velocity  $v_L^i$  we find the momentum current  $\Pi_i^k$  is

$$\begin{aligned}
 \Pi_i^k &= \left( n\phi + n_n \frac{\mu_n}{m_n} + n_p \frac{\mu_p}{m_p} - \alpha w_{np}^2 \right) \delta_i^k \\
 &\quad + n_n w_{nL}^k w_i^{nL} + n_p w_{pL}^k w_i^{pL} - 2\alpha w_{np}^k w_i^{np}
 \end{aligned} \tag{5.3.7}$$

We have defined  $n = n_n + n_p$  and assumed that the separate constituent number densities are homogeneous. This will be approximately true except near the core of the vortex. On the scale we are considering the vortex core is very small. The core itself is a similar scale to the fluid particles and so the assumption seems reasonable. The force per unit length that will act on the vortex will be due to the rate of change of momentum over a cylinder enclosing the vortex (fig 5.1).

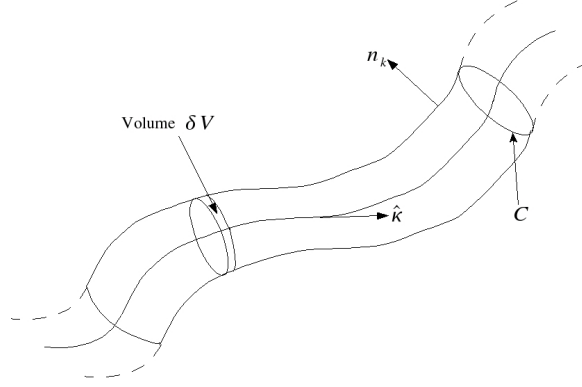


Figure 5.1: To find the force acting on the vortex we integrate the change in momentum of the surrounding fluid over a volume that encloses the vortex line. For a straight vortex we choose a cylindrical volume with the vortex line at its centre.  $\delta V$  is a small segment of this volume, while  $C$  is a closed line encircling the vortex line.  $\hat{\kappa}$  is the direction of vortex circulation and  $n_k$  is a unit vector that points out of the volume of integration.

$$F_i = \int_{\delta V} \nabla_k \Pi_i^k dV \quad (5.3.8)$$

Using Stokes theorem this is

$$F_i = \int_{\delta S} \Pi_i^k n_k dS \quad (5.3.9)$$

For a straight line vortex this reduces to

$$F_i = \oint_C \Pi_i^k n_k dl \quad (5.3.10)$$

where  $C$  encloses the vortex and  $n_k$  is the unit vector normal to the cylinder. To further simplify  $\Pi_i^k$  we rewrite the Euler equations in the frame of the vortex line.

$$\left( \frac{\partial}{\partial t} + w_j^{XL} \nabla^j \right) (w_i^{XL} + \varepsilon_X w_i^{YX}) + \nabla_i \left( \phi + \frac{\mu_X}{m_X} \right) + \varepsilon_X w_j^{YX} \nabla_i w_{XL}^j = 0 \quad (5.3.11)$$

In this frame we expect that the fluid flow will be stationary. As the neutrons and protons are superfluid they will be irrotational around the vortex line. We can also show that

$$\begin{aligned} & w_j^{XL} \nabla^j (w_i^{XL} + \varepsilon_X w_i^{YX}) + \varepsilon_X w_j^{YX} \nabla_i w_{XL}^j \\ &= \nabla_i \left( \frac{1}{2} w_{XL}^2 + \varepsilon_X w_j^{XL} w_{YX}^j \right) - \epsilon_{ijk} w_{XL}^j \epsilon^{klm} \nabla_l (w_m^{XL} + \varepsilon_X w_c^{YX}) \end{aligned} \quad (5.3.12)$$

From the assumption that the fluid is irrotational the curl of the momentum is zero. By applying the stationary assumption (5.3.11) becomes

$$\nabla_i \left( \frac{1}{2} w_{XL}^2 + \varepsilon_X w_j^{XL} w_{YX}^j + \phi + \frac{\mu_X}{m_X} \right) = 0 \quad (5.3.13)$$

By writing this out for the two constituents we find

$$C_n = \phi + \frac{\mu_n}{m_n} + \frac{1}{2} w_{nL}^2 + \varepsilon_n w_{pn}^j w_j^{nL} \quad (5.3.14)$$

$$C_p = \phi + \frac{\mu_p}{m_p} + \frac{1}{2} w_{pL}^2 + \varepsilon_p w_{np}^j w_j^{pL} \quad (5.3.15)$$

Combining these using  $n_n \varepsilon_n = n_p \varepsilon_p = 2\alpha$  gives

$$D = n\phi + n_n \frac{\mu_n}{m_n} + n_p \frac{\mu_p}{m_p} + n_n \frac{1}{2} w_{nL}^2 + n_p \frac{1}{2} w_{pL}^2 - 2\alpha w_{pn}^2 \quad (5.3.16)$$

We use this to rewrite the momentum current (5.3.7) as

$$\begin{aligned} \Pi_i^k = & \left( D - n_n \frac{1}{2} w_{nL}^2 - n_p \frac{1}{2} w_{pL}^2 + 2\alpha w_{pn}^2 - \alpha w_{np}^2 \right) \delta_i^k \\ & + n_n w_{nL}^k w_i^{nL} + n_p w_{pL}^k w_i^{pL} - 2\alpha w_{np}^k w_i^{np} \end{aligned} \quad (5.3.17)$$

For a single vortex we would expect that the flow of each constituent will be approximately the sum of a uniform flow and a flow around the vortex. We therefore assume that

$$w_i^{nL} = v_i^n - v_i^L = U_i^n + v_i^{vn} \quad w_i^{pL} = v_i^p - v_i^L = U_i^p + v_i^{vp} \quad (5.3.18)$$

where  $U_i^X$  is the constituents uniform flow and  $v_i^{vX}$  is the flow around the vortex. Substituting these into the integrand of (5.3.10) we get

$$\begin{aligned} \Pi_i^k n_k = & \left\{ D - n_n \frac{1}{2} (U_n^j + v_{vn}^j) (U_j^n + v_j^{vn}) - n_p \frac{1}{2} (U_p^j + v_{vp}^j) (U_j^p + v_j^{vp}) \right. \\ & + \alpha [(U_p^j - U_n^j) + (v_{vp}^j - v_{vn}^j)] [(U_j^p - U_j^n) + (v_j^{vp} - v_j^{vn})] \Big\} n_i \\ & + n_n (U_n^k + v_{vn}^k) (U_i^n + v_i^{vn}) n_k + n_p (U_p^k + v_{vp}^k) (U_i^p + v_i^{vp}) n_k \\ & - 2\alpha [(U_p^k - U_n^k) + (v_{vp}^k - v_{vn}^k)] [(U_i^p - U_i^n) + (v_i^{vp} - v_i^{vn})] n_k \end{aligned} \quad (5.3.19)$$

Some of these terms will disappear when integrated around the contour. The coefficients of  $n_i$  which will be constant for both fluids on the contour are

$$U_j U^j \quad v_j^{vX} v_{vX}^j \quad D \quad (5.3.20)$$



These terms will disappear when integrated around a circle. As the vector  $n_i$  in polar coordinates is proportional to the radial vector and  $v_i^{vX}$  is in the  $\theta$  direction (i.e. orthogonal to  $n_i$ ) then  $v_{vX}^j n_j = 0$ . As  $U$  is a constant flow then the integral round the vortex of  $U^k n_k U_i$  vanishes. The momentum current (5.3.19) is therefore given by

$$\begin{aligned} \Pi_i^k n_k = & n_n \left( v_i^{vn} U_n^j n_j - v_{vn}^j U_j^n n_i \right) - 2\alpha v_{vn}^j \left( U_j^p - U_j^n \right) n_i + 2\alpha v_i^{vn} \left( U_p^j - U_n^j \right) n_j \\ & + n_p \left( v_i^{vp} U_p^j n_j - v_{vp}^j U_j^p n_i \right) - 2\alpha v_{vp}^j \left( U_j^n - U_j^p \right) n_i + 2\alpha v_i^{vp} \left( U_n^j - U_p^j \right) n_j \end{aligned} \quad (5.3.21)$$

Equivalently

$$\begin{aligned} \Pi_i^k n_k = & n_n \epsilon_{ijk} \left[ U_n^j + \varepsilon_n \left( U_p^j - U_n^j \right) \right] \epsilon^{klm} v_l^{vn} n_m \\ & + n_p \epsilon_{ijk} \left[ U_p^j + \varepsilon_p \left( U_n^j - U_p^j \right) \right] \epsilon^{klm} v_l^{vp} n_m \end{aligned} \quad (5.3.22)$$

To simplify this we want to determine  $v_i^{vn}$  and  $v_i^{vp}$ . We can do this by using (5.1.2), where the number of vortices  $n_v$  is one and the surface of integration is a circle with the vortex at the center. Equivalently

$$\int_{circle} \epsilon_{ijk} \nabla^j \left[ v_n^k + \varepsilon_n \left( v_p^k - v_n^k \right) \right] dS = \frac{h}{2m} e_i^z \quad (5.3.23)$$

where  $e_i^z$  is the  $z$  axis basis vector in cylindrical polar coordinates which is aligned with the vortex line. Evaluating the integral by using Stokes theorem and noting that the distance between the contour and vortex will be constant ( $R$ ) we get

$$\Omega_i^n + \varepsilon_n (\Omega_i^p - \Omega_i^n) = \frac{\hbar}{2R^2 m} e_i^z \quad (5.3.24)$$

where  $\Omega_i^X$  is the angular velocity of constituent  $X$ . Taking the vorticity of the charged fluid as 0 then

$$v_i^{vn} + \varepsilon_n (v_i^{vp} - v_i^{vn}) = \frac{\kappa}{2\pi r} e_i^\theta \quad (5.3.25)$$

$$v_i^{vp} + \varepsilon_p (v_i^{vn} - v_i^{vp}) = 0 \quad (5.3.26)$$

where  $e_i^\theta$  is the  $\theta$  direction in polar coordinates where  $z$  is along the vortex line, and

$$\kappa = \frac{h}{2m} \quad (5.3.27)$$

This rearranges to give the vortex velocities as

$$v_i^{vn} = \left( \frac{1 - \varepsilon_p}{1 - \varepsilon_n - \varepsilon_p} \right) \frac{\kappa}{2\pi r} e_i^\theta \quad (5.3.28)$$

$$v_i^{vp} = \left( \frac{\varepsilon_p}{\varepsilon_p + \varepsilon_n - 1} \right) \frac{\kappa}{2\pi r} e_i^\theta \quad (5.3.29)$$

Substituting these into the integrand gives

$$\begin{aligned} \Pi_i^k n_k = & - \frac{(1 - \varepsilon_p)n_n}{2\pi r(1 - \varepsilon_n - \varepsilon_p)} \epsilon_{ijk} [U_n^j + \varepsilon_n (U_p^j - U_n^j)] \kappa^k \\ & + \frac{\varepsilon_p n_p}{2\pi r(1 - \varepsilon_n - \varepsilon_p)} \epsilon_{ijk} [U_p^j + \varepsilon_p (U_n^j - U_p^j)] \kappa^k \end{aligned} \quad (5.3.30)$$

Where  $\kappa_i$  is defined by  $\kappa_i = \kappa \epsilon_{ijk} e_\theta^j n^k = \kappa e_i^z$ . Noting that  $\Pi_i^k n_k$  will be constant around the integration contour in (5.3.10) the Magnus force is

$$f_i = -\rho_n \epsilon_{ijk} U_n^j \kappa^k \quad (5.3.31)$$

## 5.4 Mutual Friction

Having found the form of the Magnus force, the friction between the moving fluid and the vortex can be calculated. The Magnus force acting on the vortex will be balanced by the electrons scattering off the vortex. We expect that this force will be proportional to the difference in velocity between the vortex line and the normal fluid flow (protons and electrons).

$$f_i^e = C (v_i^p - v_i^L) \quad (5.4.1)$$

The force due to electron scattering must be equal to the Magnus force giving the relationship between them as.

$$C (v_i^p - v_i^L) = \rho_n \epsilon_{ijk} \kappa^j (v_n^k - v_L^k) \quad (5.4.2)$$

where the constant flow  $U_i^n$  has been written in the frame in which we measure the fluid velocities.  $v_i^n$  represents the uniform part of the flow in the frame of an observer. When we look at the macroscopic scale both  $v_i^p$  and  $v_i^n$  will be the measured velocities of the constituents.

$$v_i^L = v_i^p - \frac{\rho_n}{C} \epsilon_{ijk} \kappa^j (v_n^k - v_L^k) \quad (5.4.3)$$

Taking the cross product with  $\kappa_i$  gives

$$\epsilon_{ijk}\kappa^j v_L^k = \epsilon_{ijk}\kappa^j v_p^k - \frac{\rho_n}{C}\epsilon_{ijk}\kappa^j \epsilon^{klm}\kappa_l (v_m^n - v_m^L) \quad (5.4.4)$$

and again ...

$$\epsilon_{ijk}\kappa^j \epsilon^{klm}\kappa_l v_m^L = \epsilon_{ijk}\kappa^j \epsilon^{klm}\kappa_l v_m^p - \frac{\rho_n}{C}\epsilon_{ijk}\kappa^j \epsilon^{klm}\kappa_l \epsilon_{mqr}\kappa^q (v_n^r - v_L^r) \quad (5.4.5)$$

The last term expands to give

$$\begin{aligned} \frac{\rho_n}{C}\epsilon_{ijk}\kappa^j \epsilon^{klm}\kappa_l \epsilon_{mqr}\kappa^q (v_n^r - v_L^r) \\ = \frac{\rho_n}{C}\epsilon_{ijk}\kappa^j \kappa^k \kappa^l (v_l^n - v_l^L) - \frac{\rho_n}{C}\epsilon_{ijk}\kappa^j \kappa^l \kappa_l (v_n^k - v_L^k) \end{aligned} \quad (5.4.6)$$

$\epsilon_{ijk}\kappa^j \kappa^k = 0$  as this is a symmetric tensor (in  $j, k$ ) contracted by an anti-symmetric tensor. Then (5.4.5) becomes

$$\epsilon_{ijk}\kappa^j \epsilon^{klm}\kappa_l v_m^L = \epsilon_{ijk}\kappa^j \epsilon^{klm}\kappa_l v_m^p + \frac{\rho_n \kappa^2}{C}\epsilon_{ijk}\kappa^j (v_n^k - v_L^k) \quad (5.4.7)$$

Expanding (5.4.4) and substituting in (5.4.7) gives

$$\begin{aligned} \epsilon_{ijk}\kappa^j v_L^k &= \epsilon_{ijk}\kappa^j v_p^k - \frac{\rho_n}{C}\epsilon_{ijk}\kappa^j \epsilon^{klm}\kappa_l v_m^n + \frac{\rho_n}{C}\epsilon_{ijk}\kappa^j \epsilon^{klm}\kappa_l v_m^L \\ &= \epsilon_{ijk}\kappa^j v_p^k - \frac{\rho_n}{C}\epsilon_{ijk}\kappa^j \epsilon^{klm}\kappa_l v_m^n \\ &\quad + \frac{\rho_n}{C}\left[\epsilon_{ijk}\kappa^j \epsilon^{klm}\kappa_l v_m^p + \frac{\rho_n \kappa^2}{C}\epsilon_{ijk}\kappa^j (v_n^k - v_L^k)\right] \end{aligned} \quad (5.4.8)$$

This gives

$$\left(1 + \frac{\rho_n^2 \kappa^2}{C^2}\right)\epsilon_{ijk}\kappa^j v_L^k = \epsilon_{ijk}\kappa^j v_p^k + \frac{\rho_n}{C}\epsilon_{ijk}\kappa^j \epsilon^{klm}\kappa_l (v_m^p - v_m^n) + \frac{\rho_n^2 \kappa^2}{C^2}\epsilon_{ijk}\kappa^j v_n^k \quad (5.4.9)$$

Substituting this into (5.4.3)

$$\begin{aligned} v_i^L &= v_i^p - \frac{\rho_n}{C}\epsilon_{ijk}\kappa^j v_n^k + \frac{\rho_n}{C}\epsilon_{ijk}\kappa^j v_L^k \\ &= v_i^p - \frac{\rho_n}{C}\epsilon_{ijk}\kappa^j v_n^k + \frac{\rho_n}{C}\left(1 + \frac{\rho_n^2 \kappa^2}{C^2}\right)^{-1}\left[\epsilon_{ijk}\kappa^j v_p^k + \frac{\rho_n^2 \kappa^2}{C^2}\epsilon_{ijk}\kappa^j v_n^k \right. \\ &\quad \left. + \frac{\rho_n}{C}\epsilon_{ijk}\kappa^j \epsilon^{klm}\kappa_l (v_m^p - v_m^n)\right] \end{aligned} \quad (5.4.10)$$

After some rearrangement this becomes

$$\begin{aligned} v_i^L &= v_i^p + \frac{C}{\rho_n \kappa^2}\left(\frac{1}{1 + C^2/\rho_n^2 \kappa^2}\right)\epsilon_{ijk}\kappa^j (v_p^k - v_n^k) \\ &\quad + \frac{1}{\kappa^2}\left(\frac{1}{1 + C^2/\rho_n^2 \kappa^2}\right)\epsilon_{ijk}\kappa^j \epsilon^{klm}\kappa_l (v_m^p - v_m^n) \end{aligned} \quad (5.4.11)$$

Substituting this back in (5.4.1) gives the force per unit length acting on the vortex as

$$\begin{aligned} f_i^e &= C(v_i^p - v_i^L) \\ &= \frac{C^2}{\rho_n \kappa^2} \left( \frac{1}{1 + C^2/\rho_n^2 \kappa^2} \right) \epsilon_{ijk} \kappa^j (v_n^k - v_p^k) \\ &\quad + \frac{C}{\kappa^2} \left( \frac{1}{1 + C^2/\rho_n^2 \kappa^2} \right) \epsilon_{ijk} \kappa^j \epsilon^{klm} \kappa_l (v_m^n - v_m^p) \end{aligned} \quad (5.4.12)$$

The form of the mutual friction that can be used in hydrodynamic equations must be in terms of the average force per volume.  $v_i^n$  and  $v_i^p$  were just a local constant flow. If we assume that the inter-vortex spacing is large enough that there is no vortex-vortex interaction then any macroscopically measured velocities will be locally uniform on the mesoscopic scale. We can therefore take the velocities  $v_i^X$  as macroscopic quantities. By assuming that there is no vortex-vortex interaction the force on a straight vortex array in a fluid box will just be the vortex density,  $n_v$ , multiplied by the force per vortex length. This gives

$$f_i^e = n_v \left( \frac{C \rho_n}{\rho_n^2 \kappa^2 + C^2} \right) \left[ C \epsilon_{ijk} \kappa^j (v_n^k - v_p^k) + \rho_n \epsilon_{ijk} \kappa^j \epsilon^{klm} \kappa_l (v_m^n - v_m^p) \right] \quad (5.4.13)$$

From (5.3.24) we find the quantisation of vorticity gives

$$2\Omega_i^n + \varepsilon_n (2\Omega_i^p - 2\Omega_i^n) = \kappa_i \frac{n}{\pi R^2} = \kappa_i n_v \quad (5.4.14)$$

where  $n$  is the number of vortices in the area of integration and  $n_v$  is the vortex line density. Substituting this in to (5.4.13)

$$\begin{aligned} f_i^e &= [2\Omega_n + \varepsilon_n (2\Omega_p - 2\Omega_n)] \left( \frac{C \rho_n}{\rho_n^2 \kappa^2 + C^2} \right) \left[ C \epsilon_{ijk} \hat{\kappa}^j (v_n^k - v_p^k) \right. \\ &\quad \left. + \rho_n \epsilon_{ijk} \kappa^j \epsilon^{klm} \hat{\kappa}_l (v_m^n - v_m^p) \right] \end{aligned} \quad (5.4.15)$$

Rearranging this into a form similar to the mutual friction calculated in <sup>4</sup>He gives

$$\begin{aligned} f_i^e &= \left( \frac{C^2}{\rho_n^2 \kappa^2 + C^2} \right) \rho_n \epsilon_{ijk} \lambda^j (v_n^k - v_p^k) \\ &\quad + \left( \frac{C \rho_n}{\rho_n^2 \kappa^2 + C^2} \right) \rho_n \kappa \epsilon_{ijk} \lambda^j \epsilon^{klm} \hat{\kappa}_l (v_m^n - v_m^p) \end{aligned} \quad (5.4.16)$$

where

$$\begin{aligned} \lambda_i &= 2 [\Omega_n + \varepsilon_n (\Omega_p - \Omega_n)] \hat{\kappa}_i \\ &= 2\Omega_i^n + \varepsilon_n (2\Omega_i^p - 2\Omega_i^n) \end{aligned} \quad (5.4.17)$$

To clean this up we define the dimensionless coefficients,

$$\beta = \left( \frac{C}{\rho_n \kappa} \right) \left( \frac{1}{1 + C^2 / \rho_n^2 \kappa^2} \right) \quad (5.4.18)$$

$$\beta' = \left( \frac{C}{\rho_n \kappa} \right)^2 \left( \frac{1}{1 + C^2 / \rho_n^2 \kappa^2} \right) \quad (5.4.19)$$

so that the mutual friction force on the neutron fluid is given by

$$f_i^{mf} = \beta \rho_n \epsilon_{ijk} \lambda^j \epsilon^{klm} \hat{\kappa}_l (v_m^n - v_m^p) + \beta' \rho_n \epsilon_{ijk} \lambda^j (v_n^k - v_p^k) \quad (5.4.20)$$

As the force is a mutual friction, the force on the proton fluid is given by  $-f_i^{mf}$ . This looks almost identical to the equations given for mutual friction in the Helium case [38]. The difference is that  $\lambda$ ,  $\beta$  and  $\beta'$  are dependent upon entrainment.

## 5.5 Estimating the coefficients

To study the effect of the mutual friction force in neutron stars it will be useful to have some idea of the expected magnitude of the coefficients  $\beta$  and  $\beta'$ . We need to calculate the coefficient  $C$  that represents the drag between the electrons and a vortex line. The main problem at this point is that the microscopic physics becomes very important. There have been several ways in which the electron scattering has been modelled. Feibelman [21] has calculated the coefficient for superfluid neutrons mixed with a normal proton fluid. This may be more relevant in the crust. We expect the protons in the core to be superconducting. Sauls et. al. [65] have calculated the coefficients for electrons scattering off the normal fluid core of the vortex. It has since been found that the coefficient is larger if the electrons are assumed to scatter off the magnetic field produced by the protons that are entrained around the vortex [3] [57]. This effect has also been studied in the formalism that we use here [10]. The general idea is that we can write the momentum of the proton fluid [63] and then use the Maxwell equations and the assumption that there are no proton vortices to calculate the magnetic field. The coefficient is found by considering electrons scattering off this field. For expected typical values in a neutron star core we find

$$\frac{C}{\rho_n \kappa} \approx 4 \times 10^{-4} \quad (5.5.1)$$

Because this quantity is small we find

$$\beta \approx 4 \times 10^{-4} \quad \text{and} \quad \beta' \approx \beta^2 \quad (5.5.2)$$

As a result, we will tend to neglect  $\beta'$  in many of our calculations. It should be noted that in the paper by Sedrakian and Sedrakian [70], they assume that the protons that are entrained around the vortex will contain their own array of quantised vortices. This leads to an even smaller value for  $\beta$  but a larger  $\beta'$ . We should also be aware of the possibility that the coefficients may depend upon some physics that is as yet unaccounted for. If there is a mechanism by which there is strong coupling between the vortex line and the proton fluid then we would find

$$C \rightarrow \infty, \quad \beta \rightarrow 0 \quad \beta' \rightarrow 1 \quad (5.5.3)$$

The  $\beta$  coefficient is still small, but we must take into account the inertial part of the mutual friction force.

If the protons are a type I superconductor then we find that the calculation proceeds along the lines of that for type II [68]. A type I superconductor expels magnetic flux. For a neutron star this would happen over a timescale of mega years. In the meantime the flux tubes created by the entrainment of protons to the neutron vortices will be surrounded by an area of normal protons. So each neutron vortex will be enclosed by a fluid of normal protons which is surrounded by the superconducting protons. As the normal protons mean free path is of the order of the inter-vortex spacing there will not be any significant scattering of electrons off these protons. When calculating the electron scattering, this area of protons effectively just increases the apparent vortex core size. The analysis that was applied to type II superconducting protons can then be applied with a larger vortex core.

Throughout the rest of this thesis we will assume that the protons form a type II superconductor, and use  $\beta \approx 4 \times 10^{-4}$  as a typical value. We will often use the approximation  $\beta' = 0$  as  $\beta' \ll \beta$ . We can use these coefficients to work out the coupling timescale between the proton and neutron fluids due to the mutual friction. The rate of change in constituent velocity difference can be calculated

from (4.8.22) and (4.8.23) as

$$\left(1 - \frac{2\alpha\rho}{\rho_p\rho_n}\right) \frac{\partial}{\partial t} w_i^{np} + \dots \approx \frac{\rho}{\rho_p} f_i^{mf} \quad (5.5.4)$$

or

$$\frac{\partial}{\partial t} w_i^{np} + \dots \approx -\beta\kappa n_v \frac{\rho\rho_n}{\rho_n\rho_p - 2\alpha\rho} w_i^{np} \quad (5.5.5)$$

This gives us that the coupling due to the mutual friction will act on timescales of

$$\tau_{mf} = \frac{1}{\beta\kappa n_v} \frac{\rho_n\rho_p - 2\alpha\rho}{\rho\rho_n} \quad (5.5.6)$$

We will assume that  $\beta = 4 \times 10^{-4}$  and  $\rho_p/\rho_n \approx \rho_p/\rho = 0.05$ . For small entrainment and assuming that both constituents are rotating close to the observed angular velocity, we have the relation  $\kappa n_v \approx 4\pi/P$ , where  $P$  is the period of rotation of the star. This gives

$$\tau_{mf} \approx 10P \text{ s} \quad (5.5.7)$$

Comparing this to the timescale calculated by Alpar & Sauls [4] we find that their estimate is an order of magnitude larger. In their calculation, the velocity difference between the vortex motion and the electrons is fixed. They are considering the vortex motion directly, whereas we only consider the effect that the vortices have on the two fluid constituents. Even with these differences, the main astrophysical conclusions are the same. The coupling time scale is less than the resolution of pulsar timing data. This means that mutual friction is a viable coupling mechanism in the superfluid model of the glitch phenomenon, in which the jump in rotation is not resolved.

## 5.6 Curved Vortices

The mutual friction that has been calculated so far is for a straight array of vortices. This is very restrictive on the dynamics of the flow. In this model, any variation in the neutron flow from rotation around an axis is through entrainment. The angular momentum of the neutrons will in fact be aligned throughout the system. If we want to be able to model less restricted dynamics then we need to

allow the vortices to bend. In the most general case we would want to allow the vortices to move with no modelling restrictions. That is, their motion is governed by the microscopic physics. In reality this throws up some challenges. We are trying to derive a set of macroscopic equations in terms of macroscopic quantities. If the vortices end up in a tangle in which there is significant curvature of the vortex lines on the mesoscopic level then it becomes less clear how to average the forces involved over a macroscopic fluid box. If the vortices get close enough to interact with each other then the system becomes a lot more complicated. For the moment we must restrict ourselves to a less general case. We will model a curved array in which the radius of curvature of the vortex lines is a macroscopically measurable quantity. We will also ignore vortex-vortex interaction by assuming that the inter-vortex spacing is 'large enough'. In this case we can return to the mesoscopic scale and concentrate on a single vortex line. For a straight vortex, all of the forces on the vortex are acting perpendicular to the line. For a curved vortex the flow around one part of the line can effect the flow around another part of the line. In the equations of motion for  $^4\text{He}$  we find a correction to the velocities in the mutual friction known as the self induced velocity [14] [20]. This is the correction to  $v_L$  from the surrounding vortex line. To describe the vortex we define  $s(\xi, t)_i$  as the position vector of the vortex line from an arbitrary origin (see fig 5.2), where  $\xi$  is a parameter denoting position along the vortex.

### 5.6.1 Biot-Savart

To calculate the self induced velocity on a point of the vortex we must solve for the flow created by the rest of the line. This will then tell us how the rest of the line affects a single point. The method to calculate this is the same as that used to find the magnetic field from a current in a wire. The result in electromagnetism is known as the Biot-Savart law. We have the equation

$$\epsilon_{ijk} \nabla^j p_n^k = \kappa_i \quad (5.6.1)$$



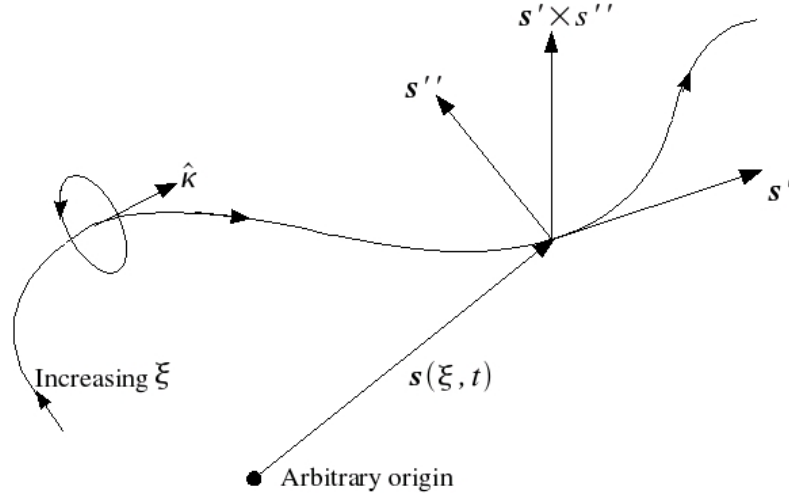


Figure 5.2: The figure shows how we parametrise the vortex. We define  $s$  as the position vector of the vortex with parameter  $\xi$  that denotes distance along the vortex from an arbitrary, but fixed, point. The tangent vector  $s' = \frac{ds}{d\xi}$  is also the direction of circulation of the vortex  $\hat{k}$ . The normal vector is defined by  $s'' = \frac{d^2s}{d^2\xi}$  and the binormal by  $s' \times s''$ .

Where  $\kappa_i$  only has support on the vortex line. As  $p_i^n$  is a vector we can assume that we can define  $A_i$  such that

$$\epsilon_{ijk} \nabla^j A^k = p_i^n \quad (5.6.2)$$

We have assumed that local to the vortex line the flow is incompressible. There is still some freedom defining  $A_i$  so we can choose that

$$\nabla^j A_j = 0 \quad (5.6.3)$$

From vector identities and (5.6.1) we find

$$\epsilon_{ijk} \nabla^j \epsilon^{klm} \nabla_l A_m = \nabla_i \nabla^j A_j - \nabla_j \nabla^j A_i = -\nabla_j \nabla^j A_i = \kappa_i \quad (5.6.4)$$

It can be noted that this is equivalent to the Poisson equation. We will solve this using a Green's function. Taking  $G$  as the solution to

$$\nabla_r^2 G(r, s) = -\delta(r - s) \quad (5.6.5)$$

where the index indicates that the operator acts on  $r$ , and integrating over a small volume  $\tau$  with surface  $\sigma$ , including the point source gives [13]

$$\int \nabla_j^r \nabla_r^j G(r, s) d\tau_r = -1 \quad (5.6.6)$$

Using Gauss law we find

$$\int \nabla_j^r G(r, s) d\sigma_r^j = -1 \quad (5.6.7)$$

We can show that (5.6.7) is satisfied if  $G$  is taken as

$$G(r, s) = \frac{1}{4\pi|r-s|} \quad (5.6.8)$$

This leads to

$$\begin{aligned} \nabla_i^r G(r, s) &= \frac{\partial|r-s|}{\partial r^i} \frac{d}{d|r-s|} \frac{1}{4\pi|r-s|} \\ &= -\frac{1}{4\pi|r-s|^2} \frac{r_i - s_i}{|r-s|} \end{aligned} \quad (5.6.9)$$

Substituting this in to (5.6.7) gives the required result as when we integrate over a sphere with center  $s$ ,  $|r-s|$  will be constant, giving

$$\int -\frac{1}{4\pi|r-s|^2} \frac{r_i - s_i}{|r-s|} d\sigma_r^j = \left( -\frac{1}{4\pi|r-s|^2} \right) (4\pi|r-s|^2) = -1 \quad (5.6.10)$$

We will use Green's theorem [13] to find

$$\begin{aligned} &\int [A_i(s) \nabla^j G(r, s) - G(r, s) \nabla^j A_i(s)] d\sigma_s^j \\ &= \int \left[ A_i(s) \underbrace{\nabla_j \nabla^j G(r, s)}_{-\delta(r-s)} - G(r, s) \underbrace{\nabla_j \nabla^j A_i(s)}_{-\kappa_i} \right] d\tau_s \end{aligned} \quad (5.6.11)$$

Integrating the delta function gives

$$A_i(r) = \int [-G(r, s)(-\kappa_i(s))] d\tau_s + \int \{G(r, s) \nabla_s^j A_i(s) - A_i(s) \nabla_s^j G(r, s)\} d\sigma_s^j \quad (5.6.12)$$

We should note here that the integral over the volume  $\tau_s$  only has support on the vortex line. The function  $\kappa$  effectively contains delta functions in the directions orthogonal to the vortex line. We should instead replace  $d\tau_s$  by  $ds$  to signify that we are integrating over the vortex line. We need to assume that the surface integral vanishes.  $G$  is inversely proportional to the distance  $(r_i - s_i)$  so as we

move the boundary of integration further from  $r_i$  then  $G \rightarrow 0$ . This assumption seems reasonable and we are left with

$$A_i(r) = \int \frac{\kappa_i}{4\pi|r-s|} ds \quad (5.6.13)$$

From (5.6.2) we get

$$p(r)_i^n = \epsilon_{ijk} \nabla_r^j \int \frac{\kappa^k}{4\pi|r-s|} ds \quad (5.6.14)$$

The variable that we are integrating over is  $s$  so the derivative  $\nabla_i^r$  can be brought inside the integral. We also note that  $\epsilon_{ijk} \nabla_r^j \kappa(s)^k = 0$  because  $\nabla_i$  is acting on  $r$ . By defining  $|R| = |r-s|$  the above equation rearranges to give

$$p_i^n = -\frac{\kappa}{4\pi} \int \frac{\epsilon_{ijk} R^j \hat{\kappa}^k}{|R|^3} ds \quad (5.6.15)$$

using

$$\nabla_i \frac{1}{(R_j R^j)^{1/2}} = -\frac{R_i}{(R_j R^j)^{3/2}} = -\frac{R_i}{|R|^3} \quad (5.6.16)$$

This is similar to the Biot-Savart law, where we have vorticity and velocity instead of current and magnetic field.

## 5.7 Induced Velocities

From (5.6.15) and assuming that there are no vortices in the proton fluid we can solve for the constituent velocities. We now want to determine the motion that this induces on the vortex line itself. We use this velocity field and take the limit as  $r_i \rightarrow s_{0i}$  where  $s_{0i}$  is a chosen point on the vortex line. This tells us how the fluid moves near the point  $s_{0i}$  due to the rest of the vortex line. This is known as the self induced velocity. To rewrite the integral form of the momentum field in a more suitable form we make the approximation that the significant contribution to the velocity field at  $s_{0i}$  will be the parts of the vortex line local to  $s_{0i}$ . This is a reasonable assumption as we have assumed that the vortex is curved on macroscopic scales and so on the mesoscopic scale the line will not curve back on itself. We can expand  $s_i$  around the point  $s_{0i}$  to give

$$s_i \approx s_{0i} + s'_{0i} \xi + \frac{1}{2} s''_{0i} \xi^2 \quad (5.7.1)$$

This gives the Taylor expansion of  $s'_i$  as

$$s'_i = \frac{\partial s_i}{\partial \xi} = s'_{0i} + s''_{0i} \xi \quad (5.7.2)$$

Rewriting the momentum field (5.6.15) in terms of  $s_i$  using  $s'_i = \hat{\kappa}_i$  gives

$$p_i^n = \frac{\kappa}{4\pi} \int \frac{\epsilon_{ijk} s'^j (r^k - s^k)}{|\mathbf{r} - \mathbf{s}|^3} ds \quad (5.7.3)$$

The Taylor expansion of the cross product in the integrand is

$$\epsilon_{ijk} (s^j - r^j) s'^k = \epsilon_{ijk} \left[ (s_0^j - r^j) + s'^j_0 \xi + \frac{1}{2} s''^j_0 \xi^2 \right] (s'^k_0 + s''^k_0 \xi) \quad (5.7.4)$$

The term  $\epsilon_{ijk} (s_0^j - r^j) s'^k_0$  will be the solution to the flow where the vortex is straight. We want to know how the flow behaves near  $s_{0i}$  and so  $(s_0^j - r^j)$  is small. This leaves

$$\epsilon_{ijk} (s^j - r^j) \hat{\kappa}^k = \underbrace{(\epsilon_{ijk} s'^j_0 s'^k_0)}_{=0} \xi + \frac{1}{2} \epsilon_{ijk} s''^j_0 s'^k_0 \xi^2 + \epsilon_{ijk} s'^j_0 s''^k_0 \xi^2 \quad (5.7.5)$$

So that

$$\epsilon_{ijk} (s^j - r^j) \hat{\kappa}^k = \frac{1}{2} \epsilon_{ijk} s'^j_0 s''^k_0 \xi^2 \quad (5.7.6)$$

Expanding the denominator of the integrand in (5.7.3) gives

$$\begin{aligned} |s - r|^3 &= \left| (s_0 - r) + s'_0 \xi + \frac{1}{2} s''_0 \xi^2 \right|^3 \\ &= |s'_0 \xi|^3 \\ &= \xi^3 \end{aligned} \quad (5.7.7)$$

where it has been used that  $|s'| = 1$  and that  $\xi$  is small. So that the notation is clearer we rewrite  $ds$  as  $d\xi$  to signify integrating along the vortex line. Substituting this in to (5.7.3) gives

$$p_i^n = \frac{\kappa}{4\pi} \int \frac{d\xi}{2\xi} \epsilon_{ijk} s'^j s''^k \quad (5.7.8)$$

We now need to decide on the limits of this integral. As the line locally has constant curvature then we will integrate as far along the vortex in each direction from  $s_{0i}$ . It makes no physical sense to integrate over the area where  $\xi < a_0$ , the vortex core size. We take the outer boundary,  $L$ , as the vortex radius of curvature. Using these integral limits we find

$$p_i^n = \frac{\kappa}{4\pi} \ln \left( \frac{L}{a_0} \right) \epsilon_{ijk} s'^j s''^k \quad (5.7.9)$$

We use this to find the induced velocities of the two fluids. Using (5.7.9) and assuming no vortices in the charged fluid we rewrite the momentum in terms of velocities to give

$$v_i^n + \varepsilon_n(v_i^p - v_i^n) = \frac{\kappa}{4\pi} \ln\left(\frac{L}{a_0}\right) \epsilon_{ijk} s'^j s''^k \quad (5.7.10)$$

$$v_i^p + \varepsilon_p(v_i^n - v_i^p) = 0 \quad (5.7.11)$$

Rearranging this gives

$$v_i^n = \frac{1 - \varepsilon_p}{1 - \varepsilon_n - \varepsilon_p} \frac{\kappa}{4\pi} \ln\left(\frac{L}{a_0}\right) \epsilon_{ijk} s'^j s''^k \quad (5.7.12)$$

$$v_i^p = \frac{-\varepsilon_p}{1 - \varepsilon_n - \varepsilon_p} \frac{\kappa}{4\pi} \ln\left(\frac{L}{a_0}\right) \epsilon_{ijk} s'^j s''^k \quad (5.7.13)$$

The difference of the velocities is

$$v_i^n - v_i^p = \frac{1}{1 - \varepsilon_n - \varepsilon_p} \frac{\kappa}{4\pi} \ln\left(\frac{L}{a_0}\right) \epsilon_{ijk} s'^j s''^k \quad (5.7.14)$$

These equations show the extra pieces that must be added to the background velocities.

## 5.8 Mutual Friction for Curved Vortices

The inclusion of curved vortices modifies the fluid motion as an addition to the flow around the vortex by

$$v_n \rightarrow v_n + v_{In} \quad (5.8.1)$$

$$v_p \rightarrow v_p + v_{Ip} \quad (5.8.2)$$

So the mutual friction for a straight vortex array (5.4.20) is modified to give

$$\begin{aligned} F_i^{MF} = & \beta \rho_n \lambda \epsilon_{ijk} s'^j \epsilon^{klm} s'_l (v_m^n - v_m^p) + \beta' \rho_n \kappa \epsilon_{ijk} s'^j (v_n^k - v_p^k) \\ & + \beta \rho_n \lambda \epsilon_{ijk} s'^j \epsilon^{klm} s'_l (v_m^{In} - v_m^{Ip}) + \beta' \rho_n \kappa \epsilon_{ijk} s'^j (v_{In}^k - v_{Ip}^k) \end{aligned} \quad (5.8.3)$$

Currently we have these induced velocities ( $v_i^{IX}$ ) in terms of  $s'_i$  and  $s''_i$ . This is not ideal as we would like to have this modification written in terms of macroscopic

quantities. We have already connected  $s'_i$  with the unit vorticity vector  $\hat{\kappa}_i$ . To write  $s''_i$  in terms of macroscopic quantities we return to the definition

$$\begin{aligned} s''_i &= \frac{\partial s'_i}{\partial \xi} \\ &= \frac{\partial x_j}{\partial \xi} \frac{\partial s'_i}{\partial x_j} = s'^j \nabla_j s'_i \end{aligned} \quad (5.8.4)$$

The right hand side comes from the fact that  $s'$  is a unit vector along the vortex. Further rearrangement gives

$$\begin{aligned} s''_i &= s'^j \nabla_j s'_i \\ &= \underbrace{s'^j \nabla_i s'_j}_0 - \epsilon_{ijk} s'^j \epsilon^{klm} \nabla_l s'_m \end{aligned} \quad (5.8.5)$$

so that

$$\begin{aligned} \epsilon_{ijk} s'^j s''^k &= -\epsilon_{ijk} s'^j \epsilon^{klm} s'_l \epsilon_{mpq} \nabla^p s'^q \\ &= \epsilon_{ipq} \nabla^p s'^q - s'^j s'_i \epsilon_{jpq} \nabla^p s'^q \end{aligned} \quad (5.8.6)$$

Note that in the mutual friction these terms are always contracted with  $\epsilon_{ijk} s'^j$  so that the second term vanishes. If we define

$$\nu = \frac{\kappa}{4\pi} \ln \left( \frac{L}{a_0} \right) \quad \text{and} \quad \tilde{\nu} = \frac{\nu}{1 - \varepsilon_n - \varepsilon_p} \quad (5.8.7)$$

One can show that

$$\begin{aligned} \beta \epsilon_{ijk} s'^j \epsilon^{klm} s'_l (v_m^{In} - v_m^{Ip}) &= \tilde{\nu} \beta \epsilon_{ijk} s'^j \epsilon^{klm} s'_l \epsilon_{mqr} \nabla^q s'^r \\ &= -\tilde{\nu} \beta \epsilon_{ijk} \nabla^j s'^k \end{aligned} \quad (5.8.8)$$

Also, by vector identities

$$\beta' \epsilon_{ijk} s'^j (v_{In}^k - v_{Ip}^k) = -\tilde{\nu} s'^j \nabla_j s'_i \quad (5.8.9)$$

Combining these results gives the modified mutual friction (5.8.3) as,

$$\begin{aligned} F_i^{MF} &= \beta \rho_n \lambda \epsilon_{ijk} \hat{\kappa}^j \epsilon^{klm} \hat{\kappa}_l (v_m^n - v_m^p) + \beta' \rho_n \lambda \epsilon_{ijk} \hat{\kappa}^j (v_n^k - v_p^k) \\ &\quad - \tilde{\nu} \beta \rho_n \lambda \epsilon_{ijk} \nabla^j \hat{\kappa}^k - \tilde{\nu} \beta' \rho_n \lambda \hat{\kappa}^j \nabla_j \hat{\kappa}_i \end{aligned} \quad (5.8.10)$$

## 5.9 Conservation of vorticity

To calculate the force density we have looked at the forces on a single vortex and multiplied this by the vortex density. We have said nothing about the stability of the array of vortices. For a simple system we expect no creation or destruction of vortex lines. They can only be destroyed when they form loops which are of the size of the vortex core. The superfluid will only create vortices if there is a driving force. For a simple case we expect conservation of vortex lines. If vorticity is conserved then the change in length of vortices per fluid element depends on the flow of vortices out of the fluid element. The total vorticity in an element  $dV$  is

$$\int_V \kappa_i n_v dV \quad (5.9.1)$$

The change in vorticity is therefore given by

$$\frac{D}{Dt} \int_V \kappa_i n_v dV = - \int \kappa_i n_v v_L^j dS_j \quad (5.9.2)$$

where the right hand side is the rate at which vortices travel through the surface of the fluid element. The fluid element is taken as fixed so that the time derivative can be brought within the volume integral. We know that the vorticity  $\omega$  is given by  $\omega_i = \kappa_i n_v$ . Using the divergence theorem,

$$\int_V \frac{\partial \omega_i}{\partial t} dV = - \int \nabla_j \omega_i v_L^j dV. \quad (5.9.3)$$

so that

$$\int_V \frac{\partial \omega_i}{\partial t} + \nabla_j \omega_i v_L^j dV = 0 \quad (5.9.4)$$

This must be true for any element  $dV$ . This means that the integrand must vanish.

$$\frac{\partial \omega_i}{\partial t} + \nabla_j (\omega_i v_L^j) = 0 \quad (5.9.5)$$

or

$$\frac{\partial \omega_i}{\partial t} + \omega_i \nabla_j v_L^j + v_L^j \nabla_j \omega_i = 0 \quad (5.9.6)$$

We expect no gradients of  $v_i^L$  in the direction of vorticity so that  $\omega^j \nabla_j v_i^L = 0$ . By vector identities we can also show that

$$\frac{1}{m} \nabla^j \epsilon_{jkl} \nabla^k p_s^l = \nabla^j \omega_j = 0 \quad (5.9.7)$$

Adding these two terms to (5.9.6) gives

$$\begin{aligned}
 0 &= \frac{\partial \omega_i}{\partial t} + \omega_i \nabla_j v_L^j + v_L^j \nabla_j \omega_i - v_i^L \nabla^j \omega_j - \omega^j \nabla^j v_i^L \\
 &= \frac{\partial \omega_i}{\partial t} + \nabla_j \omega_i v_L^j - \nabla^j \omega_j v_i^L \\
 &= \frac{\partial \omega_i}{\partial t} - \epsilon_{ijk} \nabla^j \epsilon^{klm} v_l^L \omega_m \\
 &= \epsilon_{ijk} \nabla^j \left\{ \frac{\partial}{\partial t} [v_n^k + \varepsilon_n (v_p^k - v_n^k)] - \epsilon^{klm} v_l^L \omega_m \right\} \quad (5.9.8)
 \end{aligned}$$

For this to hold it must be case that

$$\frac{\partial}{\partial t} [v_i^n + \varepsilon_n (v_i^p - v_i^n)] - \epsilon_{ijk} v_L^j \omega^k = \nabla_i \Phi \quad (5.9.9)$$

Where  $\Phi$  is any scalar potential. From the derivation of mutual friction we have seen that the Magnus force on the vortex is equal to the force due to electron scattering off the vortex (5.4.2). This gives us that

$$\rho_n \kappa \epsilon_{ijk} \hat{\kappa}^j (v_L^k - v_n^k) - \beta' \rho_n \kappa \epsilon_{ijk} \hat{\kappa}^j (v_p^k - v_n^k) - \beta \rho_n \kappa \epsilon_{ijk} \hat{\kappa}^j \epsilon^{klm} \hat{\kappa}_l (v_m^p - v_m^n) = 0 \quad (5.9.10)$$

which we can factorise to give

$$\rho_n \kappa \epsilon_{ijk} \hat{\kappa}^j \left[ (v_L^k - v_n^k) - \beta' (v_p^k - v_n^k) - \beta \epsilon^{klm} \hat{\kappa}_l (v_m^p - v_m^n) \right] = 0 \quad (5.9.11)$$

This means that

$$v_i^L = v_i^n + \beta' (v_i^p - v_i^n) + \beta \epsilon_{ijk} \hat{\kappa}^j (v_p^k - v_n^k) \quad (5.9.12)$$

Substituting this back into (5.9.9)

$$\begin{aligned}
 \frac{\partial}{\partial t} [v_i^n + \varepsilon_n (v_i^p - v_i^n)] &= \nabla_i \Phi - \epsilon_{ijk} \lambda^j v_L^k \\
 &= \nabla_i \Phi - \epsilon_{ijk} \lambda^j \left[ v_n^k + \beta' (v_p^k - v_n^k) + \beta \epsilon^{klm} \hat{\kappa}_l (v_m^p - v_m^n) \right] \quad (5.9.13)
 \end{aligned}$$

where we have used that the vorticity  $\omega_i$  has previously been written as  $\lambda_i$ . If we include the modification due to the induced velocity then we find

$$\begin{aligned}
 \frac{\partial}{\partial t} [v_i^n + \varepsilon_n (v_i^p - v_i^n)] &= \nabla_i \Phi - \epsilon_{ijk} \lambda^j (v_n^k + v_{In}^k) \\
 &\quad + \epsilon_{ijk} \kappa^j \beta' \left[ (v_n^k + v_{In}^k) - (v_p^k + v_{Ip}^k) \right] \\
 &\quad + \beta \epsilon_{ijk} \lambda^j \epsilon^{klm} \hat{\kappa}_l \left[ (v_m^n + v_m^{In}) - (v_m^p + v_m^{Ip}) \right] \quad (5.9.14)
 \end{aligned}$$



We define

$$\bar{\nu} = \frac{\nu(1 - \varepsilon_p)}{1 - \varepsilon_n - \varepsilon_p} \quad (5.9.15)$$

We expand the second term on the write hand side of (5.9.14) to get

$$\begin{aligned} -\epsilon_{ijk}\lambda^j(v_n^k + v_{In}^k) &= -\epsilon_{ijk}\lambda^j v_n^k + \bar{\nu}\lambda\hat{\kappa}^j\nabla_j\hat{\kappa}_i \\ &= \epsilon_{ijk}v_n^j\epsilon^{klm}\nabla_l[v_m^n + \varepsilon_n(v_m^p - v_m^n)] + \bar{\nu}\lambda\hat{\kappa}^j\nabla_j\hat{\kappa}_i \\ &= \nabla_i v_n^j[v_j^n + \varepsilon_n(v_j^p - v_j^n)] - [v_n^j + \varepsilon_n(v_p^j - v_n^j)]\nabla_i v_j^n \\ &\quad - v_n^j\nabla_j[v_i^n + \varepsilon_n(v_i^p - v_i^n)] + \bar{\nu}\lambda\hat{\kappa}^j\nabla_j\hat{\kappa}_i \end{aligned} \quad (5.9.16)$$

where on the right hand side the first term and first part of second term are gradients and can be absorbed into the potential term. The third term is just the transport operator that we expect on the left hand side in the equations of motion. The final term is an extra term that we have not had before. This is known as the tension and has been associated with the stability of the array [38]. This force keeps the vortex lines in the configuration which minimises the fluid internal energy. Substituting this back into (5.9.14)

$$\begin{aligned} \left(\frac{\partial}{\partial t} + v_n^j\nabla_j\right)[v_i^n + \varepsilon_n(v_i^p - v_i^n)] + \varepsilon_n(v_p^j - v_n^j)\nabla_i v_j^n \\ = \nabla_i\Phi + \bar{\nu}\lambda\hat{\kappa}^j\nabla_j\hat{\kappa}_i + \epsilon_{ijk}\lambda^j\beta'\left[(v_n^k + v_{In}^k) - (v_p^k + v_{Ip}^k)\right] \\ + \beta\epsilon_{ijk}\lambda^j\epsilon^{klm}\hat{\kappa}_l\left[(v_m^n + v_m^{In}) - (v_m^p + v_m^{Ip})\right] \end{aligned} \quad (5.9.17)$$

Combining these with the continuity equations for each constituent we have found the equations for the neutron-proton fluid that are equivalent to the HVBK equations. These equations hold as long as we have an array of vortices such that the macroscopic velocity field at a point can be described by the vortex number density and the curvature of the vortex at that point.

## 5.10 Summary

We have set up the equations of motion for a two-constituent fluid with an array of vortices. We are now in a position to investigate the consequences of the mutual friction that acts between the two constituents. We can also apply these equations

to a simple model of neutron star cores in which we are concerned with a charged fluid and a superfluid neutron fluid.

## Chapter 6

# Turbulence

Up until this point we have concentrated on arrays of superfluid vortices with a radius of curvature larger than a fluid element. That is, the structure of the vortex array can be directly matched to the velocity field on the macroscopic scale. We were able to calculate the forces involved on the macroscopic scale by multiplying the density of vortices by the force on a single vortex. If we have a tangle of vortices, or waves with a wavelength comparable to the inter-vortex spacing, this is no longer possible as not all of the vortices in a fluid box will 'act' in the same direction. The density of vortex line in a 'fluid box' is greater than that we would expect from the macroscopic velocity field. In this chapter we concentrate on the case where the tangle of vortex lines can be considered turbulent. Before looking at ways to derive the forces involved in this case we need to consider if turbulence will be relevant for neutron star modeling.

### 6.1 Conditions for turbulent flows

There have been studies of the conditions for a superfluid Helium flow to go turbulent. In Helium the mutual friction coefficients ( $\beta$  and  $\beta'$ ) can be altered by changing the temperature of the fluid, and one finds that there is some temperature at which instabilities of the vortex lines evolve into a turbulent state. Finne et. al. [23] derive a quantity which they relate to the classical fluid Reynolds num-

ber. They take the curl of the superfluid equations of motion to find an evolution equation for vorticity. Following their analysis for the neutron star case we fix the proton fluid ( $v_i^p$ ). For simplicity we also neglect the entrainment. The equations of motion will then take the form

$$\left(\frac{\partial}{\partial t} + v_n^j \nabla_j\right) v_n^k + \nabla_i(\dots) = \frac{1}{\rho_n} f_i^{mf} \quad (6.1.1)$$

It can be written as

$$\frac{\partial}{\partial t} v_i^n + \nabla_i(\dots) = \epsilon_{ijk} v_n^j \lambda_n^k + \frac{1}{\rho_n} f_i^{mf} \quad (6.1.2)$$

where for this section we take  $\lambda_i^n = \epsilon_{ijk} \nabla^j v_n^k$ . For a straight vortex array we have

$$f_i^{mf} = -\beta' \epsilon_{ijk} \lambda^j v_n^k + \beta \epsilon_{ijk} \hat{\lambda}^j \epsilon^{klm} \lambda_l v_m^n \quad (6.1.3)$$

Taking the curl of equation (6.1.2) gives

$$\frac{\partial}{\partial t} \lambda_i^n = (1 - \beta') \epsilon_{ijk} \nabla^j \left\{ \epsilon^{klm} v_l^n \lambda_m^n \right\} + \beta \epsilon_{ijk} \nabla^j \left\{ \epsilon^{klm} \hat{\lambda}_l \epsilon_{mqr} \lambda^q v_n^r \right\} \quad (6.1.4)$$

The right hand side of this equation has been written as two terms. The first is an inertial part and would act towards increasing the vorticity. The second term is dissipative and so would act to reduce the vorticity. We now define the quantity  $q$  as the ratio of the 'strengths' of these two terms

$$q = \frac{\beta}{1 - \beta'} \quad (6.1.5)$$

This is the same quantity designated  $q$  in the analysis by Finne et. al. [23]. It is suggested that it plays a similar role in quantum fluids as the Reynolds number plays in classical fluids. They suggest that when  $q > 1$  then the dissipative term will dominate and so turbulence will not develop. In particular if we consider a single vortex then Kelvin waves on a vortex will be over-damped [41]. For values  $q < 1$  the inertial term is dominant. In this situation Kelvin waves can propagate along the vortex and so instabilities can lead to turbulence [48]. For the Helium case we can compare with experiments. It is found that the onset of turbulence corresponds to  $q \approx 1.3$ . This is close enough to 1 to suggest we take this analysis seriously. For a neutron star we already have estimates of the values of  $\beta$  and  $\beta'$  as  $4 \times 10^{-4}$  and  $\beta^2$  respectively. This leads to  $q \approx 4 \times 10^{-4}$  which is a long way into the turbulent region. Though the analysis is fairly simplistic it is certainly a reason to take the possibility turbulence in neutron star cores seriously.

## 6.2 Isotropic Turbulence

Having convinced ourselves that turbulence may be an important consideration in neutron star core dynamics we need to model it. Similarly to the situation with an array of straight vortices it will be useful to calculate the force between the two fluid constituents on the macroscopic scale. We cannot approach the forces in turbulent flow in the same way as before due to the averaging problem previously discussed. As a starting case we consider a completely isotropic turbulent state. This means that the vortex lines have no preferred direction and so on the macroscopic scale the velocity field of the neutrons (neglecting entrainment) will be stationary. We will follow the analysis of both Vinen [78] and Schwarz [67]. The approaches are from slightly different view points and both are useful. Vinen tackles this problem from the macroscopic scale more directly, whereas Schwarz considers the problem from the scale of the vortex lines. We will show that the solutions are essentially equivalent.

### 6.2.1 Vinen

When deriving the macroscopic turbulent force it is important that the variables used to describe it are macroscopic. Because of this, the derivation will include more assumptions than the tangle being isotropic. The first assumption made by Vinen [78] is that the only force on the vortices is via the scattering of the normal fluid off the vortices. This ignores the effect of the Magnus force and self induced velocity on the vortex but on the average scale we would not expect any inertial terms to contribute to the force. The assumption also makes the following derivation simpler. The force per vortex line length will be given by

$$f_i^e = C w_i^{np} \quad (6.2.1)$$

This is the same force used in the derivation of the straight vortex mutual friction (5.4.1). Vinen then uses this to construct the turbulence force

$$f_i^{mf} = \frac{2L}{3} C w_i^{np} \quad (6.2.2)$$

where  $L$  is the vortex line density.  $L$  is calculated by adding up the length of vortex line in a fluid box and dividing by the volume of the box. Equation (6.2.2) is equivalent to taking the vortex line in a fluid box, extending it and calculating the force over the whole line length. There is also a geometrical factor due to the fact that the vortex is not in a straight line but in an isotropic tangle. The problem with this formulation is that the vortex line density is not a macroscopically measurable quantity. The next step in the derivation is to determine this density in terms of macroscopic quantities. To do this Vinen sets up an evolution equation for the vortex line density. He does this by considering what processes change the line length. That is, he assumes

$$\frac{dL}{dt} = \frac{dL_+}{dt} - \frac{dL_-}{dt} \quad (6.2.3)$$

where  $L_+$  and  $L_-$  designate the processes that increase and decrease the line density respectively. The increase in vortex line length will be proportional to the Magnus force acting on the vortex line. From the discussions on the derivation of the forces on straight vortices we know that the Magnus force is balanced by the dissipative force  $f_e = \beta \rho_n \kappa w_{pn}$ . Assuming that the change in line length will depend only upon  $\rho_n$ ,  $\kappa$  and  $L$  then dimensional analysis gives

$$\frac{dL_+}{dt} = \frac{\chi_1 f_e L^{3/2}}{\rho_n \kappa} \quad (6.2.4)$$

where  $\chi_1$  is a geometrical factor. At this point Vinen suggests that superfluid turbulence will be dissipated similarly to classical turbulence. e.g.

$$\frac{dL_-}{dt} = \frac{\chi_2 \kappa L^2}{2\pi} \quad (6.2.5)$$

where  $\chi_2$  is a geometrical factor. We can now construct the line density evolution equation as

$$\frac{dL}{dt} = \frac{\chi_1 f_e L^{3/2}}{\rho_n \kappa} - \frac{\chi_2 \kappa L^2}{2\pi} \quad (6.2.6)$$

We assume that fully developed turbulence will be in a stable state. This corresponds to  $\frac{\partial L}{\partial t} = 0$ . (6.2.6) now gives us an equation in terms of  $L^{1/2}$ .

$$L^{1/2} = \left( \frac{2\pi}{\kappa} \right) \left( \frac{\chi_1}{\chi_2} \right) \beta w_{np} \quad (6.2.7)$$

Finally we substitute this back into Vinen's form of the turbulent force (6.2.2) to get

$$f_i^{mf} = \frac{8\pi^2 \rho_n}{3\kappa} \left( \frac{\chi_1}{\chi_2} \right)^2 \beta^3 w_{pn}^2 w_i^{pn} \quad (6.2.8)$$

This shows that the force has a cubic relation to the velocity difference rather than the linear relation in the straight vortex case. This was first proposed by Gorter and Mellink [35] and as such is known as the Gorter-Mellink force. For isotropic turbulence Vinen takes  $\chi_1 \approx \chi_2 \approx 1$ .

### 6.2.2 Schwarz

Whereas Vinen started by assuming the form of the force on a vortex line and then calculated the vortex length, Schwarz takes the full form of the mutual friction on a single vortex [66] [67]. As we are now considering the mesoscopic scale then this is just the form of the force calculated in chapter 5 for curved vortices (5.8.10). There are still some simplifying assumptions when doing this. We are still assuming that the vortices have radius of curvature large compared to the vortex core size. The effect of vortex reconnections are not being considered. From (5.8.10) we know the force on a vortex line, per unit vortex length, is

$$f_i = \kappa \rho_n \beta [\epsilon_{ijk} s'^j \epsilon^{klm} s'_l w_m^{np} - \tilde{\nu} \epsilon_{ijk} s'^j s''^k] + \kappa \rho_n \beta' [\epsilon_{ijk} s'^j w_{np}^k - \tilde{\nu} s_i''] \quad (6.2.9)$$

Where  $s_i = s_i(\xi, t)$  is the position of the vortex line with parameter  $\xi$  that describes distance along the line from some arbitrary point on  $s_i$  (fig 5.2). Derivatives in  $\xi$  are designated by  $'$  so that  $s'_i$  is the tangent to the vortex line. The average force over a fluid element, with volume  $V$ , will be

$$\begin{aligned} f_i^{mf} &= \frac{1}{V} \int f_i d\xi \\ &= \frac{\kappa \rho_n \beta}{V} \int \left( \epsilon_{ijk} s'^j \epsilon^{klm} s'_l w_m^{np} - \tilde{\nu} \epsilon_{ijk} s'^j s''^k \right) d\xi \\ &\quad + \frac{\kappa \rho_n \beta'}{V} \int \left( \epsilon_{ijk} s'^j w_{np}^k - \tilde{\nu} s_i'' \right) d\xi \end{aligned} \quad (6.2.10)$$

We now impose that the turbulence is isotropic. Terms which have  $s'$  or it's derivative only linearly will vanish by symmetry. For this to hold we have had to assume that  $w_i^{np}$  will be a constant vector over the fluid element. Pictorially this just says

that over a fluid element the vortex line in the tangle has no preferential direction of tangent or curvature. This means that all of the  $\beta'$  terms vanish. Similarly the term with  $\epsilon_{ijk}s'^j s'^k$  will vanish over the fluid element as it is just the binormal vector which we would also expect to have no preferential direction. These simple statements are equivalent to Vinen's initial supposition that the important force on the vortices is the electron scattering (6.2.1). The force can be rewritten as

$$f_i^{mf} = \frac{\kappa\rho_n\beta'}{V} \int \epsilon_{ijk}s'^j \epsilon^{klm}s'_l w_m^{np} d\xi = \frac{\kappa\rho_n\beta'}{V} \int \left( s'^j s'_i w_j^{np} - w_i^{np} \right) d\xi \quad (6.2.11)$$

We split  $s'_i$  into a parts that are parallel and perpendicular to  $w_i^{np}$  as such,  $s'_i = s'_{\parallel i} + s'_{\perp i}$ . Then we have

$$\int \left( s'^j s'_i w_j^{np} - w_i^{np} \right) d\xi = - \int w_i^{np} (1 - s'^2_{\parallel}) d\xi + \int w_{np} s'_{\parallel} s'_{\perp i} d\xi \quad (6.2.12)$$

The second integral vanishes due to the symmetries of an isotropic tangle. We then state that the remaining

$$\int \epsilon_{ijk}s'^j \epsilon^{klm}s'_l w_m^{np} d\xi = -VLw_i^{np} I_{\parallel} \quad (6.2.13)$$

where

$$I_{\parallel} = \frac{1}{VL} \int (1 - s'^2_{\parallel}) d\xi \quad (6.2.14)$$

and we define the vortex line density explicitly as

$$L = \frac{1}{V} \int d\xi \quad (6.2.15)$$

Substituting this back into the expression for the average force on the fluid element (6.2.11)

$$f_i^{mf} = \kappa\rho_n\beta LI_{\parallel} w_i^{np} \quad (6.2.16)$$

For an isotropic tangle  $I_{\parallel} = 2/3$ . If we assume that the vortex line density will be dependent upon the magnitude of the velocity difference we can use dimensional analysis to construct

$$L = c_L^2 \left( \frac{w_{np}}{\tilde{\nu}} \right)^2 \quad (6.2.17)$$

where  $c_L$  is some dimensionless number. In making this final assumption most of the advantages gained by the clarity of the working so far have vanished. We are



back to dimensional analysis in which there are unknown constants. We can easily get Vinen's form of the turbulent force by setting

$$c_L = \frac{2\pi}{\kappa} \frac{\chi_1}{\chi_2} \beta \tilde{\nu} \quad (6.2.18)$$

The least satisfying thing about these two approaches is that at some point dimensional analysis becomes important. This makes including the dimensionless entrainment parameter in a sensible way impossible. At this point we perhaps have to accept that while investigating turbulence it makes little sense to include the effect of entrainment directly. This is slightly inconsistent as we may need the entrainment effect to have any friction at all between the two fluids. We are left in the uneasy situation of taking  $\varepsilon_X = 0$  and  $\beta \neq 0$ . Of course, this is reasonable as long as we are content to consider entrainment on the microscopic scale but neglect its macroscopic effect.

### 6.3 Digression

Having calculated the force that this idealised turbulence would contribute to the equations of motion we are in a position to consider the relevance to the neutron star model. If the effect of superfluid turbulence is negligible then we do not need to go any further in our investigations. We compare the strength of the force of turbulence with the force of a straight array of vortices by taking the ratio of their magnitudes. Remembering from chapter 5 equation (5.4.20) that the force on the constituents from a straight array of vortices is  $F_{array} = \beta \rho_n \kappa n_v w_{pn}$  then

$$\frac{F_{turb}}{F_{array}} = \frac{8\pi^2}{3n_v \kappa^2} \left( \frac{\chi_1}{\chi_2} \right)^2 \beta^2 w_{np}^2 \quad (6.3.1)$$

As we are considering a simple case we assume solid body rotation in the two constituents with some angular rotation difference. We also know that  $n_v \kappa = 2\Omega_n$  from the discussions on superfluids. It is not worth considering entrainment here as we have not included its effect in the turbulence force. We take the expected value of  $\beta$  as  $4 \times 10^{-4}$  and  $\kappa = 2 \times 10^{-4} \text{ cm}^2 \text{ s}^{-1}$ . Pulsar glitch data [55] suggests that a relative velocity difference  $\Delta\Omega/\Omega$  of  $5 \times 10^{-4}$  is attainable in a neutron star. Assuming that the geometrical constants  $\chi_1 = \chi_2 = 1$  then the ratio becomes

$$\frac{F_{turb}}{F_{array}} = 250 \left( \frac{r}{10^6 \text{ cm}} \right)^2 \left( \frac{\Delta\Omega/\Omega_n}{5 \times 10^{-4}} \right)^2 \left( \frac{P}{1 \text{ s}} \right)^{-1} \quad (6.3.2)$$

We can see that there are different regions of the star in which we would expect each arrangement of vortices to have a greater effect. Near the center of the star the straight array case will always create a larger force between the constituents. For a large enough difference in rotation, turbulence will have a greater dissipative effect at large radii.

We now consider the timescales that turbulence would be effective over. We assume that there is a situation in which the neutron constituent is in an isotropic turbulent state. In a similar way to the straight vortex array case we can calculate a characteristic time scales for the neutron and proton constituents to relax after a velocity difference is included. From before (5.5.4)

$$\frac{\partial w_i^{np}}{\partial t} \approx \left( \frac{\rho \rho_n}{\rho_n \rho_p - 2\alpha \rho} \right) f_i^{mf} \quad (6.3.3)$$

which for isotropic turbulence leads to

$$\frac{\partial w_i^{np}}{\partial t} \approx A w_{np}^3 \rightarrow w = \frac{w_0}{\sqrt{1 + A w_0^2 t}} \quad (6.3.4)$$

Where

$$A = \left( \frac{\rho \rho_n}{\rho_n \rho_p - 2\alpha \rho} \right) \frac{8\pi^2 \rho_n}{3\kappa} \left( \frac{\chi_1}{\chi_2} \right)^2 \beta^3 \quad (6.3.5)$$

This is a longer timescale than the exponential decay of the mutual friction. Defining

$$t_{linear} = \frac{1}{A w_0^2} \quad (6.3.6)$$

then in the region  $t \ll t_{linear}$  the decay of the velocity difference will be linear.

For the same typical parameters that we assumed in (6.3.2) then

$$t \approx 5 \times 10^{-3} \left( \frac{\chi_1}{\chi_2} \right)^{-2} \left( \frac{x_p}{0.05} \right) \left( \frac{P}{1 \text{ s}} \right)^2 \left( \frac{r}{10^6 \text{ cm}} \right)^{-2} \text{ s} \quad (6.3.7)$$

where  $x_p$  is the proton fraction. Near the core this has a relaxation of the order of days.

## 6.4 Polarised Turbulence

The previous sections of this chapter have dealt with completely isotropic turbulence. However, in a neutron star we would not expect this to be the case. The star will be rotating and so we would not expect that all of the neutron constituents angular momentum is shed when it goes turbulent. It is unlikely that the momentum from the superfluid could be transferred to other fluid constituents as the neutrons make up the majority of the star. We would hope to continue to benefit from work done by the superfluid Helium community. At this point we find ourselves having caught up with their progress. Very few experiments have been done on rotating turbulence, and only a few people have delved into the analysis. To make further progress we have to take a more phenomenological approach. This is not such a surprise as even for isotropic turbulence we had an element of uncertainty in the precise strength of the forces involved. Before delving into the phenomenology we will have a look at what progress has been made by the Helium community.

Currently there is only one set of experiments that investigate polarised turbulence in superfluids [75]. It was done with superfluid  $^4\text{He}$ . Throughout the description of this experiment we will use the indices  $s$  and  $n$  for the superfluid and normal fluid components, respectively. The experiment was set up as in figure 6.1. A square tube containing superfluid is heated by a resistor from below. The bulk temperature is 1.6 K. The tubes dimensions are  $1\text{cm} \times 1\text{cm} \times 40\text{cm}$ . The heater creates a flow of normal fluid along the tube which also draws superfluid down so that the mass flux of the fluid is zero. This is known as superfluid counterflow. The velocity difference between the two components is found by using

$$\rho_s v_s - \rho_n v_n = 0 \tag{6.4.1}$$

which is the previously mentioned conservation of mass flux. We also use

$$\dot{Q} = \rho T S v_n \tag{6.4.2}$$

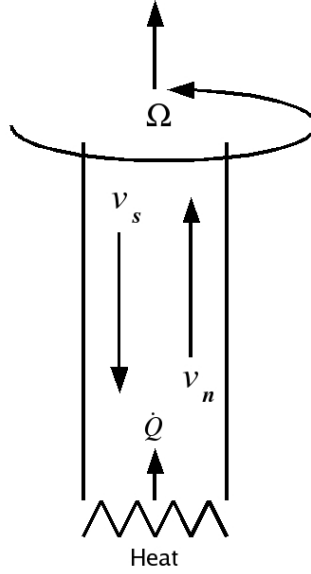


Figure 6.1: The setup of the Swanson et. al. [75] rotating counterflow experiment. A square tube filled with superfluid  $^4\text{He}$  is set into rotation with angular velocity  $\Omega$ . A heat flux  $\dot{Q}$  is applied from the heater below the tube. This induces a normal fluid flow  $v_n$  and a superfluid counterflow  $v_s$ .

Where  $\dot{Q}$  is the heat flux from the heater.  $S$  and  $T$  are the specific entropy and absolute temperature, respectively. We will also use  $V_{ns}$  to notate the constituent velocity difference for this section. This is so that the experimental data matches our notation. Combining the above equations gives

$$V_{ns} = v_n - v_s = \frac{\dot{Q}}{\rho_s T S} \quad (6.4.3)$$

The velocity difference is therefore controlled by adjusting the heat flux from the heater. The whole apparatus is placed on a rotating table. To detect the vortex line density the attenuation of second sound across the width of the tube is found. From previous discussions we know that the purely rotating superfluid will have a straight array of vortices and so the expected vortex line density relates easily to the angular velocity. The equipment can also produce a turbulent flow through the counterflow. As the velocity difference and rotation are independent we can have any combination of these two effects. The vortex line density for pure rotation is

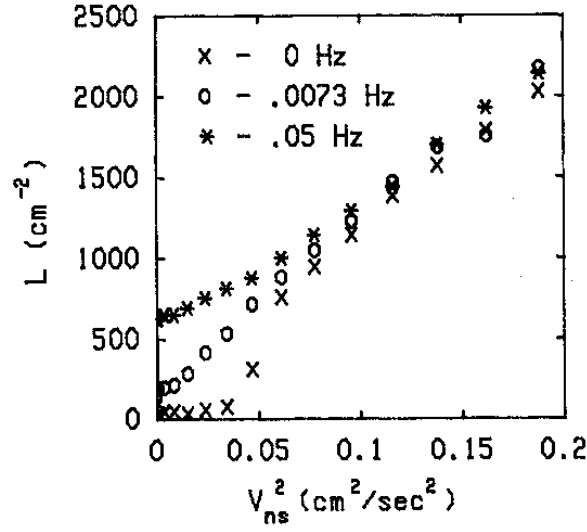


Figure 6.2: Swanson et. al. [75] results. For various fixed slow rotation rates the relation between the vortex line density and the constituent velocity difference are plotted.

given by

$$L_R = \frac{2\Omega}{\kappa} \quad (6.4.4)$$

For homogeneous turbulence the line density is

$$L_H = \gamma^2 V_{ns}^2 \quad (6.4.5)$$

Where  $\gamma$  depends upon the temperature and geometry. This relation comes from experiments, and is also the result obtained from the isotropic turbulence analysis. We shall first look at the results for slow rotation, for which the velocity difference is plotted against the vortex line density in figure 6.2. For the zero rotation case there is a sharp transition at which the density of vortex lines goes from zero to behaving like isotropic turbulence. This critical velocity seems to be non-existent as soon as rotation is introduced. The graph shows that the initial vortex line density is non-zero for the rotating superfluid as is necessary, but the plateau before the change in behaviour is not as significant as for the zero rotation case. Next we look at the results for fixed velocity difference and varying rotation (fig 6.3). The y-axis for the graph shows the vortex line density once the turbulent flow

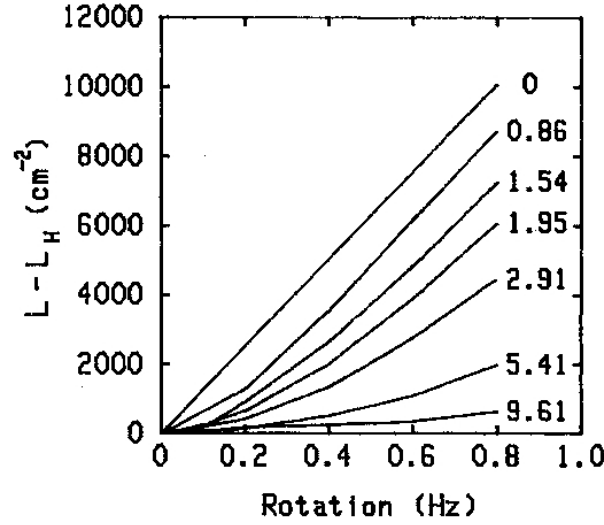


Figure 6.3: Swanson et. al. 1983 [75] results. For various fixed constituent velocity differences the relation between vortex line density and rotation is plotted. The vortex density shown is the measured density minus the expected vortex density of a turbulent flow for a particular velocity difference. The numbers to the right of the graph are  $V_{ns}^2$  in  $\text{cm}^2 \text{s}^{-2}$  calculated from the heat flux.

for the equivalent non-rotating case has been subtracted. Naively we might expect that the graph should be a set of straight lines that exactly match the density of vortex lines for pure rotation, such that

$$L = L_R + L_H \quad (6.4.6)$$

It is clear from the graph that this is not the case. The inclusion of rotation into a turbulent flow does not seem to simply add as many vortex lines as the equivalent purely rotating case would. In fact as the velocity difference gets larger, the addition of rotation seems to have less and less effect on the vortex line density. The final result comes from again comparing the vortex line density with counterflow for various rotation rates. In this case the rotation was more substantial ranging in frequency from 0.2Hz to 1Hz. By dividing the y-axis by  $L_R$  and the x-axis by  $\Omega$  all of the results overlay to give some general features (fig 6.4). From these results it seems that there are two critical velocities ( $V_{c1}$  and  $V_{c2}$ ) at which there is a change in the behaviour of the fluid. To understand what is happening we split

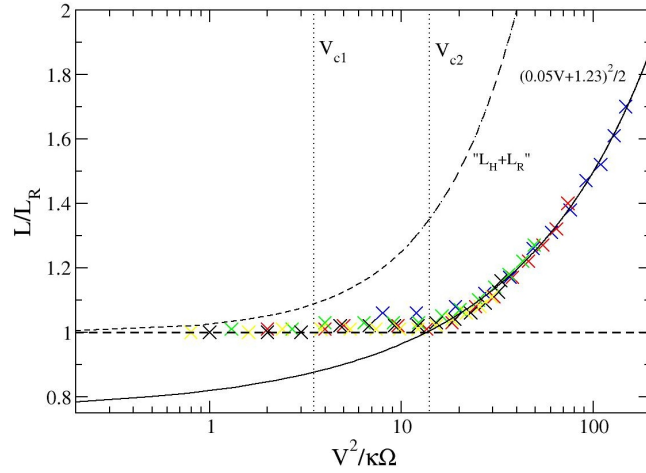


Figure 6.4: The results from Swanson et. al. [75] used to plot  $L/L_R$  vs  $V_{ns}^2/\kappa\Omega$ . Also shown are the apparent critical points at which the behaviour of the fluid changes.

the analysis into 3 regions  $V_{ns} < V_{c1}$ ,  $V_{c1} < V_{ns} < V_{c2}$  and  $V_{ns} > V_{c2}$ .

In the first region ( $V_{ns} < V_{c1}$ ) we have  $L/L_R = 1$  which means that no turbulence has developed. There is just pure rotation and so all of the vortices are in a straight array.

What then happens at the transition at  $V_{ns} = V_{c1}$ ? Swanson et. al. 1983 [75] suggest that this coincides with the onset of the Donnelly-Glaberson instability. The vortex lines themselves can oscillate by the helical Kelvin mode. At the point at which the counterflow is greater than the wave speed of the vortex line modes there is a growing instability of the oscillations [30]. Once the amplitude of the waves exceeds the inter vortex spacing the vortex lines can cross and reconnect. This produces vortex loops which themselves can reconnect with other vortex lines and we get a turbulent flow. We will discuss this instability in more detail in chapter 7 where the corresponding critical velocity difference is found for our neutron star model. For the moment we will take the result from Glaberson et. al. 1974 [30] that the critical velocity is given by

$$V_{c1} = 2\sqrt{2\nu\Omega} \quad (6.4.7)$$

Where  $\nu$  is the vortex tension. For superfluid Helium  $V_{c1}^2/\Omega\kappa \approx 3$  which we can

see from figure 6.4 matches the experiment well. More recently there have been numerical simulations of a system of straight vortices becoming unstable via the Donnelly-Glaberson instability in the presence of counterflow. The results match the experimental results well [76] [77]. Finally we need to understand why the behaviour of the fluid is different in the non-rotating case. For this instability to occur it is necessary to have vortices in the fluid initially. Therefore this instability is not relevant for the non-rotating problem. It is because of this that there is a completely different behaviour, and the critical velocity may be have to do with the counterflow needed to produce vortices on the container walls in the first place.

Now we need to look at the second region ( $V_{c1} < V_{ns} < V_{c2}$ ). Until this point the analysis was sufficient to explain the results, with the simulations acting as an extra confirmation. For this region we have to rely on the numerical results. Tsubota et. al. simulate a box of superfluid Helium containing a slightly perturbed array of vortex lines. They have a counterflow that has a velocity within this second region. The simulations then run until the turbulent state seems to be 'stable'. These simulations show that once the flow has gone turbulent the tangle of lines has some polarisation. More of the lines point along the axis of rotation. So as the rotation is increased the turbulence becomes more polarised. It is because of this that the increase in vortex density when including rotation does not correlate with the density of vortex lines for pure rotation. The turbulent flow is modified by the rotation, rather than vortex lines being added. The results shown in figure 6.3 seem to fit with this explanation.

The final thing to understand about figure 6.4 is what is happening at the critical velocity  $V_{c2}$ . We would expect that the polarised turbulence would be a reasonable picture for all higher critical velocities. Tsubota et. al. suggest that there is a change in the nature of the turbulence [77]. They suggest that there are two important timescales in the problem. The first being the decay timescale of vortex rings, and the second being the growth of Kelvin waves. In the region below  $V_{c2}$  the decay of vortex rings is the dominant timescale and so the turbulence will never fully lose its large scale structure. Above  $V_{c2}$  the dominant timescale is the growth of Kelvin waves. This leads to more reconnections and vortex rings



being created than are decaying. The flow becomes fully unstructured turbulence, though there must be some polarisation as we still have a rotating superfluid.

Unfortunately the simulations do not give us a force that we can use to model the neutron star. They were simulating directly the motion and reconnection of vortices, whereas we would like to know the macroscopic effect. When writing down a force to add to the Euler equations for the system we would like to be able to split the force into a part which comprises the usual form of the mutual friction and a part which is turbulent. The usual part would be the long range effects, the equivalent vortex array for the macroscopic velocity field of the neutrons. The turbulent part would take care of all the hidden vortex motion when considering the macroscopic scale dynamics. As seen in the Swanson et al. experiment [75] it is not as simple as adding a ratio factor, e.g.

$$\frac{dp_X}{dt} = R F_{array} + (1 - R) F_{turbulence} \quad (6.4.8)$$

The experiment suggests that the form of the turbulent force changes once rotation is included. At this point we move to the more phenomenological method. Thanks to Swanson et al. we have a useful graph of the behaviour of polarised turbulence in Helium. Jou and Mongiovi have suggested a model in this case [44] [45] [58]. As in the Vinen calculation for isotropic turbulence they start with by constructing the equation describing the change in vortex line length. They do this by introducing the two dimensionless quantities

$$\frac{W}{\kappa L^{1/2}} \quad , \quad \left( \frac{\Omega}{\kappa L} \right)^{1/2} \quad (6.4.9)$$

Where  $W$  is given by

$$W = w_{np}^j \hat{\Omega}_j \quad (6.4.10)$$

There are several reasons why the quantities are chosen in this way. Each quantity corresponds to a property that we expect to be important, the constituent velocity difference that drives the turbulence and the rotation. For a modest  $W$  we use these quantities to construct the evolution equation for the vortex line density as

$$\frac{dL}{dt} = -\gamma_1 \kappa L^2 + (\gamma_2 W + \gamma_3 \sqrt{\kappa \Omega}) L^{3/2} - \left( \gamma_4 \Omega + \gamma_5 W \sqrt{\frac{\Omega}{\kappa}} \right) L \quad (6.4.11)$$

Note that the terms involving  $\gamma_1$  and  $\gamma_2$  are exactly what we get in the Vinen analysis of isotropic turbulence. We therefore already have two of the coefficients.

$$\gamma_1 = \frac{\chi_2}{2\pi} \quad (6.4.12)$$

$$\gamma_2 = \chi_1 \beta \quad (6.4.13)$$

Solving (6.4.11) for a constant  $L$  gives

$$\begin{aligned} L^{1/2} = & \frac{\gamma_2}{2\gamma_1} \frac{W}{\kappa} + \frac{\gamma_3}{2\gamma_1} \sqrt{\frac{\Omega}{\kappa}} \\ & \pm \frac{1}{2} \sqrt{\frac{W^2}{\kappa^2} \frac{\gamma_2^2}{\gamma_1^2} + 2 \frac{W}{\kappa} \sqrt{\frac{\Omega}{\kappa}} \frac{\gamma_2}{\gamma_1} \left( \frac{\gamma_3}{\gamma_1} - 2 \frac{\gamma_5}{\gamma_2} \right) + \frac{\Omega}{\kappa} \left( \frac{\gamma_3^2}{\gamma_1^2} - 4 \frac{\gamma_4 \gamma_1}{\gamma_2^2} \right)} \end{aligned} \quad (6.4.14)$$

This can be simplified greatly by choosing,

$$\left( \frac{\gamma_3}{\gamma_1} - 2 \frac{\gamma_5}{\gamma_2} \right)^2 = \frac{\gamma_3^2}{\gamma_1^2} - 4 \frac{\gamma_4}{\gamma_1} \quad (6.4.15)$$

Equivalently

$$\frac{\gamma_4}{\gamma_1} = \frac{\gamma_5}{\gamma_2} \left( \frac{\gamma_3}{\gamma_1} - \frac{\gamma_5}{\gamma_2} \right) \quad (6.4.16)$$

which gives the two solutions

$$L^{1/2} = \frac{\gamma_5}{\gamma_2} \sqrt{\frac{\Omega}{\kappa}} \quad (6.4.17)$$

and

$$L^{1/2} = \frac{\gamma_2}{\gamma_1} \frac{W}{\kappa} + \left( \frac{\gamma_3}{\gamma_1} - \frac{\gamma_5}{\gamma_2} \right) \sqrt{\frac{\Omega}{\kappa}} = \frac{\gamma_2}{\gamma_1} \left[ \frac{W}{\kappa} + \frac{\gamma_4}{\gamma_5} \sqrt{\frac{\Omega}{\kappa}} \right] \quad (6.4.18)$$

The first of these solutions is of the form of a straight array. It is not dependent upon the velocity difference which would suggest that this is the solution to use when there is no turbulent flow. The second solution gives the vortex line length when there is a turbulent flow. We need to analyse the stability of these solutions. If they are always unstable then they are never going to describe physical states of the system. We can do this by perturbing  $L$ . Replacing  $L$  by  $L_0 + \delta L$  then (6.4.11) becomes

$$\frac{d\delta L}{dt} = \left[ -2\gamma_1 \kappa L_0 + \frac{3}{2} (\gamma_2 W + \gamma_3 \sqrt{\kappa \Omega}) L_0^{1/2} - \left( \gamma_4 \Omega + \gamma_5 W \sqrt{\frac{\Omega}{\kappa}} \right) \right] \delta L \quad (6.4.19)$$

This is stable when the factor inside the square brackets is negative. For (6.4.17) we find that

$$-2\gamma_1\kappa\frac{\gamma_5^2}{\gamma_2^2}\frac{\Omega}{\kappa} + \frac{3}{2}(\gamma_2W + \gamma_3\sqrt{\kappa\Omega})\frac{\gamma_5}{\gamma_2}\sqrt{\frac{\Omega}{\kappa}} - \left(\gamma_4\Omega + \gamma_5W\sqrt{\frac{\Omega}{\kappa}}\right) < 0 \quad (6.4.20)$$

This leads to a critical velocity difference, below which the solution (6.4.17) is stable.

$$W_c = \left(\frac{\gamma_3}{\gamma_2} - 2\frac{\gamma_4}{\gamma_5}\right)\sqrt{\kappa\Omega} \quad (6.4.21)$$

In this model the straight array will be stable until the critical velocity difference  $W_c$  is reached. This is exactly what we need our phenomenological model to do. Above  $W_c$  the second solution is stable. We now have a model in which there are two different behaviours in different regions. It therefore makes sense to choose the critical velocity such that it corresponds to the onset of turbulence from a normally rotating fluid. It is known that for Helium the onset of turbulence is due to the Donnelly-Glaberson instability. The critical velocity difference at which the instability first occurs is found to be (6.4.7). Comparing with the critical velocity in the model this leads to

$$2^{3/2}\sqrt{\frac{\nu}{\kappa}} = \left(\frac{\gamma_3}{\gamma_2} - 2\frac{\gamma_4}{\gamma_5}\right) \quad (6.4.22)$$

Below the critical velocity we would expect the behaviour to be that of a straight array of vortices. The vortex density will be given by

$$L = \frac{2\Omega}{\kappa} \quad (6.4.23)$$

Giving

$$\gamma_5 = \sqrt{2}\gamma_2 \quad (6.4.24)$$

Using (6.4.22) and (6.4.16) we get

$$\gamma_4 = \frac{\chi_2}{\pi} - 4\left(\frac{\nu}{\kappa}\right)^{1/2}\chi_1\beta \approx 2\gamma_1 \quad (6.4.25)$$

$$\gamma_3 = \sqrt{2}\left[\frac{\chi_2}{\pi} - 2\left(\frac{\nu}{\kappa}\right)^{1/2}\chi_1\beta\right] \approx 2^{3/2}\gamma_1 \quad (6.4.26)$$

since  $\beta \ll 1$ . Returning to the experimental results found by Swanson et. al. (fig 6.4) we can see that we have modeled two of the three regions. We have a region

with a straight array and a region of fully developed polarised turbulence. We have not accounted for the region  $V_{c1} < V_{ns} < V_{c2}$ . This is the region in which the dynamics are more involved and there are fewer assumptions that we can make in trying to analyse the behaviour. We must be aware that the superfluid needs to be in a fully developed turbulent state to use our model.

### 6.4.1 Applying this to Neutron Stars

Having found the length of vortex in a fluid box, how do we now extend this to derive a force that can be used in the equations of motion? We must make an educated guess. The force must account for long range effects and also the hidden details. It is this that guides us to split the vortex line length into a long range rotational effect plus a tangle. The picture shifts from the tangle having some over all direction, to the picture of a tangle added to an ordered array. This sounds suspiciously like the picture that we discarded at the beginning. However, the original picture didn't deal with the fact that the rotation modifies the form of the turbulent part of the force as well as adding a large scale rotation force. We can also think of this as splitting small segments off from the tangle that are aligned with the rotation. These segments will act as a large scale array and the rest of the tangle will be left as a dissipative force on the fluid. We split up the vortex line length as

$$L = L_R + L_T \quad (6.4.27)$$

It is straight forward to calculate  $L_R$ . On the macroscopic scale (neglecting entrainment) we have,

$$\left\langle \epsilon_{ijk} \nabla^j v_n^k \right\rangle = 2\Omega_i = n_v \kappa_i \quad (6.4.28)$$

where  $\Omega$  is the macroscopic angular velocity. Taking the magnitude of this,

$$\left| \left\langle \epsilon_{ijk} \nabla^j v_n^k \right\rangle \right| = 2\Omega_n = L_R \kappa \quad (6.4.29)$$

where  $L_R = n_v$  is the vortex line density of an array producing the observed rotation. We can now rewrite the total vortex line length in terms of  $L_R$

$$L = \frac{\gamma_2^2}{\gamma_1^2} \left[ \frac{W}{\kappa} + \frac{\gamma_4}{\gamma_5} \sqrt{\frac{L_R}{2}} \right]^2 \quad (6.4.30)$$

Expanding this and substituting in the necessary coefficients

$$L = \left( \frac{2\pi\chi_1\beta}{\chi_2} \right)^2 \left( \frac{W}{\kappa} \right)^2 + \frac{4\pi\chi_1\beta}{\chi_2} \frac{W}{\kappa} \sqrt{L_R} + L_R \quad (6.4.31)$$

The geometrical coefficient  $\chi_1$  is usually taken as 1. Assuming this to be true then we get

$$\begin{aligned} L_T &= L - L_R \\ &= 4\pi^2\beta^2 \left( \frac{W}{\kappa} \right)^2 + 4\pi\beta \frac{W}{\kappa} \sqrt{L_R} \end{aligned} \quad (6.4.32)$$

We then assume that the mutual friction force is of the form

$$\begin{aligned} F_i^{MF} &= \rho_n L_R \left\{ \beta' \epsilon_{ijk} \kappa^j w_{np}^k + \beta \epsilon_{ijk} \epsilon^{klm} \hat{\kappa}^j \kappa_l w_m^{np} \right. \\ &\quad \left. - \tilde{\nu} \left[ \beta' \hat{\kappa}^j \nabla_j \kappa_i + \beta \epsilon_{ijk} \kappa^j \hat{\kappa}^l \nabla_l \hat{\kappa}^k \right] \right\} + \frac{2L_T}{3} \rho_n \kappa \beta w_i^{pn} \end{aligned} \quad (6.4.33)$$

This represents our best guess at the form of the turbulent flow force. There have been assumptions made along the way, and the whole model is phenomenological, but it is currently the best we can do. We should note here that there has been work done on a more algebraic derivation of polarised turbulence (see [24] - [29]). The vortex tangle is treated as a third fluid and we would hope to investigate this further in the future. More experimental work is currently being done on superfluid Helium which will hopefully improve our understanding of polarised turbulence and reduce the number of ‘guesses’ involved in the modeling process [79].

## 6.5 Summary

We have shown the derivation of the forces on the fluid constituents when the neutron superfluid is turbulent. It has been argued that we should consider the possibility of turbulence seriously in neutron star cores. As neutron stars rotate we have had to extend the isotropic turbulence model to one in which the turbulence is polarised. We have obtained this force phenomenologically using results from experiments with superfluid Helium [75]. Now that we have this force we can apply

it to models of neutron star phenomena, e.g. glitches and free precession. It may be necessary to use numerical methods to simulate these phenomena, in particular, since turbulence may be localised in neutron stars. This makes analytical work on global models very tough and so a numerical approach would be more appropriate. Some work has already been done on this with isotropic turbulence [60] [61].

## Chapter 7

# Plane Waves

We now have a system of equations that describes some of the effects that may be found in the neutron star core superfluid. This allows us to investigate how the fluid properties influence motions in the fluid. We can claim only that some of the effects have been included as our discussions have been based on a comparison with He II. We have included the properties that we expect to be the most important but as we don't have direct access to a fluid of neutrons, protons and electrons at nucleonic densities we can't do much more at this point. To gain useful information from our proposed system we can look at how the fluid reacts in different situations. If an event occurs in the neutron star we would expect waves to travel through the fluid. We can model a wave traveling through the fluid as a perturbation on a background solution. This can give us an idea of how different fluid properties affect the oscillations. Solving the full equations including all the different property variables will be too difficult without using a computer. A numerical approach may seem the next natural step but this would lose the detail of how each included property of the system affects the wave. To gain some insight into this, it is useful to find the dispersion relation of a plane wave, relating the frequency of a wave to its phase speed. Throughout this chapter we will consider various dispersion relations to investigate different properties. These include rotation of the fluid, entrainment, mutual friction and vortex tension. Throughout the plane wave analysis the wave is taken as a perturbation on a simple background. To simplify the algebra the

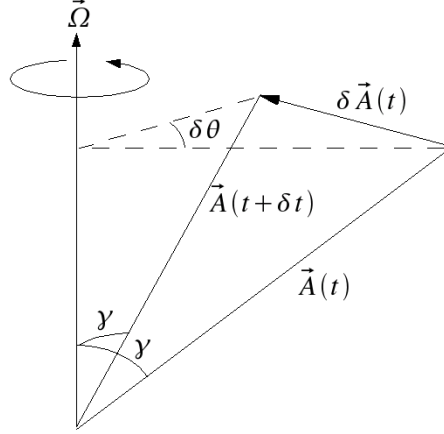


Figure 7.1: The vector  $\mathbf{A}$  is being rotated by  $\mathbf{\Omega}$ , this is shown at time  $t$  and  $t + \delta t$ .  $\mathbf{A}$  is at an angle  $\gamma$  to the axis of rotation. In time  $\delta t$  the vector has rotated by angle  $\delta\theta$ , which is a change of  $\delta\mathbf{A}$  in the vector  $\mathbf{A}$ .

equations are transformed into a rotating frame so that when rotation is included some of the hard work has already been done. The background velocities can be then be taken as zero in the rotating frame.

## 7.1 Time Derivative of a Vector

Rewriting the equations of motion in a rotating frame is a standard piece of undergraduate mathematics. We include the derivation here as a check that the entrainment does not enter into the terms that are added to our equations due to rotation. We first consider a constant vector  $\mathbf{A}$  which we rotate with angular velocity  $\mathbf{\Omega}$  (fig. 7.1). The total time derivative of this rotating vector can be found by calculating the change in the vector between times  $t$  and  $t + \delta t$ . We define  $\gamma$  as the angle between the vector  $\mathbf{A}$  and the axis of rotation. The difference in the vector between times  $t$  and  $t + \delta t$  is therefore given by

$$\mathbf{A}(t + \delta t) - \mathbf{A}(t) \equiv \delta\mathbf{A} = \mathbf{n} |\mathbf{A}| \sin(\gamma) \delta\theta + O((\delta\theta)^2) \quad (7.1.1)$$

Where  $\mathbf{n}$  is the direction of  $\delta\mathbf{A}$

$$\mathbf{n} = \frac{\mathbf{\Omega} \times \mathbf{A}}{|\mathbf{\Omega} \times \mathbf{A}|} \quad (7.1.2)$$



As  $\delta t$  tends to zero we have

$$\frac{\delta \mathbf{A}}{\delta t} = \frac{d\mathbf{A}}{dt} = |A| \sin(\gamma) \frac{d\theta}{dt} \frac{\boldsymbol{\Omega} \times \mathbf{A}}{|\boldsymbol{\Omega} \times \mathbf{A}|} \quad (7.1.3)$$

but

$$|\boldsymbol{\Omega} \times \mathbf{A}| = |\boldsymbol{\Omega}| |\mathbf{A}| \sin(\gamma) \quad (7.1.4)$$

so

$$\frac{d\mathbf{A}}{dt} = \boldsymbol{\Omega} \times \mathbf{A} \quad (7.1.5)$$

Now we take an arbitrary vector and compare it in an inertial frame and a rotating frame. Calling the vector  $\mathbf{B}$ , seen in the rotating frame as

$$\mathbf{B} = B_1 \mathbf{i} + B_2 \mathbf{j} + B_3 \mathbf{k} \quad (7.1.6)$$

According to an observer in the rotating frame we have

$$\left( \frac{d\mathbf{B}}{dt} \right)_R = \frac{dB_1}{dt} \mathbf{i} + \frac{dB_2}{dt} \mathbf{j} + \frac{dB_3}{dt} \mathbf{k} \quad (7.1.7)$$

The coordinates will not move relative to the frame. The  $R$  is to emphasis that the differentiation is with respect to the rotating frame. For an inertial observer it will no longer be the case that the coordinates of  $\mathbf{B}$  are stationary. We get

$$\left( \frac{d\mathbf{B}}{dt} \right)_I = \frac{dB_1}{dt} \mathbf{i} + \frac{dB_2}{dt} \mathbf{j} + \frac{dB_3}{dt} \mathbf{k} + B_1 \frac{d\mathbf{i}}{dt} + B_2 \frac{d\mathbf{j}}{dt} + B_3 \frac{d\mathbf{k}}{dt} \quad (7.1.8)$$

and as the coordinate vectors are of constant magnitude then we can use (7.1.5) to give

$$\left( \frac{d\mathbf{B}}{dt} \right)_I = \left( \frac{d\mathbf{B}}{dt} \right)_R + \boldsymbol{\Omega} \times \mathbf{B} \quad (7.1.9)$$

Now if  $\mathbf{B}$  is a velocity measured in the respective frames

$$\mathbf{B}_I = \mathbf{B}_R + \boldsymbol{\Omega} \times \mathbf{r} \quad (7.1.10)$$

where  $\mathbf{r}$  is measured in the rotating frame Then

$$\left( \frac{d\mathbf{B}_I}{dt} \right)_I = \left( \frac{d\mathbf{B}_R}{dt} \right)_R + 2\boldsymbol{\Omega} \times \mathbf{B}_R - \nabla \varphi \quad (7.1.11)$$

where the rotation has been taken to be uniform and the centrifugal force ( $\boldsymbol{\Omega} \times \boldsymbol{\Omega} \times \mathbf{r}$ ) has been re-written as the gradient of a potential ( $\varphi$ ). For a slowly rotating frame we can make the assumption that the centrifugal force is negligible.

## 7.2 Equations of Motion in a Slowly Rotating Frame

Throughout this section the centrifugal force is neglected. The equations of motion in an inertial frame are

$$\left(\frac{\partial}{\partial t} + v_j^X \nabla^j\right) [v_i^X + \epsilon_X (v_i^Y - v_i^X)] + \nabla_i \left(\phi + \frac{\mu_X}{m_X}\right) + \epsilon_X (v_j^Y - v_j^X) \nabla_i v_X^j = F_i^{YX} \quad (7.2.1)$$

The momentum expressed in the rotating frame is

$$m [v_i^X + \epsilon_X (v_i^Y - v_i^X)] + m \epsilon_{ijk} \Omega^j r_X^k \quad (7.2.2)$$

The first term in a rotating frame becomes

$$\left(\frac{\partial}{\partial t} + v_j^X \nabla^j\right) [v_i^X + \epsilon_X (v_i^Y - v_i^X)] + \epsilon_{ijk} \Omega^j [2v_X^k + \epsilon_X (v_Y^k - v_X^k)] - O(\Omega^2) \quad (7.2.3)$$

while the second term is given by

$$\begin{aligned} & \epsilon_X (v_Y^j - v_X^j) \nabla_i v_j^X + \epsilon_X (v_Y^j - v_X^j) \nabla_i \epsilon_{jkl} \Omega^k r^l \\ &= \epsilon_X (v_Y^j - v_X^j) \nabla_i v_j^X + \epsilon_X (v_Y^j - v_X^j) \epsilon_{jkl} \Omega^k \delta_i^l \\ &= \epsilon_X (v_Y^j - v_X^j) \nabla_i v_j^X - \epsilon_{ijk} \Omega^j \epsilon_X (v_Y^k - v_X^k) \end{aligned} \quad (7.2.4)$$

The gradient of a scalar will not change when rotated and neither will the force.

The equations of motion with a moderate frame rotation then become

$$\left(\frac{\partial}{\partial t} + v_j^X \nabla^j\right) [v_i^X + \epsilon_X (v_i^Y - v_i^X)] + 2\epsilon_{ijk} \Omega^j v_X^k + \nabla_i \left(\phi + \frac{\mu_X}{m_X}\right) + \epsilon_X (v_j^Y - v_j^X) \nabla_i v_X^j = F_i^{YX} \quad (7.2.5)$$

This shows that the entrainment does not enter the new terms. It was necessary to check this as the entrainment is a modification of the momentum and as such it would not be surprising if it entered as new force terms. On the other hand entrainment is connected to the velocity difference between the two fluid constituent velocities. Rotating the fluid does not modify this velocity difference.

## 7.3 Single Fluid

Before leaping into the analysis of waves in the two constituent case it is worth examining the simpler case of a single fluid. The main purpose is to introduce the method and observe some properties of this simple system. In this way we will have a base from which we can observe how the inclusion of a second constituent changes various properties. The equations of motion for a single fluid are

$$\left(\frac{\partial}{\partial t} + v^j \nabla_j\right) v_i + 2\epsilon_{ijk} \Omega^j v^k + \nabla_i(\tilde{\mu}) = 0 \quad (7.3.1)$$

The continuity equation is

$$\frac{\partial \rho}{\partial t} + \nabla_j(\rho v^j) = 0 \quad (7.3.2)$$

To analyse the behaviour of waves in this fluid we will assume some simple background velocity field and perturb this. To simplify things we take the background velocity field as stationary and the background density as constant (both in space and time). We also take the background chemical potential as constant. Denoting perturbations by  $\delta$  and background pieces with a subscript 0, these quantities will be rewritten as,

$$v_i \rightarrow \delta v_i \quad (7.3.3)$$

$$\rho \rightarrow \rho_0 + \delta \rho \quad (7.3.4)$$

$$\tilde{\mu} \rightarrow \tilde{\mu}_0 + \delta \tilde{\mu} \quad (7.3.5)$$

To perturb the equations we also assume that the energy  $E$  of the system is dependent only upon the density. Therefore the chemical potential is given by

$$\tilde{\mu} = \frac{dE}{d\rho} \rightarrow \delta \tilde{\mu} = \frac{d\tilde{\mu}}{d\rho} \delta \rho = \frac{c^2}{\rho} \delta \rho \quad (7.3.6)$$

where the sound speed is defined by

$$c^2 = \frac{\partial \tilde{\mu}}{\partial \rho} \rho \quad (7.3.7)$$

The perturbed equations are therefore

$$\frac{\partial \delta \rho}{\partial t} + \rho_0 \nabla_j(\delta v^j) = 0 \quad (7.3.8)$$

and

$$\frac{\partial}{\partial t} \delta v_i + 2\epsilon_{ijk} \Omega^j \delta v^k + \frac{c^2}{\rho_0} \nabla_i (\delta \rho) = 0 \quad (7.3.9)$$

We will assume that the perturbations are plane waves and so can be written as

$$\delta v_i = \bar{v}_i e^{i(\omega t - k^j x_j)} \quad (7.3.10)$$

$$\delta \rho = \bar{\rho} e^{i(\omega t - k^j x_j)} \quad (7.3.11)$$

Where  $\bar{v}_i$  is a constant vector and  $\bar{\rho}$  is a constant scalar. This assumption is useful as spatial gradients of these quantities can be replaced by  $-ik_i$  and time derivatives by  $i\omega$ . The equations of motion and continuity are therefore,

$$i\omega \bar{v}_i + 2\epsilon_{ijk} \Omega^j \bar{v}^k - ik_i c^2 \frac{\bar{\rho}}{\rho_0} = 0 \quad (7.3.12)$$

and

$$i\omega \bar{\rho} - i\rho_0 k_j \bar{v}^j = 0 \quad (7.3.13)$$

The latter rearranges to give

$$\bar{\rho} = \frac{\rho_0 k_j \bar{v}^j}{\omega} \quad (7.3.14)$$

Substituting (7.3.14) into (7.3.12) gives

$$i\omega \bar{v}_i + 2\epsilon_{ijk} \Omega^j \bar{v}^k - ik_i c^2 \frac{k_j \bar{v}^j}{\omega} = 0 \quad (7.3.15)$$

### 7.3.1 Finding the frequencies

We have now reduced the problem to one in which the only perturbed quantity in the equation is the velocity. We would like to find the relationship between the frequency and phase velocity. To continue we split the vector equation into 3 scalar equations by taking the dot product with  $k^i$ ,  $\Omega^i$  and  $\Omega_j \epsilon^{jki} k_k$ . At this point we use vector notation, where vectors are shown in bold. This is to make a connection with the two fluid calculation later on where we will define vectors where the elements are constructed from various vector products. Contracting (7.3.15) with  $k^i$

$$i(\mathbf{v} \cdot \mathbf{k}) \left( \omega - \frac{c^2 k^2}{\omega} \right) + 2[\mathbf{v} \cdot (\mathbf{k} \times \boldsymbol{\Omega})] = 0 \quad (7.3.16)$$

Contracting the perturbed equations of motion with  $\Omega^i$  gives

$$(\mathbf{v} \cdot \boldsymbol{\Omega}) = (\mathbf{k} \cdot \boldsymbol{\Omega}) \frac{c^2}{\omega^2} (\mathbf{v} \cdot \mathbf{k}) \quad (7.3.17)$$

Contracting with  $\Omega_j \epsilon^{jki} k_k$  gives

$$-i\omega(\mathbf{v} \cdot (\mathbf{k} \times \boldsymbol{\Omega})) + 2\Omega^2(\mathbf{v} \cdot \mathbf{k}) - 2(\mathbf{k} \cdot \boldsymbol{\Omega})(\mathbf{v} \cdot \boldsymbol{\Omega}) = 0 \quad (7.3.18)$$

We now define  $\theta$  as the angle between  $\mathbf{k}$  and  $\boldsymbol{\Omega}$  so that  $(\mathbf{k} \cdot \boldsymbol{\Omega}) = k\Omega \cos \theta$ . Substituting (7.3.17) into (7.3.16) and (7.3.18) we get

$$i(\mathbf{v} \cdot \mathbf{k})\left(\omega - \frac{c^2 k^2}{\omega}\right) + 2(\mathbf{v} \cdot (\mathbf{k} \times \boldsymbol{\Omega})) = 0 \quad (7.3.19)$$

and

$$-\omega(\mathbf{v} \cdot (\mathbf{k} \times \boldsymbol{\Omega})) = 2i\Omega^2(\mathbf{v} \cdot \mathbf{k}) - 2ik\Omega \cos \theta (\mathbf{k} \cdot \boldsymbol{\Omega}) \frac{c^2}{\omega^2} (\mathbf{v} \cdot \mathbf{k}) \quad (7.3.20)$$

or

$$(\mathbf{v} \cdot (\mathbf{k} \times \boldsymbol{\Omega})) = -2i \frac{\Omega^2}{\omega} (\mathbf{v} \cdot \mathbf{k}) (1 - \cos^2 \theta \frac{k^2 c^2}{\omega^2}) \quad (7.3.21)$$

Combining these gives

$$(\mathbf{v} \cdot \mathbf{k}) \left[ \left( \omega - \frac{c^2 k^2}{\omega} \right) - 4 \frac{\Omega^2}{\omega} \left( 1 - \cos^2 \theta \frac{k^2 c^2}{\omega^2} \right) \right] = 0 \quad (7.3.22)$$

This means that for waves that are not purely transverse ( $\mathbf{k} \cdot \mathbf{v} \neq 0$ ) then

$$\omega^4 - \omega^2 [c^2 k^2 + 4\Omega^2] + 4\Omega^2 \cos^2 \theta k^2 c^2 = 0 \quad (7.3.23)$$

Solving this as a quadratic in  $\omega$  gives

$$\omega^2 = \frac{c^2 k^2}{2} + 2\Omega^2 \pm \frac{1}{2} \sqrt{c^4 k^4 \left( 1 + \frac{8\Omega^2}{c^2 k^2} + \frac{16\Omega^4}{c^4 k^4} - \frac{16\Omega^2 \cos^2 \theta}{c^2 k^2} \right)} \quad (7.3.24)$$

For slow rotation to first order

$$\omega^2 = \frac{c^2 k^2}{2} + 2\Omega^2 \pm \left( \frac{c^2 k^2}{2} + 2\Omega^2 - 4\Omega^2 \cos^2 \theta \right) \quad (7.3.25)$$

This gives the solutions

$$\omega = \pm ck \pm 2 \frac{\Omega^2}{ck} \sin^2 \theta \approx \pm ck \quad (7.3.26)$$

$$\omega = \pm 2\Omega \cos \theta \quad (7.3.27)$$

These are sound waves and inertial modes respectively. Remembering that (7.3.23) only applies for a wave that is not transverse, we need to consider this situation. Taking the cross product of the perturbed equations of motion with  $\boldsymbol{\Omega}$  and then assuming that the wave is purely transverse ( $\mathbf{k} \cdot \mathbf{v} = 0$ ) leaves

$$i\omega\boldsymbol{\Omega} \times \mathbf{v} + 2\boldsymbol{\Omega} \times (\boldsymbol{\Omega} \times \mathbf{v}) = 0 \quad (7.3.28)$$

which together with (7.3.15) simply gives the dispersion relation

$$\omega = \pm 2\Omega \quad (7.3.29)$$

This is the limit of the inertial waves at  $\theta = 0$ . By contracting (7.3.15) with  $\mathbf{v}$  we can also see that

$$v^2 = 0 \quad (7.3.30)$$

So it must be true that, for a non-trivial mode that in Cartesian coordinates where the  $z$ -axis is aligned with the rotation vector, we have  $v_x = \pm i v_y$ . This represents a helical oscillation.

## 7.4 Two Fluids

At this stage we can begin the plane wave analysis for two constituents. As a first step in modeling possible situations in neutron star cores we would like to have a rotating fluid. As well as the obvious reason that neutron stars rotate, it also allows us to consistently include the effect of an array of vortices in the neutron fluid. This is only a first step so we will assume a straight array. To include rotation in the dispersion relation we use the equations of motion in a rotating frame. To find a dispersion relation it will be assumed that the fluid components are stationary in the rotating frame. On top of this simple background solution we add a plane wave perturbative term. This is a slightly simplified situation, but to keep the analysis manageable it is necessary at this point to avoid velocity differences in the background solutions of the two components. The equations of motion with

an array of straight vortices in the neutron fluid are,

$$\begin{aligned} & \left( \frac{\partial}{\partial t} + v_X^j \nabla_j \right) [v_i^X + \varepsilon_X (v_i^Y - v_i^X)] + \varepsilon_X (v_j^Y - v_j^X) \nabla_i v_X^j + \nabla_i (\psi + \tilde{\mu}_X) \\ & + 2\epsilon_{ijk} \Omega^j v_X^k = \frac{\rho_n}{\rho_X} \beta' \epsilon_{ijk} \lambda^j (v_X^k - v_Y^k) + \frac{\rho_n}{\rho_X} \beta \epsilon_{ijk} \hat{\kappa}^j \epsilon^{klm} \lambda_l (v_m^X - v_m^Y) \end{aligned} \quad (7.4.1)$$

Where

$$\lambda_i = 2\Omega_i + \epsilon_{ijk} \nabla^j [v_n^k + \varepsilon_n (v_p^k - v_n^k)] \quad (7.4.2)$$

The rotation of the frame has been denoted  $\Omega_i$ . As usual mass conservation gives

$$\frac{\partial \rho_X}{\partial t} + \nabla^j (\rho_X v_j^X) = 0 \quad (7.4.3)$$

Perturbing the background solutions according to

$$\begin{aligned} v_i^X & \rightarrow \delta v_i^X \\ \rho_X & \rightarrow \rho_{0X} + \delta \rho_X \end{aligned} \quad (7.4.4)$$

where we again denote background quantities by the index 0 and perturbations by  $\delta$ . The continuity equations therefore become

$$\frac{\partial \delta \rho_X}{\partial t} + \nabla^j (\rho_{0X} \delta v_j^X) = 0 \quad (7.4.5)$$

Using the Cowling approximation ( $\nabla_i \delta \psi = 0$ ) the perturbed equations of motion become

$$\begin{aligned} & \frac{\partial}{\partial t} (\delta v_i^X + \varepsilon_X [\delta v_i^Y - \delta v_i^X]) + \nabla_i (\delta \tilde{\mu}_X) + 2\epsilon_{ijk} \Omega^j \delta v_X^k \\ & = \frac{\rho_{0n}}{\rho_{0X}} \beta' \epsilon_{ijk} \lambda_0^j (\delta v_X^k - \delta v_Y^k) + \frac{\rho_{0n}}{\rho_{0X}} \beta \epsilon_{ijk} \hat{\kappa}^j \epsilon^{klm} \lambda_l^0 (\delta v_m^X - \delta v_m^Y) \end{aligned} \quad (7.4.6)$$

It can be seen here in the mutual friction terms that taking the background rotation as that of the frame has greatly reduced the complexity of the equation. If there was a velocity difference in the background then we would also have to perturb  $\lambda_i$ . Note that the background quantity  $\lambda_i^0 = 2\Omega_i = 2\Omega \hat{\kappa}_i$ . This is because the background velocity field has been taken as vanishing in the rotating frame. Moreover, the array of vortices is aligned with the rotation vector. We again assume that the perturbations are plane waves;

$$\delta v_i^X = \bar{v}_i^X e^{i(\omega t - x^j k_j)} \quad (7.4.7)$$

$$\delta \rho_X = \bar{\rho}_X e^{i(\omega t - x^j k_j)} \quad (7.4.8)$$

Where  $\bar{v}_i^X$  and  $\bar{\rho}_X$  are constant vectors. The continuity equation then becomes

$$0 = i\omega\bar{\rho}_X - i\rho_{0X}k_j\bar{v}_X^j \quad (7.4.9)$$

$$k_j\bar{v}_X^j = \frac{\bar{\rho}_X}{\rho_{0X}}\omega \quad (7.4.10)$$

To perturb the equations of motion we need to know how to deal with the chemical potential. We will assume that the background quantity is constant so that its derivative vanishes. For a two-constituent fluid a perturbation in the chemical potential is generally given by

$$\delta\tilde{\mu}_X = \frac{\partial\tilde{\mu}_X}{\partial\rho_X}\delta\rho_X + \frac{\partial\tilde{\mu}_X}{\partial\rho_Y}\delta\rho_Y + \frac{\partial\tilde{\mu}_X}{\partial w^2}\delta w^2 \quad (7.4.11)$$

But for our problem there is no background velocity difference between the two fluid constituents. This means that

$$\delta w^2 = 2w^j\delta w_j = 0 \quad (7.4.12)$$

So if we define  $\frac{\partial\tilde{\mu}_X}{\partial\rho_X} = \tilde{\mu}_{XX}$  and  $\frac{\partial\tilde{\mu}_X}{\partial\rho_Y} = \tilde{\mu}_{XY}$  then

$$\delta\tilde{\mu}_X = \tilde{\mu}_{XX}\delta\rho_X + \tilde{\mu}_{XY}\delta\rho_Y \quad (7.4.13)$$

The perturbed momentum equations (7.4.6) then become

$$\begin{aligned} i\omega(\bar{v}_i^X + \varepsilon_X(\bar{v}_i^Y - \bar{v}_i^X)) - ik_i(\tilde{\mu}_{XX}\bar{\rho}_X + \tilde{\mu}_{XY}\bar{\rho}_Y) + 2\epsilon_{ijk}\Omega^j\bar{v}_X^k \\ = \frac{\rho_{0n}}{\rho_{0X}}\beta'\epsilon_{ijk}\lambda_0^j(\bar{v}_X^k - \bar{v}_Y^k) + \frac{\rho_{0n}}{\rho_{0X}}\beta\epsilon_{ijk}\hat{\kappa}^j\epsilon^{klm}\lambda_l^0(\bar{v}_m^X - \bar{v}_m^Y) \end{aligned} \quad (7.4.14)$$

Rearranging this and using the perturbed continuity equation (7.4.9) gives

$$\begin{aligned} \bar{v}_m^X \left[ i\omega(1 - \varepsilon_X)\delta_i^m + \left( 2 - 2\frac{\rho_{0n}}{\rho_{0X}}\beta' \right) \epsilon_{ij}{}^m \Omega^j \right. \\ \left. - 2\frac{\rho_{0n}}{\rho_{0X}}\beta\epsilon_{ijk}\hat{\kappa}^j\epsilon^{klm}\Omega_l - ik_i\tilde{\mu}_{XX}\frac{\rho_{0X}}{\omega}k^m \right] \\ + \bar{v}_m^Y \left[ i\omega\varepsilon_X\delta_i^m + 2\frac{\rho_{0n}}{\rho_{0X}}\beta'\epsilon_{ij}{}^m\Omega^j + 2\frac{\rho_{0n}}{\rho_{0X}}\beta\epsilon_{ijk}\hat{\kappa}^j\epsilon^{klm}\Omega_l - ik_i\tilde{\mu}_{XY}\frac{\rho_{0Y}}{\omega}k^m \right] = 0 \end{aligned} \quad (7.4.15)$$



As in the single fluid analysis we separate this into three equations by contracting with three vectors. Firstly we contract with  $k^i$  giving

$$\begin{aligned} \bar{v}_m^X \left[ i\omega(1 - \varepsilon_X)k^m + \left( 2 - 2\frac{\rho_{0n}}{\rho_{0X}}\beta' \right) k^i \epsilon_{ij}{}^m \Omega^j \right. \\ \left. - 2k^i \frac{\rho_{0n}}{\rho_{0X}} \beta \epsilon_{ijk} \hat{\kappa}^j \epsilon^{klm} \Omega_l - ik^2 \tilde{\mu}_{XX} \frac{\rho_{0X}}{\omega} k^m \right] \\ + \bar{v}_m^Y \left[ i\omega \varepsilon_X k^m + 2\frac{\rho_{0n}}{\rho_{0X}} \beta' k^i \epsilon_{ij}{}^m \Omega^j + 2\frac{\rho_{0n}}{\rho_{0X}} \beta k^i \epsilon_{ijk} \hat{\kappa}^j \epsilon^{klm} \Omega_l \right. \\ \left. - ik^2 \tilde{\mu}_{XY} \frac{\rho_{0Y}}{\omega} k^m \right] = 0 \quad (7.4.16) \end{aligned}$$

Contracting with  $\Omega^i$

$$\begin{aligned} \bar{v}_m^X \left[ i\omega(1 - \varepsilon_X) \Omega^m - ik_i \Omega^i \tilde{\mu}_{XX} \frac{\rho_{0X}}{\omega} k^m \right] \\ + \bar{v}_m^Y \left[ i\omega \varepsilon_X \Omega^m - ik_i \Omega^i \tilde{\mu}_{XY} \frac{\rho_{0Y}}{\omega} k^m \right] = 0 \quad (7.4.17) \end{aligned}$$

Finally contracting with  $\Omega^j \epsilon_{jki} k^k$

$$\begin{aligned} \bar{v}_m^X \left[ i\omega(1 - \varepsilon_X) \Omega_i \epsilon^{ikm} k_k + \left( 2 - 2\frac{\rho_{0n}}{\rho_{0X}} \beta' \right) \Omega_i \epsilon^{ikl} \epsilon_{lj}{}^m k_k \Omega^j \right. \\ \left. - 2\frac{\rho_{0n}}{\rho_{0X}} \beta \Omega_i \epsilon^{iqr} \epsilon_{rjk} \epsilon^{klm} k_q \hat{\kappa}^j \Omega_l \right] \\ + \bar{v}_m^Y \left[ i\omega \varepsilon_X \Omega_i \epsilon^{ijm} k_j + 2\frac{\rho_{0n}}{\rho_{0X}} \beta' \Omega_i \epsilon^{ikl} \epsilon_{lj}{}^m k_k \Omega^j \right. \\ \left. + 2\frac{\rho_{0n}}{\rho_{0X}} \beta \Omega_i^0 \epsilon^{iqr} \epsilon_{rjk} \epsilon^{klm} k_q \hat{\kappa}^j \Omega_l \right] = 0 \quad (7.4.18) \end{aligned}$$

At this point we could push on with the analysis, but we are now working with 8 equations and it will get messy. Instead we introduce a set of vectors and matrices that take advantage of the symmetry in the equations between the two constituents. To introduce the notation we write (7.4.17) explicitly as two equations.

$$\begin{aligned} \bar{v}_m^n \left[ i\omega(1 - \varepsilon_n) \Omega^m - ik_i \Omega^i \tilde{\mu}_{nn} \frac{\rho_{0n}}{\omega} k^m \right] \\ + \bar{v}_m^p \left[ i\omega \varepsilon_n \Omega^m - ik_i \Omega^i \tilde{\mu}_{np} \frac{\rho_{0p}}{\omega} k^m \right] = 0 \quad (7.4.19) \end{aligned}$$

$$\begin{aligned} \bar{v}_m^p \left[ i\omega(1 - \varepsilon_p) \Omega^m - ik_i \Omega^i \tilde{\mu}_{pp} \frac{\rho_{0p}}{\omega} k^m \right] \\ + \bar{v}_m^n \left[ i\omega \varepsilon_p \Omega^m - ik_i \Omega^i \tilde{\mu}_{pn} \frac{\rho_{0n}}{\omega} k^m \right] = 0 \quad (7.4.20) \end{aligned}$$

We then define

$$\begin{aligned}\boldsymbol{\xi} &= \begin{pmatrix} 1 - \varepsilon_n & \varepsilon_n \\ \varepsilon_p & 1 - \varepsilon_p \end{pmatrix} & \tilde{\boldsymbol{\mu}} &= \begin{pmatrix} \tilde{\mu}_{nn}\rho_{0n} & \tilde{\mu}_{np}\rho_{0p} \\ \tilde{\mu}_{pn}\rho_{0n} & \tilde{\mu}_{pp}\rho_{0p} \end{pmatrix} \\ \mathbf{v}_\Omega &= \begin{pmatrix} \Omega^j \bar{v}_j^n \\ \Omega^j \bar{v}_j^p \end{pmatrix} & \mathbf{v}_k &= \begin{pmatrix} k^j \bar{v}_j^n \\ k^j \bar{v}_j^p \end{pmatrix}\end{aligned}\quad (7.4.21)$$

which allows us to write (7.4.17) simply as

$$\frac{\omega^2}{k_j \Omega^j} \boldsymbol{\xi} \mathbf{v}_\Omega = \tilde{\boldsymbol{\mu}} \mathbf{v}_k \quad (7.4.22)$$

As a note for future reference

$$\begin{aligned}\boldsymbol{\xi}^{-1} &= \frac{1}{\xi} \begin{pmatrix} 1 - \varepsilon_p & -\varepsilon_n \\ -\varepsilon_p & 1 - \varepsilon_n \end{pmatrix} & \xi &= \det(\boldsymbol{\xi}) = 1 - \varepsilon_n - \varepsilon_p \\ \mathbf{v}_\epsilon &= \begin{pmatrix} \Omega^i \epsilon_{ijk} k^j \bar{v}_n^k \\ \Omega^i \epsilon_{ijk} k^j \bar{v}_p^k \end{pmatrix} & \boldsymbol{\rho}_0 &= \begin{pmatrix} \rho_{0p} & -\rho_{0p} \\ -\rho_{0n} & \rho_{0n} \end{pmatrix}\end{aligned}\quad (7.4.23)$$

Here we have made the assumption that  $1 - \varepsilon_n - \varepsilon_p \neq 0$ . Writing out (7.4.16) in it's separate constituents gives

$$\begin{aligned}\bar{v}_m^n &\left[ i\omega(1 - \varepsilon_n)k^m + (2 - 2\beta') k^i \epsilon_{ij}{}^m \Omega^j \right. \\ &\quad \left. - 2k^i \beta \epsilon_{ijk} \hat{\kappa}^j \epsilon^{klm} \Omega_l - ik^2 \tilde{\mu}_{nn} \frac{\rho_{0n}}{\omega} k^m \right] \\ &+ \bar{v}_m^p \left[ i\omega \varepsilon_n k^m + 2\beta' k^i \epsilon_{ij}{}^m \Omega^j + 2\beta k^i \epsilon_{ijk} \hat{\kappa}^j \epsilon^{klm} \Omega_l - ik^2 \tilde{\mu}_{np} \frac{\rho_{0p}}{\omega} k^m \right] = 0\end{aligned}\quad (7.4.24)$$

and

$$\begin{aligned}\bar{v}_m^p &\left[ i\omega(1 - \varepsilon_p)k^m + \left( 2 - 2\frac{\rho_{0n}}{\rho_{0p}} \beta' \right) k^i \epsilon_{ij}{}^m \Omega^j \right. \\ &\quad \left. - 2k^i \frac{\rho_{0n}}{\rho_{0p}} \beta \epsilon_{ijk} \hat{\kappa}^j \epsilon^{klm} \Omega_l - ik^2 \tilde{\mu}_{pp} \frac{\rho_{0p}}{\omega} k^m \right] \\ &+ \bar{v}_m^n \left[ i\omega \varepsilon_p k^m + 2\frac{\rho_{0n}}{\rho_{0p}} \beta' k^i \epsilon_{ij}{}^m \Omega^j + 2\frac{\rho_{0n}}{\rho_{0p}} \beta k^i \epsilon_{ijk} \hat{\kappa}^j \epsilon^{klm} \Omega_l - ik^2 \tilde{\mu}_{pn} \frac{\rho_{0p}}{\omega} k^m \right] = 0\end{aligned}\quad (7.4.25)$$

These equations can be combined as

$$\left[ i\omega \boldsymbol{\xi} - i\frac{k^2}{\omega} \tilde{\boldsymbol{\mu}} + 2\frac{\beta}{\rho_{0p}} \Omega \boldsymbol{\rho}_0 \right] \mathbf{v}_k - \left[ 2\mathbf{I} - 2\frac{\beta'}{\rho_{0p}} \boldsymbol{\rho}_0 \right] \mathbf{v}_\epsilon - 2\frac{\beta}{\rho_{0p}\Omega} (k \cdot \Omega) \boldsymbol{\rho}_0 \mathbf{v}_\Omega = 0 \quad (7.4.26)$$

Writing (7.4.18) out in separate components we get

$$\begin{aligned} \bar{v}_m^n \left[ i\omega(1 - \varepsilon_n) \Omega_i \epsilon^{ikm} k_k + (2 - 2\beta') \Omega_i \epsilon^{ikl} \epsilon_{lj}^m k_k \Omega^j \right. \\ \left. - 2\beta \Omega_i \epsilon^{iqr} \epsilon_{rjk} \epsilon^{klm} k_q \hat{\kappa}^j \Omega_l \right] \\ + \bar{v}_m^p \left[ i\omega \varepsilon_n \Omega_i \epsilon^{ijm} k_j + 2\beta' \Omega_i \epsilon^{ikl} \epsilon_{lj}^m k_k \Omega^j + 2\beta \Omega_i \epsilon^{iqr} \epsilon_{rjk} \epsilon^{klm} k_q \hat{\kappa}^j \Omega_l \right] = 0 \end{aligned} \quad (7.4.27)$$

and

$$\begin{aligned} \bar{v}_m^n \left[ i\omega(1 - \varepsilon_p) \Omega_i \epsilon^{ikm} k_k + \left( 2 - 2\frac{\rho_{0n}}{\rho_{0p}} \beta' \right) \Omega_i \epsilon^{ikl} \epsilon_{lj}^m k_k \Omega^j \right. \\ \left. - 2\frac{\rho_{0n}}{\rho_{0p}} \beta \Omega_i \epsilon^{iqr} \epsilon_{rjk} \epsilon^{klm} k_q \hat{\kappa}^j \Omega_l \right] \\ + \bar{v}_m^p \left[ i\omega \varepsilon_p \Omega_i \epsilon^{ijm} k_j + 2\frac{\rho_{0n}}{\rho_{0p}} \beta' \Omega_i \epsilon^{ikl} \epsilon_{lj}^m k_k \Omega^j \right. \\ \left. + 2\frac{\rho_{0n}}{\rho_{0p}} \beta \Omega_i \epsilon^{iqr} \epsilon_{rjk} \epsilon^{klm} k_q \hat{\kappa}^j \Omega_l \right] = 0 \end{aligned} \quad (7.4.28)$$

Again writing this into matrix form gives

$$\left[ i\omega \boldsymbol{\xi} + 2\frac{\beta \Omega}{\rho_{0p}} \boldsymbol{\rho}_0 \right] \mathbf{v}_\epsilon + \left[ 2\mathbf{I} - 2\frac{\beta'}{\rho_{0p}} \boldsymbol{\rho}_0 \right] \Omega^2 \mathbf{v}_k - \left[ 2\mathbf{I} - 2\frac{\beta'}{\rho_{0p}} \boldsymbol{\rho}_0 \right] (k \cdot \Omega) \mathbf{v}_\Omega = 0 \quad (7.4.29)$$

From (7.4.22) we know that

$$\mathbf{v}_\Omega = \frac{(k \cdot \Omega)}{\omega^2} \boldsymbol{\xi}^{-1} \tilde{\boldsymbol{\mu}} \mathbf{v}_k \quad (7.4.30)$$

Substituting this into (7.4.26) and (7.4.29)

$$\left[ i\omega \boldsymbol{\xi} - i\frac{k^2}{\omega} \tilde{\boldsymbol{\mu}} + 2\frac{\beta}{\rho_{0p}} \Omega \boldsymbol{\rho}_0 \right] \mathbf{v}_k - \left[ 2\mathbf{I} - 2\frac{\beta'}{\rho_{0p}} \boldsymbol{\rho}_0 \right] \mathbf{v}_\epsilon - 2\frac{\beta}{\rho_{0p} \Omega} \boldsymbol{\rho}_0 \frac{(k \cdot \Omega)^2}{\omega^2} \boldsymbol{\xi}^{-1} \tilde{\boldsymbol{\mu}} \mathbf{v}_k \quad (7.4.31)$$

and

$$\left[ i\omega \boldsymbol{\xi} + 2\frac{\beta \Omega}{\rho_{0p}} \boldsymbol{\rho}_0 \right] \mathbf{v}_\epsilon + \left[ 2\mathbf{I} - 2\frac{\beta'}{\rho_{0p}} \boldsymbol{\rho}_0 \right] \Omega^2 \mathbf{v}_k - \left[ 2\mathbf{I} - 2\frac{\beta'}{\rho_{0p}} \boldsymbol{\rho}_0 \right] \frac{(k \cdot \Omega)^2}{\omega^2} \boldsymbol{\xi}^{-1} \tilde{\boldsymbol{\mu}} \mathbf{v}_k = 0 \quad (7.4.32)$$

These rearrange to give

$$\left[ i\omega \boldsymbol{\xi} - i\frac{k^2}{\omega} \tilde{\boldsymbol{\mu}} + 2\frac{\beta}{\rho_{0p} \Omega} \boldsymbol{\rho}_0 \left( \Omega^2 - \frac{(k \cdot \Omega)^2}{\omega^2} \boldsymbol{\xi}^{-1} \tilde{\boldsymbol{\mu}} \right) \right] \mathbf{v}_k - \left[ 2\mathbf{I} - 2\frac{\beta'}{\rho_{0p}} \boldsymbol{\rho}_0 \right] \mathbf{v}_\epsilon = 0 \quad (7.4.33)$$

and

$$\left[ i\omega \boldsymbol{\xi} + 2\frac{\beta \Omega}{\rho_{0p}} \boldsymbol{\rho}_0 \right] \mathbf{v}_\epsilon = - \left[ (2\mathbf{I} - 2\frac{\beta'}{\rho_{0p}} \boldsymbol{\rho}_0) \left( \Omega^2 - \frac{(k \cdot \Omega)^2}{\omega^2} \boldsymbol{\xi}^{-1} \tilde{\boldsymbol{\mu}} \right) \right] \mathbf{v}_k \quad (7.4.34)$$

Note that up to this point the only assumption in the algebra is that  $1 - \varepsilon_n - \varepsilon_p \neq 0$ .

The matrix from the left hand side of equation (7.4.34) has determinant

$$\begin{aligned} \det \left( i\omega \boldsymbol{\xi} + 2 \frac{\beta \Omega}{\rho_{0p}} \boldsymbol{\rho}_0 \right) &= [i\omega(1 - \varepsilon_n) + 2\beta\Omega] \left[ i\omega(1 - \varepsilon_p) + 2 \frac{\rho_{0n}}{\rho_{0p}} \beta \Omega \right] \\ &\quad - [i\omega\varepsilon_n - 2\beta\Omega] \left[ i\omega\varepsilon_p - 2 \frac{\rho_{0n}}{\rho_{0p}} \beta \Omega \right] \\ &= -\omega^2(1 - \varepsilon_n - \varepsilon_p) + i2\omega\Omega\beta \left( 1 + \frac{\rho_{0n}}{\rho_{0p}} \right) \end{aligned} \quad (7.4.35)$$

This means that the inverse of the matrix is

$$-\frac{1}{\omega^2\xi - i2\omega\Omega\beta \left( 1 + \frac{\rho_{0n}}{\rho_{0p}} \right)} \begin{pmatrix} i\omega(1 - \varepsilon_p) + 2 \frac{\rho_{0n}}{\rho_{0p}} \beta \Omega & -i\omega\varepsilon_n + 2\beta\Omega \\ -i\omega\varepsilon_p + 2 \frac{\rho_{0n}}{\rho_{0p}} \beta \Omega & i\omega(1 - \varepsilon_n) + 2\beta\Omega \end{pmatrix} \quad (7.4.36)$$

To continue working with this notation we define

$$\boldsymbol{\rho}_0^{zero} = \begin{pmatrix} \rho_{0n} & \rho_{0p} \\ \rho_{0n} & \rho_{0p} \end{pmatrix} \quad (7.4.37)$$

Noting that  $\boldsymbol{\rho}_0 \boldsymbol{\rho}_0^{zero} = \mathbf{0}$  then (7.4.34) can be rewritten as

$$\mathbf{v}_\epsilon = \frac{i\omega\xi\boldsymbol{\xi}^{-1} + 2 \frac{\beta\Omega}{\rho_{0p}} \boldsymbol{\rho}_0^{zero}}{\omega^2\xi - i2\omega\Omega\beta \left( 1 + \frac{\rho_{0n}}{\rho_{0p}} \right)} \left[ \left( 2\mathbf{I} - 2 \frac{\beta'}{\rho_{0p}} \boldsymbol{\rho}_0 \right) \left( \Omega^2 - \frac{(k \cdot \Omega)^2}{\omega^2} \boldsymbol{\xi}^{-1} \tilde{\boldsymbol{\mu}} \right) \right] \mathbf{v}_k \quad (7.4.38)$$

Substituting into (7.4.33) gives

$$\begin{aligned} &\left[ i\omega\boldsymbol{\xi} - i \frac{k^2}{\omega} \tilde{\boldsymbol{\mu}} + 2 \frac{\beta}{\rho_{0p}\Omega} \boldsymbol{\rho}_0 \left( \Omega^2 - \frac{(k \cdot \Omega)^2}{\omega^2} \boldsymbol{\xi}^{-1} \tilde{\boldsymbol{\mu}} \right) \right] \mathbf{v}_k \\ &- \left( 2\mathbf{I} - 2 \frac{\beta'}{\rho_{0p}} \boldsymbol{\rho}_0 \right) \frac{i\omega\xi\boldsymbol{\xi}^{-1} + 2 \frac{\beta\Omega}{\rho_{0p}} \boldsymbol{\rho}_0^{zero}}{\omega^2\xi - i2\omega\Omega\beta \left( 1 + \frac{\rho_{0n}}{\rho_{0p}} \right)} \\ &\quad \left[ \left( 2\mathbf{I} - 2 \frac{\beta'}{\rho_{0p}} \boldsymbol{\rho}_0 \right) \left( \Omega^2 - \frac{(k \cdot \Omega)^2}{\omega^2} \boldsymbol{\xi}^{-1} \tilde{\boldsymbol{\mu}} \right) \right] \mathbf{v}_k = 0 \end{aligned} \quad (7.4.39)$$

This expands to give

$$\begin{aligned}
 \mathbf{v}_k \left\{ i\omega \boldsymbol{\xi} - i \frac{k^2}{\omega} \tilde{\boldsymbol{\mu}} + 2 \frac{\beta}{\rho_{0p} \Omega} \boldsymbol{\rho}_0 \left( \Omega^2 - \frac{(k \cdot \Omega)^2}{\omega^2} \boldsymbol{\xi}^{-1} \tilde{\boldsymbol{\mu}} \right) - \frac{\Omega^2}{\omega^2 \boldsymbol{\xi} - i 2 \omega \Omega \beta \left( 1 + \frac{\rho_{0n}}{\rho_{0p}} \right)} \right. \\
 \left. \left\langle 4i\omega \boldsymbol{\xi} \boldsymbol{\xi}^{-1} - 4i\omega \boldsymbol{\xi} \frac{\beta'}{\rho_{0p}} [\boldsymbol{\rho}_0 \boldsymbol{\xi}^{-1} + \boldsymbol{\xi}^{-1} \boldsymbol{\rho}_0] + i 4 \omega \boldsymbol{\xi} \left( \frac{\beta'}{\rho_{0p}} \right)^2 \boldsymbol{\rho}_0 \boldsymbol{\xi}^{-1} \boldsymbol{\rho}_0 + 8 \frac{\beta \Omega}{\rho_{0p}} \boldsymbol{\rho}_0^{zero} \right. \right. \\
 \left. \left. - \frac{(k \cdot \Omega)^2}{\omega^2 \Omega^2} \left[ 4i\omega \boldsymbol{\xi}^{-1} \boldsymbol{\xi}^{-1} \tilde{\boldsymbol{\mu}} - 4i\omega \frac{\beta'}{\rho_{0p}} (\boldsymbol{\rho}_0 \boldsymbol{\xi}^{-1} + \boldsymbol{\xi}^{-1} \boldsymbol{\rho}_0) \boldsymbol{\xi}^{-1} \tilde{\boldsymbol{\mu}} \right. \right. \right. \\
 \left. \left. \left. + i 4 \omega \left( \frac{\beta'}{\rho_{0p}} \right)^2 \boldsymbol{\rho}_0 \boldsymbol{\xi}^{-1} \boldsymbol{\rho}_0 \boldsymbol{\xi}^{-1} \tilde{\boldsymbol{\mu}} + 8 \frac{\beta \Omega}{\rho_{0p} \boldsymbol{\xi}} \boldsymbol{\rho}_0^{zero} \boldsymbol{\xi}^{-1} \tilde{\boldsymbol{\mu}} \right] \right\rangle \right\} = 0 \quad (7.4.40)
 \end{aligned}$$

For  $\mathbf{v}_k \neq 0$  the determinant of the matrix part of the above must vanish. This leads to waves which are not transverse. As an aside, if we consider the transverse case ( $\mathbf{v}_k = 0$ ) then we can see from (7.4.33) and (7.4.34) that these two conditions must be satisfied unless either the wave direction vector or oscillation vectors are aligned with the rotation,

$$\begin{aligned}
 \det \left( i\omega \boldsymbol{\xi} + 2 \frac{\beta \Omega}{\rho_{0p}} \boldsymbol{\rho}_0 \right) &= 0 \\
 \det \left( 2\mathbf{I} - 2 \frac{\beta'}{\rho_{0p}} \boldsymbol{\rho}_0 \right) &= 0 \quad (7.4.41)
 \end{aligned}$$

That is, we would have to demand that

$$\begin{aligned}
 0 &= \omega^2 (1 - \varepsilon_n - \varepsilon_p) - i 2 \omega \Omega \beta \left( 1 + \frac{\rho_{0n}}{\rho_{0p}} \right) \\
 0 &= 4 - 4\beta' \left( 1 + \frac{\rho_{0n}}{\rho_{0p}} \right) \quad (7.4.42)
 \end{aligned}$$

The second condition is very restrictive and so a purely transverse wave in which  $k_i$  and  $\Omega_i$  are not parallel seems unlikely. In the single fluid problem we found a dispersion relation for the parallel case. The calculation for two constituents is more complicated. Later on we shall look at a similar case but with no perturbation of the proton fluid and  $\beta$  taken as small.

## 7.5 Solutions

The equation that we now have to solve represents a very general case that includes a lot of different properties of our two fluid system. It is useful to consider some

simple situations to get a feel for how each fluid property included in the model affects the waves.

### 7.5.1 No rotation, coupling, or friction

We start with the simplest case with the two fluids completely decoupled. This is equivalent to saying that the equation of state is given by

$$E = f(n_n) + g(n_p) \quad (7.5.1)$$

The equation that gives the dispersion relation when  $\Omega = \beta = \beta' = \varepsilon_X = \tilde{\mu}_{XY} = 0$  is

$$\left| i\omega \mathbf{I} - i \frac{k^2}{\omega} \tilde{\boldsymbol{\mu}} \right| = 0 \quad (7.5.2)$$

This expands to give

$$\omega^2 \left( 1 - \frac{k^2}{\omega^2} \tilde{\mu}_{nn} \rho_{0n} \right) \left( 1 - \frac{k^2}{\omega^2} \tilde{\mu}_{pp} \rho_{0p} \right) = 0 \quad (7.5.3)$$

which gives solutions as

$$\omega^2 = k^2 \tilde{\mu}_{nn} \rho_{0n} \quad \omega^2 = k^2 \tilde{\mu}_{pp} \rho_{0p} \quad (7.5.4)$$

Defining the sound speed of each fluid by  $c_X^2 = \tilde{\mu}_{XX} \rho_{0X}$  these become

$$\begin{aligned} \omega &= \pm k c_n \\ \omega &= \pm k c_p \end{aligned} \quad (7.5.5)$$

These can be associated with the neutron and proton longitudinal sound waves respectively. There is no interaction between the two fluids as there is no coupling mechanism included.

### 7.5.2 Entrainment

At this point we can begin to investigate how various parameters modify these modes. Including entrainment allows the equation of state to depend on relative velocities. We denote the relative velocity of the two constituents by  $w_{np}$  and take

$$E = f(n_n) + g(n_p) + h(w_{np}^2) \quad (7.5.6)$$

The assumption that we can separate the velocity difference and the densities in the energy is equivalent to Taylor expanding for small  $w_i^{np}$ . In this case we take  $\Omega = \beta = \beta' = \tilde{\mu}_{XY} = 0$ , and obtain the equation,

$$\left| i\omega \boldsymbol{\xi} - i \frac{k^2}{\omega} \tilde{\boldsymbol{\mu}} \right| = 0 \quad (7.5.7)$$

We expand this to get

$$\omega^2 \left[ \left( 1 - \varepsilon_n - \frac{k^2}{\omega^2} c_n^2 \right) \left( 1 - \varepsilon_p - \frac{k^2}{\omega^2} \tilde{\mu}_{pp} \rho_{0p} \right) - \varepsilon_n \varepsilon_p \right] = 0 \quad (7.5.8)$$

Solving for  $\omega^2$  gives

$$\begin{aligned} \omega^2 = \frac{1}{2\xi} & \left[ (1 - \varepsilon_n) k^2 c_p^2 + (1 - \varepsilon_p) k^2 c_n^2 \right] \\ & \pm \frac{k^2}{2\xi} \left\{ \left[ (1 - \varepsilon_n) c_p^2 + (1 - \varepsilon_p) c_n^2 \right]^2 - 4\xi c_n^2 c_p^2 \right\}^{1/2} \end{aligned} \quad (7.5.9)$$

To make further progress it is useful to assume that the entrainment is a small effect and use Taylor expansions on  $\varepsilon_X$ . From (7.5.8) we can see that the frequencies then are

$$\omega = \pm \left( 1 + \frac{1}{2} \varepsilon_n \right) k c_n \quad (7.5.10)$$

$$\omega = \pm \left( 1 + \frac{1}{2} \varepsilon_p \right) k c_p \quad (7.5.11)$$

(7.5.10) and (7.5.11) are sound waves with a correction due to entrainment. Even though entrainment is a coupling between the constituents there appears to be no interaction between the two fluids wave speeds. These effects are of higher order in the entrainment parameter.

### 7.5.3 Chemical coupling

For completeness we consider the effect that “chemical coupling” has on the frequency. The equation of state for this situation is of the form

$$E = f(n_n, n_p) \quad (7.5.12)$$

This allows the chemical potential of one fluid to be affected by the population density of the other constituent. This gives

$$\left| \omega \mathbf{I} - \frac{k^2}{\omega} \tilde{\boldsymbol{\mu}} \right| = 0 \quad (7.5.13)$$

which expands to give

$$\omega^4 - \omega^2 [k^2 (c_n^2 + c_p^2)] + k^4 \left( c_n^2 c_p^2 - \frac{\rho_{0p}}{\rho_{0n}} C^2 \right) \quad (7.5.14)$$

where  $C = \mu_{XY} \rho_{0n} = \mu_{YX} \rho_{0n}$ . Solving this quadratic for  $\omega^2$ , taking  $C^2$  as small, gives the dispersion relation as either

$$\omega = \pm \left( k c_n + \frac{\rho_{0p}}{2\rho_{0n}} k \frac{C^2}{c_n(c_n^2 - c_p^2)} \right) \quad (7.5.15)$$

or

$$\omega = \pm \left( k c_p + \frac{\rho_{0p}}{2\rho_{0n}} k \frac{C^2}{c_p(c_p^2 - c_n^2)} \right) \quad (7.5.16)$$

These are still modified sound waves in each constituent.

#### 7.5.4 Slow rotation

We now move on to the case of slow rotation. As well as finding the appropriate modes associated with rotation, this is done in order to later be able to include mutual frictional effects. To first order mutual friction will affect waves when the background rotation is non-zero. For the moment we take the mutual friction coefficients as zero. To keep the problem tractable, we will be taking zero coupling in the equation of state. That is

$$E = f(n_n) + g(n_p) \quad (7.5.17)$$

Taking  $\beta = \beta' = \varepsilon_X = \tilde{\mu}_{XY} = 0$  the equation to solve is

$$\left| i\omega \mathbf{I} - i \frac{k^2}{\omega} \tilde{\boldsymbol{\mu}} - \frac{\Omega^2}{\omega^2} \left( 4i\omega \mathbf{I} - 4i \frac{k^2}{\omega} \cos^2 \theta \tilde{\boldsymbol{\mu}} \right) \right| = 0 \quad (7.5.18)$$

Defining  $\theta$  as the angle between  $k_i$  and  $\Omega_i$  such that  $k^j \Omega_j = k\Omega \cos \theta$ , this expands to give

$$\left( \omega - \frac{k^2}{\omega} c_n^2 - \frac{4\Omega^2}{\omega} + 4 \frac{\Omega^2 k^2}{\omega^3} \cos^2 \theta c_n^2 \right) \left( \omega - \frac{k^2}{\omega} c_p^2 - \frac{4\Omega^2}{\omega} + 4 \frac{\Omega^2 k^2}{\omega^3} \cos^2 \theta c_p^2 \right) = 0 \quad (7.5.19)$$

The solutions can thus be found from either

$$0 = \omega^4 - \omega^2 [k^2 c_n^2 + 4\Omega^2] + 4\Omega^2 k^2 \cos^2 \theta c_n^2 \quad (7.5.20)$$

$$0 = \omega^4 - \omega^2 [k^2 c_p^2 + 4\Omega^2] + 4\Omega^2 k^2 \cos^2 \theta c_p^2 \quad (7.5.21)$$



These are both quadratics in  $\omega^2$ . Solving these and using the assumption of slow rotation ( $\Omega \ll kc_X$ ) the dispersion relations are

$$\omega = \pm (kc_n + 2\Omega^2 \sin^2 \theta) \quad (7.5.22)$$

$$\omega = \pm 2\Omega \cos \theta \quad (7.5.23)$$

and

$$\omega = \pm (kc_p + 2\Omega^2 \sin^2 \theta) \quad (7.5.24)$$

$$\omega = \pm 2\Omega \cos \theta \quad (7.5.25)$$

(7.5.23) and (7.5.25) are inertial modes which were trivial in the previous calculations. These solutions appear degenerate because the background rotations of the two constituents is the same. If higher powers of  $\Omega$  are included then these two solutions are no longer degenerate. The frequencies found in (7.5.22) and (7.5.24) are the sound waves with a correction due to rotation. All of these solutions are exactly what we expect from comparing with the single fluid case.

### 7.5.5 Mutual friction with slow rotation

Up until now there have not been any dissipative mechanisms included so that the waves were not damped. By including mutual friction in the calculation we should gain some insight into how oscillations inside a neutron star are damped. Due to the complicated nature of the system of equations we would like to simplify the problem as much as possible. We will therefore take the chemical coupling and entrainment as negligible ( $\varepsilon_X = \tilde{\mu}_{XY} = 0$ ). In principle it is not quite consistent to ignore the entrainment as it is necessary for the interaction between the two constituents that leads to the mutual friction force. We are, however, concerned here with the dissipative effects of mutual friction, which the explicitly written entrainment term in the equations should not effect too much. We are forced to set a non-zero rotation as it directly relates to how mutual friction affects the fluid. It is by the neutron fluid rotating that we have vortices in the fluid by which we get the force between the constituents. Carrying on from the previous section we take  $\Omega$  as small. It is also sensible to take  $\beta$  as small as we have seen previously that we

might expect  $\beta \ll 1$ . As  $\beta' \approx \beta^2$  we will neglect  $\beta'$ . To find the dispersion relation we will use the solution found for slow rotation and assume that the addition of mutual friction into the problem will be a small correction to the frequency. So we replace the frequency  $\omega$  by  $\omega_0 + \delta\omega$ .  $\omega_0$  is the frequency when  $\beta = 0$  and  $\delta\omega$  is the correction. The equation to solve is

$$\left| i\omega \mathbf{I} - \frac{ik^2}{\omega} \tilde{\boldsymbol{\mu}} + \frac{2\beta}{\rho_{0p}\Omega} \boldsymbol{\rho}_0 \left( \Omega^2 \mathbf{I} - \frac{(k \cdot \Omega)^2}{\omega^2} \tilde{\boldsymbol{\mu}} \right) - \frac{\Omega^2}{\omega^2 - i2\omega\Omega\beta \left( 1 + \frac{\rho_{0p}}{\rho_{0n}} \right)} \left[ i4\omega \mathbf{I} + 8\frac{\beta\Omega}{\rho_{0p}} \boldsymbol{\rho}_0^{zero} - \frac{(k \cdot \Omega)^2}{\omega^2\Omega^2} \left( i4\omega \tilde{\boldsymbol{\mu}} + 8\frac{\beta\Omega}{\rho_{0p}} \boldsymbol{\rho}_0^{zero} \tilde{\boldsymbol{\mu}} \right) \right] \right| = 0 \quad (7.5.26)$$

Before choosing the form of  $\omega$  it is useful to take  $\beta$  as small so that,

$$\frac{\Omega^2}{\omega^2 - i2\omega\Omega\beta \left( 1 + \frac{\rho_{0n}}{\rho_{0p}} \right)} = \frac{\Omega^2}{\omega^2} \left[ 1 + i\frac{2\Omega\beta}{\omega} \left( 1 + \frac{\rho_{0n}}{\rho_{0p}} \right) \right] \quad (7.5.27)$$

At this point we rewrite (7.5.26) with the assumed form of  $\omega$ .

$$\left| i\omega_0 \left( 1 + \frac{\delta\omega}{\omega_0} \right) \mathbf{I} - \frac{ik^2}{\omega_0} \left( 1 - \frac{\delta\omega}{\omega_0} \right) \tilde{\boldsymbol{\mu}} + \frac{2\beta}{\rho_{0p}\Omega} \boldsymbol{\rho}_0 \left[ \Omega^2 \mathbf{I} - \frac{(k \cdot \Omega)^2}{\omega_0^2} \left( 1 - 2\frac{\delta\omega}{\omega_0} \right) \tilde{\boldsymbol{\mu}} \right] - \frac{\Omega^2}{\omega_0^2} \left[ 1 - 2\frac{\delta\omega}{\omega_0} + i\frac{2\Omega\beta}{\omega_0} \left( 1 + \frac{\rho_{0n}}{\rho_{0p}} \right) \right] \left\{ i4\omega_0 \left( 1 + \frac{\delta\omega}{\omega_0} \right) \mathbf{I} + 8\frac{\beta\Omega}{\rho_{0p}} \boldsymbol{\rho}_0^{zero} - \frac{(k \cdot \Omega)^2}{\omega_0^2\Omega^2} \left( 1 - 2\frac{\delta\omega}{\omega_0} \right) \left[ i4\omega_0 \left( 1 + \frac{\delta\omega}{\omega_0} \right) \tilde{\boldsymbol{\mu}} + 8\frac{\beta\Omega}{\rho_{0p}} \boldsymbol{\rho}_0^{zero} \tilde{\boldsymbol{\mu}} \right] \right\} \right| = 0 \quad (7.5.28)$$

This can be written in the form

$$\left| \begin{pmatrix} a & \beta b \\ \beta c & d \end{pmatrix} \right| = 0 \quad (7.5.29)$$

As  $\beta$  is small then solutions are found from either  $a = 0$  or  $d = 0$ . This means that we need to solve either

$$\begin{aligned} & i\omega_0 \left( 1 + \frac{\delta\omega}{\omega_0} \right) - \frac{ik^2}{\omega_0} \left( 1 - \frac{\delta\omega}{\omega_0} \right) c_n^2 + \frac{2\beta}{\Omega} \left( \Omega^2 - \frac{(k \cdot \Omega)^2}{\omega_0^2} c_n^2 \right) \\ & - \frac{\Omega^2}{\omega_0^2} \left[ 1 - 2\frac{\delta\omega}{\omega_0} + i\frac{2\Omega\beta}{\omega_0} \left( 1 + \frac{\rho_{0n}}{\rho_{0p}} \right) \right] \left\{ i4\omega_0 \left( 1 + \frac{\delta\omega}{\omega_0} \right) + 8\frac{\beta\Omega}{\rho_{0p}} \rho_{0n} \right. \\ & \quad \left. - \frac{(k \cdot \Omega)^2}{\omega_0^2\Omega^2} \left( 1 - 2\frac{\delta\omega}{\omega_0} \right) \left[ i4\omega_0 \left( 1 + \frac{\delta\omega}{\omega_0} \right) c_n^2 + 8\frac{\beta\Omega}{\rho_{0p}} \rho_{0n} c_n^2 \right] \right\} = 0 \end{aligned} \quad (7.5.30)$$

or

$$\begin{aligned}
 & i\omega_0 \left(1 + \frac{\delta\omega}{\omega_0}\right) - \frac{ik^2}{\omega_0} \left(1 - \frac{\delta\omega}{\omega_0}\right) c_p^2 + \frac{2\beta\rho_n}{\Omega\rho_p} \left(\Omega^2 - \frac{(k \cdot \Omega)^2}{\omega_0^2} c_p^2\right) \\
 & - \frac{\Omega^2}{\omega_0^2} \left[1 - 2\frac{\delta\omega}{\omega_0} + i\frac{2\Omega\beta}{\omega_0} \left(1 + \frac{\rho_{0n}}{\rho_{0p}}\right)\right] \left\{ i4\omega_0 \left(1 + \frac{\delta\omega}{\omega_0}\right) + 8\beta\Omega \right. \\
 & \quad \left. - \frac{(k \cdot \Omega)^2}{\omega_0^2\Omega^2} \left(1 - 2\frac{\delta\omega}{\omega_0}\right) \left[ i4\omega_0 \left(1 + \frac{\delta\omega}{\omega_0}\right) c_p^2 + 8\beta\Omega c_p^2 \right] \right\} = 0
 \end{aligned} \tag{7.5.31}$$

Expanding (7.5.30) and collecting small terms we get

$$\begin{aligned}
 & \omega_0 - \frac{k^2}{\omega_0} c_n^2 - 4\frac{\Omega^2}{\omega_0} + 4\frac{\Omega^2}{\omega_0^3} k^2 \cos^2 \theta c_n^2 \\
 & + \delta\omega \left[ 1 + \frac{k^2}{\omega_0^2} c_n^2 + 4\frac{\Omega^2}{\omega_0^2} - 12\frac{k^2\Omega^2 \cos^2 \theta}{\omega_0^4} c_n^2 \right] \\
 & - i2\beta\Omega \left[ 1 + 4\frac{\Omega^2}{\omega_0^2} \right] \left[ 1 - \frac{k^2 \cos^2 \theta}{\omega_0^2} c_n^2 \right] = 0
 \end{aligned} \tag{7.5.32}$$

The first line is exactly the equation we solved for the slow rotation, no friction case. If we substitute the solutions (7.5.22) or (7.5.23) this line will cancel out. Solving for  $\delta\omega$ , we get

$$\delta\omega = i2\beta\Omega \frac{[\omega_0^2 + 4\Omega^2] [\omega_0^2 - k^2 \cos^2 \theta c_n^2]}{\omega_0^4 + k^2\omega_0^2 c_n^2 + 4\Omega^2\omega_0^2 - 12k^2\Omega^2 \cos^2 \theta c_n^2} \tag{7.5.33}$$

Looking first at the inertial modes we use  $\omega_0^2 = 4\Omega^2 \cos^2 \theta$  to get

$$\delta\omega = i2\beta\Omega \frac{[1 + \cos^2 \theta] [4\Omega^2 - k^2 c_n^2]}{4\Omega^2 (1 + \cos^2 \theta) - 2k^2 c_n^2} \tag{7.5.34}$$

To first order in  $\Omega$  this is

$$\delta\omega = i\beta\Omega [1 + \cos^2 \theta] \tag{7.5.35}$$

The other solution is for sound waves in the neutron fluid. We make the substitution  $\omega_0^2 = k^2 c_n^2 + 4\Omega^2 \sin^2 \theta$  into (7.5.33) and find

$$\begin{aligned}
 \delta\omega &= i2\beta\Omega \frac{[k^2 c_n^2 + 4\Omega^2 \sin^2 \theta + 4\Omega^2] [k^2 c_n^2 + 4\Omega^2 \sin^2 \theta - k^2 \cos^2 \theta c_n^2]}{2k^4 c_n^4 + 12k^2 c_n^2 \Omega^2 \sin^2 \theta - 12k^2 c_n^2 \Omega^2 \cos^2 \theta + 4k^2 c_n^2 \Omega^2 + 32\Omega^4 \sin^4 \theta} \\
 &= i\beta\Omega [1 - \cos^2 \theta] \\
 &= i\beta\Omega \sin^2 \theta
 \end{aligned} \tag{7.5.36}$$

We now use (7.5.31) to find the other set of solutions. Again expanding this and collecting small terms we obtain

$$\begin{aligned} \omega_0 - \frac{k^2}{\omega_0} c_p^2 - 4 \frac{\Omega^2}{\omega_0} + 4 \frac{k^2 \Omega^2 \cos^2 \theta}{\omega_0^3} c_p^2 \\ + \delta\omega \left[ 1 + \frac{k^2}{\omega_0^2} c_p^2 + 4 \frac{\Omega^2}{\omega_0^2} - 12 \frac{k^2 \Omega^2 \cos^2 \theta}{\omega_0^4} c_p^2 \right] \\ - i2\beta\Omega \frac{\rho_n}{\rho_p} \left[ 1 + 4 \frac{\Omega^2}{\omega_0^2} \right] \left[ 1 - \frac{k^2 c_p^2 \cos^2 \theta}{\omega_0^2} \right] = 0 \end{aligned} \quad (7.5.37)$$

Again the first line equals zero for the two previously found solutions (7.5.24) and (7.5.25) of  $\omega_0$ . Solving for  $\delta\omega$  gives

$$\delta\omega = i2\beta\Omega \frac{\rho_n}{\rho_p} \frac{[\omega_0^2 + 4\Omega^2] [\omega_0^2 - k^2 \cos^2 \theta c_p^2]}{\omega_0^4 + k^2 \omega_0^2 c_p^2 + 4\Omega^2 \omega_0^2 - 12k^2 \Omega^2 \cos^2 \theta c_p^2} \quad (7.5.38)$$

Again looking at inertial modes we use the substitution  $\omega_0^2 = 4\Omega^2 \cos^2 \theta$  giving,

$$\delta\omega = i\beta\Omega \frac{\rho_n}{\rho_p} [1 + \cos^2 \theta] \quad (7.5.39)$$

The second solution for  $\omega_0$  is for the sound waves in the charged fluid. Using the substitution  $\omega_0^2 = k^2 c_p^2 + 4\Omega^2 \sin^2 \theta$  (7.5.38) becomes,

$$\delta\omega = i\beta\Omega \frac{\rho_n}{\rho_p} \sin^2 \theta \quad (7.5.40)$$

To summarise the results of this section we have two sets of sound waves with frequency

$$\omega = \pm (kc_n + 2\Omega^2 \sin^2 \theta) + i\beta\Omega \sin^2 \theta \quad (7.5.41)$$

$$\omega = \pm (kc_p + 2\Omega^2 \sin^2 \theta) + i\beta\Omega \frac{\rho_n}{\rho_p} \sin^2 \theta \quad (7.5.42)$$

We also have two sets of inertial modes. Previously these solutions were degenerate, but they become distinct with the inclusion of the damping effects of mutual friction. We have

$$\omega = \pm 2\Omega \cos \theta + i\beta\Omega [1 + \cos^2 \theta] \quad (7.5.43)$$

$$\omega = \pm 2\Omega \cos \theta + i\beta\Omega \frac{\rho_n}{\rho_p} [1 + \cos^2 \theta] \quad (7.5.44)$$

(7.5.41) and (7.5.42) show that there will be no dissipation of sound waves when they are travelling along the axis of rotation. On the other hand the inertial modes

(7.5.43) and (7.5.44) always feel the effect of dissipation. In fact, the greatest effect is when the wave travels along the direction of rotation ( $\theta = 0$ ). To investigate in more detail why the dissipation acts like this on the various modes we return to the single fluid case.

### 7.5.6 A More Detailed Look at the Waves

The single fluid case can help show why the different types of wave are affected in different ways by the mutual friction. In the two fluid case we have assumed that straight vortices create friction between the two constituents. All frictional forces are orthogonal to the direction of circulation. This means that any flow along a vortex will not be modified by the inclusion of these forces. It is therefore only modes in which the particles move orthogonally to the circulation that will be damped. To see how much mutual friction is expected to affect each type of wave it is useful to find  $|\mathbf{v} \times \boldsymbol{\Omega}|$  and  $\mathbf{v} \cdot \boldsymbol{\Omega}$ . The vortex array will be taken as parallel to the rotation of the frame. These two quantities will therefore give a measure of how much of the velocity field points in the directions parallel and perpendicular to the vortex array. For sound waves we found the dispersion relation  $\omega = \pm kc$  (7.3.26). Substituting this into the perturbed equations (7.3.15) and dotting with the unit vector  $\hat{\Omega}_i$  we get

$$\pm ikc\bar{v}_i\hat{\Omega}^i - i\frac{c}{k}\hat{\Omega}^ik_ik_j\bar{v}^j = 0 \quad (7.5.45)$$

Rewriting this and dividing by  $|v|$  gives

$$\pm ik^2c^2\left(\hat{v} \cdot \hat{\Omega}\right) - ik^2c^2\left(\hat{\Omega} \cdot \hat{k}\right)\left(\hat{k} \cdot \hat{v}\right) = 0 \quad (7.5.46)$$

so that

$$\pm ik^2c^2\left(\hat{v} \cdot \hat{\Omega}\right) - ik^2c^2\left(\hat{\Omega} \cdot \hat{k}\right)\left(\hat{k} \cdot \hat{v}\right) = 0 \quad (7.5.47)$$

This rearranges to give

$$\pm\left(\hat{v} \cdot \hat{\Omega}\right) = \cos\theta\left(\hat{k} \cdot \hat{v}\right) \quad (7.5.48)$$

Dotting (7.3.15) with  $\hat{v}$  gives

$$\pm ikc\bar{v}_i\hat{v}^i - i\frac{c}{k}\hat{v}_ik_ik_j\bar{v}^j = 0 \quad (7.5.49)$$

Finally, rearrange to get

$$\pm 1 = (\hat{v} \cdot \hat{k})^2 \quad (7.5.50)$$

As expected for sound waves, the above equation says that the perturbations are completely longitudinal. Substituting this in to (7.5.48) shows the angle between the vectors  $\Omega_i$  and  $v_i$  as

$$(\hat{v} \cdot \hat{\Omega}) = \cos \theta \quad (7.5.51)$$

This shows that  $v_i$  is parallel to  $\Omega_i$  when  $\cos \theta = 1$ . This suggests that when a sound wave travels along the direction of rotation we would expect no mutual friction effects in the two fluid problem. Comparing with the sound wave dispersion relations in the two fluid case, (7.5.41) and (7.5.42), this is exactly what we found. Let us now consider the inertial modes. Substituting  $\omega = \pm 2\Omega \cos \theta$  into (7.3.15) we have

$$\pm 4\Omega^2 \cos \theta \epsilon_{ijk} \hat{\Omega}_0^j \hat{v}^k = ik^2 c^2 \hat{k}_i \hat{k}_j \hat{v}^j - i4\Omega^2 \cos^2 \theta \hat{v}_i \quad (7.5.52)$$

Rearranging and squaring this gives

$$\left( \epsilon_{ijk} \hat{\Omega}_0^j \hat{v}^k \right)^2 = -\frac{1}{16\Omega^4 \cos^2 \theta} \left[ k^4 c^4 (\hat{k} \cdot \hat{v})^2 + 16\Omega^4 \cos^4 \theta - 8k^2 c^2 (\hat{k} \cdot \hat{v})^2 \Omega^2 \cos^2 \theta \right] \quad (7.5.53)$$

Dotting (7.3.15) with  $\Omega_i$  and  $v_i$  gives

$$4\Omega^2 \cos^2 \theta = k^2 c^2 (\hat{k} \cdot \hat{v})^2 \quad (7.5.54)$$

and

$$4\Omega^2 \cos^2 \theta (\hat{v} \cdot \hat{\Omega}) = k^2 c^2 \cos \theta (\hat{k} \cdot \hat{v}) \quad (7.5.55)$$

This gives

$$(\hat{k} \cdot \hat{v}) = \pm \frac{2\Omega \cos \theta}{kc} \quad (7.5.56)$$

Finally substitution of (7.5.56) into (7.5.53) gives

$$\left( \epsilon_{ijk} \hat{\Omega}_0^j \hat{v}^k \right)^2 = \frac{-1}{16\Omega^4 \cos^2 \theta} [4k^2 c^2 \Omega^2 \cos^2 \theta - 16\Omega^4 \cos^4 \theta] \quad (7.5.57)$$

We see that there is no wave motion orthogonal to the rotation when  $kc = 2\Omega \cos \theta$ . It is worthwhile noting that this is when the wave speed of the inertial modes equals the speed of sound. We find from (7.5.55) and (7.5.56) that

$$(\hat{v} \cdot \hat{\Omega}) = \frac{kc}{2\Omega} \quad (7.5.58)$$

This means that the vector  $v_i$  will be parallel to  $\Omega_i$  only when  $kc = 2\Omega$ . Comparing this with what we have just found it seems that the only situation in which there will be an inertial wave in the fluid which has no motion orthogonal to the rotation axis is when  $kc = 2\Omega$ . The wave is then longitudinal and travels in the direction of rotation. The two types of wave have a degeneracy for  $kc = 2\Omega \cos \theta$  and are both longitudinal. Except for this special case we would expect mutual friction to dissipate the inertial modes as there will always be some part of the fluid velocity orthogonal to the axis of rotation. This correlates with the two fluid dispersion relations (7.5.43) and (7.5.44).

## 7.6 Hall modes

So far the superfluid neutron vortices have been assumed to be in a straight array. We have not accounted for the possibility of the vortex lines bending and so the tension term has been zero. Hall [37] found modes by including the vortex tension and constraining the direction of wave propagation to be parallel to the rotation axis, the  $z$ -axis in the following. Redoing this calculation with our equations will show how entrainment affects these modes. Mutual friction will be neglected for this calculation. The equations of motion in a rotating frame are now

$$\begin{aligned} \left( \frac{\partial}{\partial t} + v_n^j \nabla_j \right) [v_i^n + \varepsilon_n (v_i^p - v_i^n)] + \varepsilon_n (v_j^p - v_j^n) \nabla_i v_n^j + \nabla_i (\tilde{\mu}_n) + 2\epsilon_{ijk} \Omega^j v_n^k \\ = \nu \lambda^j \nabla_j \hat{\lambda}_i \end{aligned} \quad (7.6.1)$$

$$\begin{aligned} \left( \frac{\partial}{\partial t} + v_p^j \nabla_j \right) [v_i^p + \varepsilon_p (v_i^n - v_i^p)] + \varepsilon_p (v_j^n - v_j^p) \nabla_i v_p^j + \nabla_i (\tilde{\mu}_p) + 2\epsilon_{ijk} \Omega^j v_p^k \\ = 0 \end{aligned} \quad (7.6.2)$$

The  $\lambda_i$  in the tension term is the average circulation in the neutron fluid at a point. It is therefore defined as,

$$\lambda_i = n_v \kappa_i = 2\Omega_i + \epsilon_{ijk} \nabla^j [v_n^k + \varepsilon_n (v_p^k - v_n^k)] \quad (7.6.3)$$

The gravitational potential has been ignored. To proceed we assume that the background flows of the two fluids are both zero in the rotating frame. Except for

the tension term these two equations have been perturbed before, so we concentrate on the tension. Perturbing  $v_i^n$  and  $\lambda_i$  we use the substitution

$$v_i^n \rightarrow \delta v_i^n \quad (7.6.4)$$

$$\lambda_i \rightarrow \lambda_i^0 + \delta \lambda_i = 2\Omega_i + \frac{1}{m_n} \epsilon_{ijk} \nabla^j \delta p_n^k \quad (7.6.5)$$

Where, as before, the subscript 0 denotes the background part and the  $\delta$  denotes the perturbation.  $p_i^n$  is the momentum of the neutrons and as before, see (4.5.5), it is defined by

$$p_n = m_n [v_i^n + \varepsilon_n (v_i^p - v_i^n)] \quad (7.6.6)$$

As the background part of  $\hat{\lambda}_i$  is a constant unit vector in the  $z$  direction;

$$\delta(\lambda^j \nabla_j \hat{\lambda}_i) = \lambda_0^j \nabla_j \delta \hat{\lambda}_i \quad (7.6.7)$$

To find  $\delta \hat{\lambda}_i$  we expand  $\hat{\lambda}_i$  to get

$$\hat{\lambda}_i^0 + \delta \hat{\lambda}_i = \frac{\frac{1}{m_n} \epsilon_{ijk} \nabla^j \delta p_n^k + 2\Omega_i}{\left| \frac{1}{m_n} \epsilon_{rst} \nabla^s \delta p_n^t + 2\Omega_r \right|} \quad (7.6.8)$$

Expanding the denominator of this fraction we have

$$\left| \frac{1}{m_n} \epsilon_{ijk} \nabla^j \delta p_n^k + 2\Omega_i \right| = \sqrt{\left( \frac{1}{m_n} \epsilon_{ijk} \nabla^j \delta p_n^k + 2\Omega_i \right) \left( \frac{1}{m_n} \epsilon^{ilm} \nabla^l \delta p_n^m + 2\Omega^i \right)} \quad (7.6.9)$$

To first order in  $\delta p_i^n$  this becomes

$$\begin{aligned} \left| \epsilon_{ijk} \nabla^j \frac{1}{m_n} p_n^k + 2\Omega_i \right| &= \sqrt{(2\Omega)^2 \left( 1 + \frac{\Omega^i}{\Omega^2} \frac{1}{m_n} \epsilon_{ijk} \nabla^j \delta p_n^k \right)} \\ &= 2\Omega \left( 1 + \frac{1}{m_n} \frac{\Omega^i}{2\Omega^2} \epsilon_{ijk} \nabla^j \delta p_n^k \right) \end{aligned} \quad (7.6.10)$$

Note that at this point we can no longer take the  $\Omega \rightarrow 0$  limit. Substituting (7.6.10) back into (7.6.8) and using  $\hat{\lambda}_0 = \Omega_i/\Omega$  we find the perturbed tension is

$$\begin{aligned} \lambda_0^j \nabla_j \delta \hat{\lambda}_i &= (2\Omega^j \nabla_j) \left\{ \left( \frac{\frac{1}{m_n} \epsilon_{ijk} \nabla^j \delta p_n^k + 2\Omega_i}{2\Omega} \right) \left( 1 - \frac{\Omega^i}{2\Omega^2} \frac{1}{m_n} \epsilon_{ijk} \nabla^j \delta p_n^k \right) - \frac{\Omega_i}{\Omega} \right\} \\ &= (2\Omega^j \nabla_j) \left( \frac{\frac{1}{m_n} \epsilon_{ijk} \nabla^j \delta p_n^k - \Omega_i \frac{\Omega^m}{\Omega^2} \frac{1}{m_n} \epsilon_{mjk} \nabla^j \delta p_n^k}{2\Omega} \right) \end{aligned} \quad (7.6.11)$$



We again assume that the perturbations are plane waves. For reasons of clarity, we also add the assumption that the waves travel along the axis of rotation ( $k_z = k$ ). This gives  $\Omega^m \epsilon_{mjk} \nabla^j \delta p_n^k = 0$  in (7.6.11). After dividing by the oscillating part  $e^{i(\omega t - k^j x_j)}$  (as we have done for the rest of the equation of motion) we find that the tension term that needs to be included in the perturbed equations of motion is,

$$-\frac{1}{m_n} k_z \epsilon_{ijk} k_z^j p_n^k = -k_z \epsilon_{ijk} k_z^j \left[ \bar{v}_n^k + \varepsilon_n \left( \bar{v}_p^k - \bar{v}_n^k \right) \right] \quad (7.6.12)$$

It can be seen that the tension will have no effect on longitudinal waves along the axis of rotation. As we are concentrating on the modes found by Hall [37] the perturbations are now taken as completely transverse waves. By the continuity equation this means that there are no density perturbations. The perturbed equations of motion are therefore,

$$i\omega \left[ \bar{v}_i^n + \varepsilon_n \left( \bar{v}_i^p - \bar{v}_i^n \right) \right] + 2\Omega \epsilon_{ijk} \hat{\Omega}^j \bar{v}_n^k = -\tilde{\nu} k_z^2 \epsilon_{ijk} \hat{\Omega}^j \left[ \bar{v}_n^k + \varepsilon_n \left( \bar{v}_p^k - \bar{v}_n^k \right) \right] \quad (7.6.13)$$

$$i\omega \left[ \bar{v}_i^p + \varepsilon_p \left( \bar{v}_i^n - \bar{v}_i^p \right) \right] + 2\Omega \epsilon_{ijk} \hat{\Omega}^j \bar{v}_p^k = 0 \quad (7.6.14)$$

To solve these equations we take the cross product with  $\Omega_i$ .

$$i\omega \left[ \epsilon_{ijk} \hat{\Omega}_0^j \bar{v}_n^k (1 - \varepsilon_n) + \varepsilon_n \epsilon_{ijk} \hat{\Omega}_0^j \bar{v}_p^k \right] = \left[ \tilde{\nu} k_z^2 (1 - \varepsilon_n) + 2\Omega \right] \bar{v}_i^n + \tilde{\nu} k_z^2 \varepsilon_n \bar{v}_i^p \quad (7.6.15)$$

$$i\omega \left[ \epsilon_{ijk} \hat{\Omega}_0^j \bar{v}_p^k (1 - \varepsilon_p) + \varepsilon_p \epsilon_{ijk} \hat{\Omega}_0^j \bar{v}_n^k \right] - 2\Omega \bar{v}_i^p = 0 \quad (7.6.16)$$

We now use (7.6.15) and (7.6.16) to solve for  $\epsilon_{ijk} \hat{\Omega}_0^j \bar{v}_n^k$  and  $\epsilon_{ijk} \hat{\Omega}_0^j \bar{v}_p^k$ . These results can then be substituted into (7.6.13) and (7.6.14) to give

$$\begin{aligned} \bar{v}_i^n & \left\{ [2\Omega + (1 - \varepsilon_n) \tilde{\nu} k_z^2]^2 - \omega^2 (1 - \varepsilon_n) \left[ 1 - \varepsilon_n - \frac{\varepsilon_n \varepsilon_p \omega^2 \tilde{\nu} k_z^2}{2\Omega} \right] - \frac{\varepsilon_n \varepsilon_p \omega^2}{2\Omega} \right\} \\ & = \bar{v}_i^p \left\{ \omega^2 \varepsilon_n (1 - \varepsilon_n) \left[ 1 - \frac{(1 - \varepsilon_p) \tilde{\nu} k_z^2}{\Omega} \right] + \frac{\varepsilon_n (1 - \varepsilon_p) \omega^2}{2\Omega} \right. \\ & \quad \left. - [2\Omega + (1 - \varepsilon_n) \tilde{\nu} k_z^2] \varepsilon_n \tilde{\nu} k_z^2 \right\} \end{aligned} \quad (7.6.17)$$

and

$$[4\Omega^2 - (1 - \varepsilon_p)^2 \omega^2] \bar{v}_i^p = \omega^2 \varepsilon_p^2 \bar{v}_i^n \quad (7.6.18)$$

From these two relations we see that the required dispersion relation is

$$\begin{aligned}
 & [4\Omega^2 - (1 - \varepsilon_p)^2 \omega^2] \left\{ [2\Omega + (1 - \varepsilon_n) \bar{\nu} k_z^2]^2 \right. \\
 & \quad \left. - \omega^2 (1 - \varepsilon_n) \left[ 1 - \varepsilon_n - \frac{\varepsilon_n \varepsilon_p \omega^2 \bar{\nu} k_z^2}{2\Omega} \right] - \frac{\varepsilon_n \varepsilon_p \omega^2}{2\Omega} \right\} \\
 & = \omega^2 \varepsilon_p^2 \left\{ \omega^2 \varepsilon_n (1 - \varepsilon_n) \left[ 1 - \frac{(1 - \varepsilon_p) \bar{\nu} k_z^2}{2\Omega} \right] \right. \\
 & \quad \left. + \frac{\varepsilon_n (1 - \varepsilon_p) \omega^2}{2\Omega} - [2\Omega + (1 - \varepsilon_n) \bar{\nu} k_z^2] \varepsilon_n \bar{\nu} k_z^2 \right\} \quad (7.6.19)
 \end{aligned}$$

We now have a quadratic in  $\omega^2$ . This is possible to solve but even with all the assumptions we've included the result is very messy. As a starting point we ignore entrainment to get

$$[4\Omega^2 - \omega^2] [(2\Omega + \bar{\nu} k_z^2)^2 - \omega^2] = 0 \quad (7.6.20)$$

This gives the solutions

$$\omega = \pm (2\Omega + \bar{\nu} k_z^2) \quad (7.6.21)$$

$$\omega = \pm 2\Omega \quad (7.6.22)$$

We see that the second solution is just the proton inertial modes. The first solution is the inertial mode in the neutron fluid. This mode is modified by the tension and is the same relation found by Hall [37] for superfluid Helium. To extend this result we reintroduce the entrainment. As in the mutual friction case we assume that the entrainment is a small quantity and that its inclusion will be a small modification of the previously found solutions. To first order in entrainment the dispersion relation is,

$$[4\Omega^2 - (1 - \varepsilon_p)^2 \omega^2] \left\{ [2\Omega + (1 - \varepsilon_n) \bar{\nu} k_z^2]^2 - \omega^2 (1 - \varepsilon_n)^2 \right\} = 0 \quad (7.6.23)$$

Hence, we can see that the solutions are

$$\omega = \pm [2\Omega(1 + \varepsilon_n) + \bar{\nu} k_z^2] \quad (7.6.24)$$

$$\omega = \pm 2\Omega(1 + \varepsilon_p) \quad (7.6.25)$$

There is no reason why the entrainment should be small, but the assumption makes the solutions more tractable. The purpose of this section was to get some

feel, analytically, for the way that entrainment comes into the problem. We can see that for weak entrainment the frequency is modified via the rotation rather than the tension.

## 7.7 The Donnelly-Glaberson Instability

A logical next step in pushing this analysis forwards is to include a background velocity difference between the two constituents. This will greatly complicate the analysis and so we are forced to look at special cases. In a paper by Glaberson et. al. [30] unstable modes were found by introducing a velocity difference along the axis of rotation. They also confine themselves to looking at transverse waves that travel in the direction of the velocity difference. In their paper they show that the unstable modes are due to mutual friction. It would be interesting to see if other coupling effects like entrainment can do the same job. The investigation of instabilities is important in discussions of the onset of turbulence. In fact, it is the instability found by Glaberson et. al. [30] that is thought to lead to turbulence. It is known as the Donnelly-Glaberson instability and was already discussed in section 6.4. It is clearly important that we understand this instability in the neutron star case.

We will consider a transverse wave traveling parallel to the axis of rotation and velocity difference. This will again be labelled as the  $z$  axis. To gain as full a picture of the instability as possible we include the mutual friction force for curved vortices, the tension and entrainment. We will take  $\beta$  as a small quantity. The problem will lead to a complicated set of equations so we will clamp the proton fluid. That is, we assume that the proton velocity is zero in the rotating frame. This means that the velocity difference between the two constituents will just lead to a term in the neutron fluid background. This is not so unreasonable. If the coupling terms are taken as small, as we have done here, then one constituents velocity field only affects the dispersion relation of the other constituent at the second order level.

To summarise, the assumed velocity fields are

$$\begin{aligned} v_i^{0n} &= V_i & v_i^{0p} &= 0 \\ \delta v_i^n &= \bar{v}_i^n e^{i\omega - k^j x_j} & \delta v_i^p &= 0 \end{aligned} \quad (7.7.1)$$

where  $k_i = k_i^z$ . The perturbed continuity equation for the neutrons is given as

$$\hat{\rho}_n = \rho_{0n} \frac{k^j \bar{v}_j^n}{(\omega - kV)} = 0 \quad (7.7.2)$$

The right hand side of the equation vanishes as the wave is transverse. We therefore have a set of three equations from the neutron equations of motion. When perturbed and the assumptions are implemented these equations lead to

$$i(\omega - Vk)\bar{v}_i^n(1 - \varepsilon_n) + 2\epsilon_{ijk}\Omega^j v_n^k = \delta F_i^n \quad (7.7.3)$$

As discussed above the perturbed force will consist of a perturbed tension, mutual friction and a self induced velocity piece. The previous section has given us that for a transverse wave the perturbed tension is given by

$$\delta F_i^{tension} = -\nu k_z \epsilon_{ijk} k^j \bar{v}_n^k (1 - \varepsilon_n) \quad (7.7.4)$$

Previously we calculated the perturbed mutual friction force for a straight vortex array. This, however, did not allow for a background velocity difference. The perturbed force before implementing the assumptions is given by,

$$\delta F_i^{mutual} = \delta \left( \beta \epsilon_{ijk} \lambda^j \epsilon^{klm} \hat{\lambda}_l (v_m^n - v_m^p) \right) \quad (7.7.5)$$

Applying the assumed form of the velocity fields and remembering that  $\lambda_i^0 = 2\Omega_i$ , we get

$$\begin{aligned} \delta F_i^{mutual} &= \beta \delta \left( \lambda^j \hat{\lambda}_i v_j^n - \lambda^j \hat{\lambda}_j v_i^n \right) \\ &= \beta \left( \delta \lambda^j \frac{\Omega_i}{\Omega} V_j + V 2\Omega \delta \hat{\lambda}_i - \delta |\lambda| V_i + 2\Omega^j \frac{\Omega_i}{\Omega} \delta v_j^n - 2\Omega \delta v_i^n \right) \end{aligned} \quad (7.7.6)$$

For a transverse wave we know that  $k^j \bar{v}_j^X = 0$  and  $\delta \lambda_i$  is perpendicular to  $k_i$ . After dividing by  $e^{i(\omega t - k^j x_j)}$  then the perturbed mutual friction for a straight array is

$$\delta F_i^{mutual} = -i\beta V \epsilon_{ijk} k^j \bar{v}_n^k (1 - \varepsilon_n) - 2\beta \Omega \bar{v}_i^n \quad (7.7.7)$$

Lastly we need to find the perturbed force due to the vortex self induced velocity;

$$\delta F_i^{induced} = \delta \left( -\nu\beta\lambda\epsilon_{ijk}\nabla^j\hat{\lambda}^k \right) = -2\nu\beta\Omega\epsilon_{ijk}\nabla^j\delta\hat{\lambda}^k \quad (7.7.8)$$

Using (7.6.8) this becomes

$$\begin{aligned} \delta F_i^{induced} &= \nu\beta\epsilon_{ijk}k^j\epsilon^{klm}k_lv_m^n(1-\varepsilon_n) \\ &= \nu\beta k^j k_i v_j^n(1-\varepsilon_n) - \nu\beta k^2 v_i^n(1-\varepsilon_n) \end{aligned} \quad (7.7.9)$$

Substituting (7.7.4), (7.7.7) and (7.7.9) into (7.7.3) gives us the perturbed equations of motion.

$$\begin{aligned} [i(\omega - Vk)(1-\varepsilon_n) + 2\beta\Omega + \nu\beta k^2(1-\varepsilon_n)] \bar{v}_i^n \\ = [-2\Omega - \nu k^2(1-\varepsilon_n) - i\beta Vk(1-\varepsilon_n)] \epsilon_{ijk}\hat{k}^j v_n^k \end{aligned} \quad (7.7.10)$$

Contracting this with  $\epsilon_{ijk}\hat{k}^j$  and combining the two equations we find that

$$\begin{aligned} [(\omega - Vk)(1-\varepsilon_n) - i2\beta\Omega - i\nu\beta k^2(1-\varepsilon_n)]^2 \\ = [2\Omega + \nu k^2(1-\varepsilon_n) + i\beta Vk(1-\varepsilon_n)]^2 \end{aligned} \quad (7.7.11)$$

which for small entrainment gives the dispersion relation

$$\omega - Vk = \pm [2\Omega(1+\varepsilon_n) + \nu k^2] + i2\beta\Omega(1+\varepsilon_n) + i\nu\beta k^2 \pm i\beta Vk \quad (7.7.12)$$

There will be a growing unstable mode when  $\omega$  has a negative imaginary part.

This means that the amplitude of the oscillations grows for

$$V > \frac{2\Omega}{k}(1+\varepsilon_n) + \nu k \quad (7.7.13)$$

Neglecting entrainment for the moment we have found a velocity at which the wave will become unstable that depends upon the wave vector  $k$ . To find the critical velocity at which the instability will set in we simply need to minimise the right hand side of the equation. This gives

$$\nu - \frac{2\Omega}{k^2} = 0 \rightarrow k_z = \sqrt{\frac{2\Omega}{\nu}} \quad (7.7.14)$$

So we will have an instability when

$$V > V_c = 2\sqrt{2\Omega\nu} \quad (7.7.15)$$

This is exactly the relation found for the Helium case by Glaberson et. al. [30]. From the discussion of Glaberson et. al., we know that these are helical Kelvin waves that travel along the vortex lines. We have shown that they are inertial waves on the macroscopic scale. For a neutron star we will have entrainment as well. When we include entrainment as a small quantity then the critical wave vector is

$$k_z = \sqrt{\frac{2\Omega}{\nu}} \left( 1 + \frac{1}{2}\varepsilon_n \right) \quad (7.7.16)$$

while the critical velocity becomes

$$V_c = 2\sqrt{2\Omega\nu} \left( 1 + \frac{1}{2}\varepsilon_n \right) \quad (7.7.17)$$

We would like to know what is physically significant about this velocity. We can find the phase velocity ( $\sigma_p$ ) of the wave from

$$\sigma_p = \frac{\Re(\omega)}{k} \quad (7.7.18)$$

For the inertial waves this leads to

$$\sigma_p = V \pm \left[ \frac{2\Omega}{k} (1 + \varepsilon_n) + \nu k \right] \quad (7.7.19)$$

We can see from this that the critical velocity corresponds to  $\sigma_p = 0$ . This is when the velocity of the wave is the same as the counterflow velocity. So the critical velocity coincides with the point at which the counterflow is at the same speed as the helical oscillations that travel along the vortex line. This instability is one of a more general class of two stream instabilities [9]. The instability found here is the same one that was discussed in chapter 6 as the onset of turbulent flows. We need to check that this instability is reasonable for neutron stars. For these rough estimates we neglect entrainment. From (7.7.14) we find that the critical wave vector is

$$k_z \approx 250 \left( \frac{\Omega}{100s^{-1}} \right)^{1/2} \text{ cm}^{-1} \quad (7.7.20)$$

This corresponds to a wavelength of

$$\lambda_z = 4 \times 10^{-3} \left( \frac{\Omega}{100s^{-1}} \right)^{-1/2} \text{ cm} \quad (7.7.21)$$

We expect that the inter vortex spacing to be

$$d_v = 3.4 \times 10^{-3} \left( \frac{\Omega}{100 \text{ s}^{-1}} \right)^{-1/2} \text{ cm} \quad (7.7.22)$$

Hence there would be a large range of wavelengths for which the modes would be unstable. The corresponding critical velocity is

$$V_c \approx 5.7 \left( \frac{\Omega}{100 \text{ s}^{-1}} \right)^{-1/2} \text{ cm s}^{-1} \quad (7.7.23)$$

For a star with an angular velocity of  $100 \text{ s}^{-1}$  the critical velocity is as small as  $5.7 \text{ cm s}^{-1}$ . This seems to be a very low velocity and so it seems likely that there will be situations in which this is relevant.

## 7.8 Turbulence

To conclude this chapter we now introduce turbulence into the discussion. The previous section showed that the instability that is thought to be crucial in setting up a turbulent flow is physically possible. In fact the calculations showed that the necessary conditions are likely to be satisfied. It is important to understand oscillations in a turbulent flow as it may significantly influence neutron star dynamics. We will approach this in a similar way to the calculation for the Donnelly-Glaberson instability. In this way we can see how turbulence affects the instability. All assumptions used in the previous section still hold except that we use the polarised turbulent force given in chapter 6 as,

$$\begin{aligned} f_i^{mf} = \rho_n L_R \left[ \beta' \epsilon_{ijk} \lambda^j w_{np}^k + \beta \epsilon_{ijk} \epsilon^{klm} \hat{\lambda}^j \lambda_l w_m^{np} \right. \\ \left. - \nu \left( \beta' \hat{\lambda}^j \nabla_j \lambda_i + \beta \lambda \epsilon_{ijk} \nabla^j \hat{\lambda}^k \right) \right] + \frac{2}{3} \rho_n \beta \lambda w_i^{pn} L_T \end{aligned} \quad (7.8.1)$$

Hence we have

$$L_T = 4\pi^2 \beta^2 \left( \frac{W}{\kappa} \right)^2 + 4\pi \beta \frac{W}{\kappa} \sqrt{L_R} \quad (7.8.2)$$

and

$$L_R = \frac{2\Omega}{\kappa} \quad (7.8.3)$$

moreover,  $\rho_n$  is constant for a transverse wave and  $\bar{v}_p = 0$  when the proton fluid is clamped. We are also taking  $\beta$  as small so  $\beta'$  is negligible.  $W$  is defined by

$$W = |w_{pn}^j k_j| = |v_n^j k_j| \quad (7.8.4)$$

Perturbing this gives

$$\delta W = \left| \delta v_n^j k_j + V^j \epsilon_{jkl} k^k \delta v_n^l \right| = 0 \quad (7.8.5)$$

where the first term vanishes due to the wave being transverse, while the second is the cross product of two parallel vectors. We also have

$$\delta L_R = 0 \quad (7.8.6)$$

as  $L_R$  relates directly to the fixed quantity  $\Omega$ . As we were not able to include the entrainment in the derivation of the turbulent force it does not make sense to include the parameter here. We therefore take  $\varepsilon_X = 0$ . This means that the perturbed equations of motion of the neutron fluid are given by

$$\begin{aligned} i(\omega - Vk)\bar{v}_i^n + 2\epsilon_{ijk}\Omega^j v_n^k &= -\nu k_z \epsilon_{ijk} k^j \bar{v}_n^k - i\beta V \epsilon_{ijk} k^j \bar{v}_n^k - 2\beta\Omega \bar{v}_i^n \\ &+ \nu\beta k^j k_i v_j^n - \nu\beta k^2 v_i^n - \frac{2}{3}\beta\kappa \bar{v}_n^i L_{0T} \end{aligned} \quad (7.8.7)$$

Rearranging gives

$$\begin{aligned} \left[ i(\omega - Vk) + 2\beta\Omega + \nu\beta k^2 + \frac{2}{3}\kappa\beta L_{0T} \right] \bar{v}_i^n \\ = [-2\Omega - \nu k^2 - i\beta Vk] \epsilon_{ijk} \hat{k}^j v_n^k \end{aligned} \quad (7.8.8)$$

Contracting this with  $\epsilon_{ijk} \hat{k}^j$  and combining the two equations gives

$$\left[ (\omega - Vk) - i2\beta\Omega - i\nu\beta k^2 - i\frac{2}{3}\kappa\beta L_{0T} \right]^2 = [2\Omega + \nu k^2 + i\beta Vk]^2 \quad (7.8.9)$$

so that

$$\omega - Vk = i2\beta\Omega + i\nu\beta k^2 + i\frac{2}{3}\kappa\beta L_{0T} \pm [2\Omega + \nu k^2 + i\beta Vk] \quad (7.8.10)$$

Written out in full the dispersion relation is

$$\begin{aligned} \omega - Vk &= i2\beta\Omega + i\nu\beta k^2 + i\frac{2}{3}\kappa\beta \left[ 4\pi^2 \beta^2 \left( \frac{V}{\kappa} \right)^2 + 4\pi\beta \frac{V}{\kappa^{3/2}} (2\Omega)^{1/2} \right] \\ &\pm [2\Omega + \nu k^2 + i\beta Vk] \end{aligned} \quad (7.8.11)$$



This shows that there will be a growing instability when

$$2\Omega + \nu k^2 + \frac{2}{3}\kappa \left[ 4\pi^2 \beta^2 \left( \frac{V}{\kappa} \right)^2 + 4\pi\beta \frac{V}{\kappa^{3/2}} (2\Omega)^{1/2} \right] \pm V k < 0 \quad (7.8.12)$$

We can see from this that the turbulence has a damping effect and so stabilises the instability. On the other hand as  $\beta \ll 1$  this will be a small effect. For small  $\beta$  the critical velocity becomes

$$V > \left( \frac{2\Omega}{k} + \nu k \right) \left[ 1 + \frac{8}{3} \frac{\pi\beta}{k} \left( \frac{2\Omega}{\kappa} \right)^{1/2} \right] \quad (7.8.13)$$

For a larger  $\beta$  we can see that there will be a second root in which the system would become stable again for larger  $V$ .

## 7.9 Summary

We have investigated the nature of the waves that will be present in a two-constituent fluid with a mutual friction due to vortices. The role of various fluid properties has been discussed, in particular the mutual friction force. We have shown that the presence of vortices, and hence mutual friction, can make the inertial waves unstable. This instability is a mechanism that can create turbulence in the fluid. A further step in this work would be to find the relevance of the mutual friction coefficient  $\beta'$ . For a strong coupling between the proton fluid and the vortices this coefficient can no longer be neglected. Strong coupling may be important for a number of neutron star phenomena [32].

## Chapter 8

# Boundary Effects

In previous chapters we have studied the behaviour of waves in a fluid with no boundaries. However, we know that boundaries and interfaces can have significant effect on fluid motion. Hence, it is interesting to see how entrainment and mutual friction affect the motion of a fluid at a boundary. This will hopefully provide insight into how energy is exchanged between the neutron star crust and the core. The discussion here will only be a very simple first step as in reality the crust is not a solid wall like boundary but a lattice structure for which elastic effects would be important.

Following a similar philosophy to the approach taken in the plane wave analysis in chapter 7 we will first investigate a simple single fluid problem and then introduce a second fluid component. The general strategy for all of these calculations is to set up an oscillation in the fluid with no boundary by adding a 'hand of God' force. Then a boundary is inserted with a no-slip condition (i.e. the fluid velocity vanishes on the boundary). The velocity field can then be solved for. In this way the modelled fluid is forced to oscillate far from the boundary, but the flow is modified by viscosity over some length scale near the boundary. The oscillations will be assumed to be small enough that non linear velocity terms can be neglected.

## 8.1 One Fluid

The simplest case that we shall investigate is a single viscous rotating fluid. The equations of motion in a rotating frame for this situation are,

$$\left( \frac{\partial}{\partial t} + v^j \nabla_j \right) v_i + \nabla_i \tilde{\mu} + 2\epsilon_{ijk} \Omega^j v^k = \nu \nabla^2 v_i + F_i \quad (8.1.1)$$

Where  $F_i$  is some force that drives the system with a prescribed oscillation. We will ignore chemical potential gradients from now on. For a stationary (in this frame) velocity with a small oscillation added this is equivalent to an incompressibility condition. In reality we are making this assumption for simplicity. Once we have set up an oscillation in the fluid we will insert a boundary at  $z = 0$  in Cartesian coordinates. The length scale over which the boundary effects are important is known as the Ekman boundary layer. Setting  $v_i$  to oscillate so that in the rotating frame (in Cartesian coordinates)  $v_i = [V_0 \cos(\omega t), 0, 0]$  we find that the form of the force is

$$F_i = [-\omega V_0 \sin(\omega t), 2\Omega V_0 \cos(\omega t), 0] \quad (8.1.2)$$

We now want to substitute this back into the full equations of motion. Before returning to the algebra we take a detour to discuss the methodology of this type of problem.

For problems in which the fluid is spun down by a boundary that is rotating slower than the fluid, the Ekman boundary layer is an important part of the evolution of the flow. In these problems it is assumed that  $\nu^{1/2}$  is small and  $v_i$  is expanded in powers of  $\nu^{1/2}$  [36]. At each order of  $\nu^{1/2}$  it is assumed that there is a background flow that is not dependent upon the boundary, and a small correction due to the boundary. The spatial derivative of the correction term is taken as proportional to  $\nu^{-1/2}$ . This just assumes that the characteristic size of the boundary layer is proportional to the inverse square root of the viscosity. To first order the expansion of  $v_i$  is.

$$v_i = v_i^0 + \tilde{v}_i^0 + \nu^{1/2} (v_i^1 + \tilde{v}_i^1) \quad (8.1.3)$$

where the corrections are denoted by tildes. When applying this to the equations of motion we find that we have a set of equations at each order of  $\nu$ . Applying

this method to our problem it is found that the first order terms in  $v_i$  vanish. Reinvestigating the types of problems that have non-zero first order terms we find that they are situations in which there is time dependence. In problems where the boundary rotates faster than the fluid the first order terms are the part of the flow that helps spin the whole fluid up. In our case nothing is being spun up. We are looking for a stable solution, in the sense that the solution is periodic with no time dependent decay. It also signifies the lack of any secondary large scale motion.

For our problem, in which we are looking for stable solutions, we do not need to consider the higher order terms. This method is equivalent to solving for a background oscillating solution and then inserting the boundary as a separate calculation. The difference is that we do not need to assume the dependence of the correction term on  $\nu^{1/2}$  as we have not needed to consider  $\nu$  as small. If we take the oscillations as small then we only need to solve the linearized Euler equation. In Cartesian coordinates we take  $v_i = [V_X(z)e^{i\omega t}, V_Y(z)e^{i\omega t}, V_Z(z)e^{i\omega t}]$ . Since we have assumed that the oscillations themselves are linear, the only dependence will be on the distance from the boundary. We have also taken  $\omega$  as constant so that we have a periodic solution. As the equations are now linearized we can divide through by  $e^{i\omega t}$  to get the component equations

$$\begin{aligned} i\omega V_X - 2\Omega V_Y - i\omega V_0 - \nu \frac{\partial^2 V_X}{\partial z^2} &= 0 \\ i\omega V_Y + 2\Omega V_X - 2\Omega V_0 - \nu \frac{\partial^2 V_Y}{\partial z^2} &= 0 \\ i\omega V_Z - \nu \frac{\partial^2 V_Z}{\partial z^2} &= 0 \end{aligned} \tag{8.1.4}$$

We can see from this that we need 6 boundary conditions. We get 3 from the non-slip condition on the boundary. The other conditions are found by assuming that the velocity field will not be affected by the boundary at infinity and so will oscillate as in the no boundary case. That is, we have

$$\begin{aligned} \lim_{z \rightarrow \infty} V_i &= (V_0, 0, 0) \\ \lim_{z \rightarrow 0} V_i &= (0, 0, 0) \end{aligned} \tag{8.1.5}$$

We can see that the  $z$  component is completely decoupled. The solutions to these

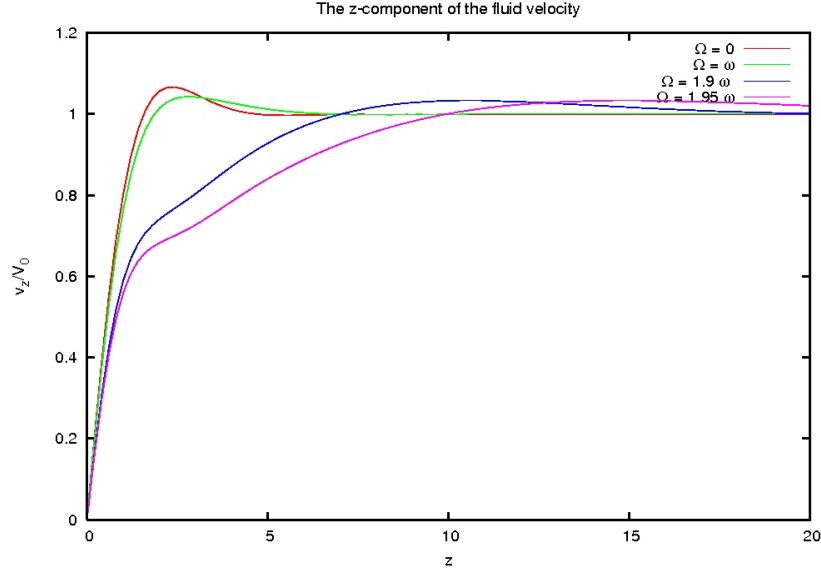


Figure 8.1: The velocity field of the rotating boundary problem at time  $t = 0$ . The boundary is at  $z = 0$ . We can see that the field is only significantly modified from the non-rotating case when the rotation is large.

equations are found to be

$$\begin{aligned}
 V_X &= V_0 - \frac{V_0}{2} \exp \left[ -(1+i) \sqrt{\frac{\omega+2\Omega}{2\nu}} z \right] - \frac{V_0}{2} \exp \left[ -(1+i) \sqrt{\frac{\omega-2\Omega}{2\nu}} z \right] \\
 V_Y &= \frac{iV_0}{2} \exp \left[ -(1+i) \sqrt{\frac{\omega+2\Omega}{2\nu}} z \right] - \frac{iV_0}{2} \exp \left[ -(1+i) \sqrt{\frac{\omega-2\Omega}{2\nu}} z \right] \\
 V_Z &= 0
 \end{aligned} \tag{8.1.6}$$

Defining  $\omega_1 = \omega + 2\Omega$  and  $\omega_2 = \omega - 2\Omega$ , this gives the physical velocity field as

$$\begin{aligned}
 v_X &= V_0 \cos(\omega t) - \frac{V_0}{2} e^{-\sqrt{\frac{\omega_1}{2\nu}} z} \cos \left( \sqrt{\frac{\omega_1}{2\nu}} z - \omega t \right) - \frac{V_0}{2} e^{-\sqrt{\frac{\omega_2}{2\nu}} z} \cos \left( \sqrt{\frac{\omega_2}{2\nu}} z - \omega t \right) \\
 v_Y &= \frac{V_0}{2} e^{-\sqrt{\frac{\omega_1}{2\nu}} z} \sin \left( \sqrt{\frac{\omega_1}{2\nu}} z - \omega t \right) - \frac{V_0}{2} e^{-\sqrt{\frac{\omega_2}{2\nu}} z} \sin \left( \sqrt{\frac{\omega_2}{2\nu}} z - \omega t \right) \\
 v_Z &= 0
 \end{aligned} \tag{8.1.7}$$

Figure 8.1 shows the velocity field plotted at time  $t = 0$  for various  $\Omega$ . We have taken  $\nu = 1 \text{ cm}^2 \text{ s}^{-1}$  and  $\omega = 2 \text{ s}^{-1}$ . This is not for any physical reason but just to have a visual way of seeing the effect of rotation. We can see that there is not a great difference in the solutions when  $\Omega = 0$  and  $\Omega = \omega$ . For larger  $\Omega$  the solution

is more significantly modified. Having solved this problem we now look specifically at the no rotation case. Setting  $\Omega = 0$  the velocity field is

$$\begin{aligned} v_X &= V_0 \cos(\omega t) - V_0 e^{-\sqrt{\frac{\omega}{2\nu}}z} \cos\left(\sqrt{\frac{\omega}{2\nu}}z - \omega t\right) \\ v_Y &= 0 \\ v_Z &= 0 \end{aligned} \tag{8.1.8}$$

We can see that the solution is made of two parts, the original oscillation and a flow modification near the boundary. The modification has characteristic length scale  $\sqrt{\omega/2\nu}$ . This is known as the size of the Ekman boundary layer. This second term will be negligible far from the boundary. Now that we have a solution to compare to we reintroduce the rotation. We can see from the velocity field that the effect of rotation is to split the frequency of the oscillations into two. To investigate the effect of rotation further we Taylor expand the velocity field in  $\Omega$  near the boundary. So,

$$\begin{aligned} \exp\left[-(1+i)\sqrt{\frac{\omega+2\Omega}{2\nu}}z\right] &\approx \exp\left[-(1+i)\sqrt{\frac{\omega}{2\nu}}\left(1+\frac{\Omega}{\omega}\right)z\right] \\ &\approx \exp\left[-(1+i)\sqrt{\frac{\omega}{2\nu}}z\right]\left[1-(1+i)\frac{\Omega}{\sqrt{2\nu\omega}}z\right] \end{aligned} \tag{8.1.9}$$

Substituting this back into (8.1.6) gives to first order in  $\Omega z$

$$\begin{aligned} V_X &= V_0 - V_0 \exp\left(-\sqrt{\frac{\omega}{2\nu}}z\right) \\ V_Y &= (i-1)\frac{\Omega V_0 z}{\sqrt{2\nu\omega}} \exp\left(-\sqrt{\frac{\omega}{2\nu}}z\right) \\ V_Z &= 0 \end{aligned} \tag{8.1.10}$$

We can see from these equations that to first order the  $x$ -component does not depend on  $\Omega$ . This suggests that for slow rotation it is approximately the case that the  $x$ -component of the velocity is unchanged. This is the result we saw in figure 8.1, that for small values of  $\Omega$  the solution is only slightly modified. When we introduce a second fluid component we expect the problem will be much more complicated. We also know that physically we need rotation in the fluid to have a mutual friction. The above calculation suggests that for slow rotation the

single fluid solution is not significantly modified. It will thus not be completely inconsistent to include the mutual friction in the two fluid problem while neglecting the centrifugal force. This will simplify the two fluid problem so that we can concentrate on the coupling effect of mutual friction. It is obviously inconsistent to ignore rotation while including mutual friction as the force originates from the superfluid vortices, but for calculating purposes we can still show how the mutual friction modifies the velocity field. It is also worth noting that to first order in rotation the  $y$ -component will vanish for  $z \ll 1$  and  $z \gg 1$ . In these regions the  $y$ -component of the velocity field is equivalent to the non-rotating case.

## 8.2 Two Fluids

We now move on to the situation with two fluid constituents. We shall consider one fluid as normal fluid (protons) and one as superfluid (neutrons). The equations for protons and neutrons with mutual friction are

$$\begin{aligned}
& \left( \frac{\partial}{\partial t} + v_n^j \nabla_j \right) [v_i^n + \varepsilon_n (v_i^p - v_i^n)] + \varepsilon_n (v_p^j - v_n^j) \nabla_i v_j^n + \nabla_i \tilde{\mu}_n + \epsilon_{ijk} \Omega^j v_n^k \\
& \quad = \beta \epsilon_{ijk} \lambda^j \epsilon^{klm} \hat{\lambda}_l (v_m^n - v_m^p) + F_i^n \\
& \left( \frac{\partial}{\partial t} + v_p^j \nabla_j \right) [v_i^p + \varepsilon_p (v_i^n - v_i^p)] + \varepsilon_p (v_n^j - v_p^j) \nabla_i v_j^p + \nabla_i \tilde{\mu}_p + \epsilon_{ijk} \Omega^j v_p^k \\
& \quad = \nu \nabla^2 v_i^p + \beta \frac{\rho_n}{\rho_p} \epsilon_{ijk} \lambda^j \epsilon^{klm} \hat{\lambda}_l (v_m^p - v_m^n) + F_i^p
\end{aligned} \tag{8.2.1}$$

where  $F_i^X$  is the force that we shall use to impose an oscillation in the fluid. The equations assume that the superfluid vortices are in a straight array and the usual  $\beta'$  coefficient is negligible. These are assumptions that we would like to relax in the future, but for now we consider this constrained problem.

### 8.2.1 No Mutual Friction

As in the single fluid case we will ignore perturbations in the chemical potentials and linearise in  $v_i^X$ . We consider the no rotation case as we discussed in the single fluid section. To investigate the effect of entrainment we will first set the mutual

friction coefficients to zero. The equations of motion are therefore

$$\begin{aligned}\frac{\partial}{\partial t} [v_i^n + \varepsilon_n(v_i^p - v_i^n)] &= F_i^n \\ \frac{\partial}{\partial t} [v_i^p + \varepsilon_p(v_i^n - v_i^p)] &= \nu \nabla^2 v_i^p + F_i^p\end{aligned}\quad (8.2.2)$$

Setting the velocities in a similar way to the single fluid case the field is given, in Cartesian coordinates, by

$$v_i^n = [V_{0n} \cos(\omega t), 0, 0] \quad (8.2.3)$$

$$v_i^p = [V_{0p} \cos(\omega t), 0, 0] \quad (8.2.4)$$

The oscillation amplitudes in the two constituents have been assumed to be different so that we can see what happens when each fluid is driving the motion. Substituting (8.2.3) into (8.2.1) we find that the driving force is

$$F_i^n = [-\{\omega V_{0n}(1 - \varepsilon_n) + \varepsilon_n \omega V_{0p}\} \sin(\omega t), 0, 0] \quad (8.2.5)$$

$$F_i^p = [-\{\omega V_{0p}(1 - \varepsilon_p) + \varepsilon_p \omega V_{0n}\} \sin(\omega t), 0, 0] \quad (8.2.6)$$

Substituting this back into (8.2.1) we have the equations of motion in which we can include a boundary and solve for the velocity field. We assume that the fluid motion is only dependent upon time and the distance from the boundary. As in the single fluid case we insert a non-slip boundary at  $z = 0$ . The form of the component velocities are therefore taken as,

$$v_i^n = [V_X^n(z)e^{i\omega t}, V_Y^n(z)e^{i\omega t}, V_Z^n(z)e^{i\omega t}] \quad v_i^p = [V_X^p(z)e^{i\omega t}, V_Y^p(z)e^{i\omega t}, V_Z^p(z)e^{i\omega t}] \quad (8.2.7)$$

Once this assumed form of the velocity is substituted into the equations of motion (8.2.1) we divide through by  $e^{i\omega t}$  to get

$$\begin{aligned}0 &= i\omega [V_X^n + \varepsilon_n(V_X^p - V_X^n)] - i\omega [V_{0n}(1 - \varepsilon_n) + \varepsilon_n \omega V_{0p}] \\ 0 &= i\omega [V_Y^n + \varepsilon_n(V_Y^p - V_Y^n)] \\ 0 &= i\omega [V_Z^n + \varepsilon_n(V_Z^p - V_Z^n)] \\ 0 &= i\omega [V_X^p + \varepsilon_p(V_X^n - V_X^p)] - i\omega [V_{0p}(1 - \varepsilon_p) + \varepsilon_p \omega V_{0n}] - \nu \frac{\partial^2 V_X^p}{\partial z^2} \\ 0 &= i\omega [V_Y^p + \varepsilon_p(V_Y^n - V_Y^p)] - \nu \frac{\partial^2 V_Y^p}{\partial z^2} \\ 0 &= i\omega [V_Z^p + \varepsilon_p(V_Z^n - V_Z^p)] - \nu \frac{\partial^2 V_Z^p}{\partial z^2}\end{aligned}\quad (8.2.8)$$



For this set of equations we need six boundary conditions. These are taken by fixing the velocity of the protons at the boundary and infinity (similar to the single fluid example). That is, we have

$$\begin{aligned}\lim_{z \rightarrow \infty} V_i^p &= (V_{0p}, 0, 0) \\ \lim_{z \rightarrow 0} V_i^p &= (0, 0, 0)\end{aligned}\tag{8.2.9}$$

For the neutron fluid we do not need to set boundary conditions as it is superfluid.

This gives the solutions

$$\begin{aligned}V_X^n &= V_{0n} + \frac{\varepsilon_n V_{0p}}{1 - \varepsilon_n} \exp \left[ -(1+i) \sqrt{\frac{\omega}{2\nu}} \left( \sqrt{\frac{1 - \varepsilon_n - \varepsilon_p}{1 - \varepsilon_n}} \right) z \right] \\ V_X^p &= V_{0p} - V_{0p} \exp \left[ -(1+i) \sqrt{\frac{\omega}{2\nu}} \left( \sqrt{\frac{1 - \varepsilon_n - \varepsilon_p}{1 - \varepsilon_n}} \right) z \right]\end{aligned}\tag{8.2.10}$$

where the other components vanish. We define

$$\aleph = \frac{1 - \varepsilon_n - \varepsilon_p}{1 - \varepsilon_n}\tag{8.2.11}$$

The form of the velocity fields are therefore

$$\begin{aligned}v_X^n &= V_{0n} \cos(\omega t) + \frac{\varepsilon_n V_{0p}}{1 - \varepsilon_n} e^{\left(-\sqrt{\frac{\omega \aleph}{2\nu}} z\right)} \cos \left( \sqrt{\frac{\omega \aleph}{2\nu}} z - \omega t \right) \\ v_X^p &= V_{0p} \cos(\omega t) - V_{0p} e^{\left(-\sqrt{\frac{\omega \aleph}{2\nu}} z\right)} \cos \left( \sqrt{\frac{\omega \aleph}{2\nu}} z - \omega t \right)\end{aligned}\tag{8.2.12}$$

All the other velocity components vanish. In the proton fluid we can see that the entrainment enters as a modification to the Ekman layer size. For the neutrons the coupling due to entrainment has introduced an Ekman layer into the neutron velocity field. This is shown in figure 8.2 where the  $x$ -components of the two constituent velocity fields have been plotted for  $t = 0$  and  $\varepsilon_n = 0$  and  $\varepsilon_n = 0.1$ . All other free parameters have been set to unity. The purpose of the plot is not to give physical velocities, but to sketch the effect that the entrainment has on the velocity field. We can see the shift in the proton fluid velocity due to modifying the Ekman boundary layer size. We can also see that the velocity field of the neutrons only varies with position when  $\varepsilon_n$  is non-zero.

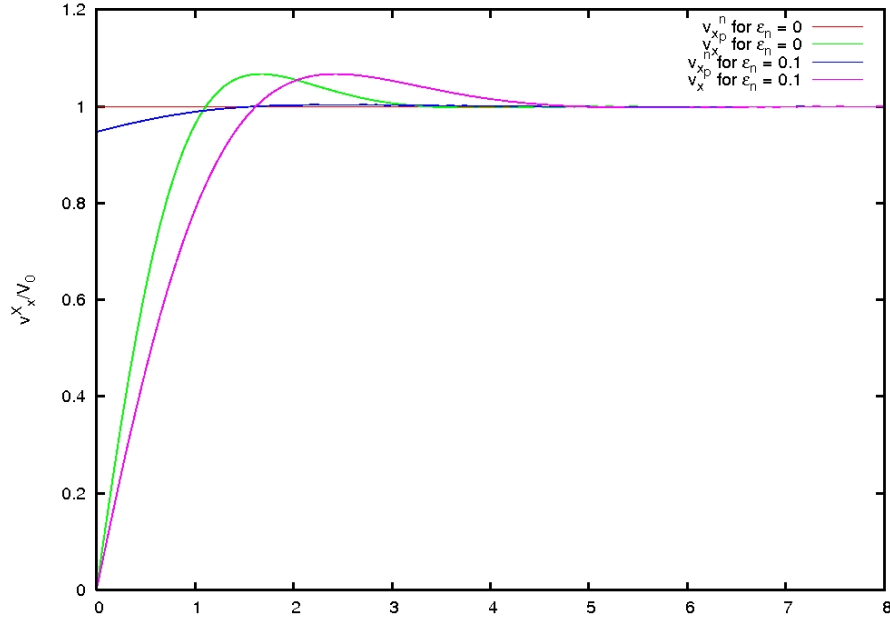


Figure 8.2: The  $x$ -direction velocity field of the two constituent rotating boundary problem at time  $t = 0$ . The boundary is at  $z = 0$ .

### 8.2.2 Mutual Friction

Finally we include the mutual friction. We ignore the chemical potentials and linearise in  $v_i$ . It is at this point that we introduce a rotation into the mutual friction term, but neglect it otherwise. This corresponds to effectively inserting vortices in the fluid but ignoring the associated large scale rotation. This is a reasonable assumption to make as we showed in the single fluid case that to first order the velocity field in the  $x$  direction is not modified for slow rotation. The equations are now

$$\begin{aligned} \frac{\partial}{\partial t} [v_i^n + \varepsilon_n (v_i^p - v_i^n)] &= 2\beta \epsilon_{ijk} \Omega^j \epsilon^{klm} \hat{\Omega}_l (v_m^n - v_m^p) + F_i^n \\ \frac{\partial}{\partial t} (v_i^p + \varepsilon_p (v_i^n - v_i^p)) &= \nu \nabla^2 v_i^p + 2\beta \frac{\rho_n}{\rho_p} \epsilon_{ijk} \Omega^j \epsilon^{klm} \hat{\Omega}_l (v_m^p - v_m^n) + F_i^p \end{aligned} \quad (8.2.13)$$

Using the same method as before we set the velocity as

$$v_i^n = [V_{0n} \cos(\omega t), 0, 0] \quad (8.2.14)$$

$$v_i^p = [V_{0p} \cos(\omega t), 0, 0] \quad (8.2.15)$$

This gives us the 'hand of God' force

$$\begin{aligned} F_X^n &= [-\omega V_{0n}(1 - \varepsilon_n) - \varepsilon_n \omega V_{0p}] \sin(\omega t) + [2\beta\Omega(V_{0n} - V_{0p})] \cos(\omega t) \\ F_X^p &= [-\omega V_{0p}(1 - \varepsilon_p) - \varepsilon_p \omega V_{0n}] \sin(\omega t) + \left[ 2\beta\Omega \frac{\rho_n}{\rho_p} (V_{0p} - V_{0n}) \right] \cos(\omega t) \end{aligned} \quad (8.2.16)$$

The other components of the force vanish. Substituting this back into the equations of motion (8.2.13) and dividing through by  $e^{i\omega t}$  gives

$$\begin{aligned} 0 &= i\omega [V_X^n + \varepsilon_n(V_X^p - V_X^n)] - i\omega [V_{0n}(1 - \varepsilon_n) + \varepsilon_n \omega V_{0p}] \\ &\quad + 2\beta\Omega [(V_X^n - V_X^p) - (V_{0n} - V_{0p})] \\ 0 &= i\omega [V_Y^n + \varepsilon_n(V_Y^p - V_Y^n)] + 2\beta\Omega (V_Y^n - V_Y^p) \\ 0 &= i\omega [V_Z^n + \varepsilon_n(V_Z^p - V_Z^n)] \\ 0 &= i\omega [V_X^p + \varepsilon_p(V_X^n - V_X^p)] - i\omega [V_{0n}(1 - \varepsilon_n) + \varepsilon_n \omega V_{0p}] \\ &\quad + 2\beta\Omega \frac{\rho_n}{\rho_p} [(V_X^p - V_X^n) - (V_{0p} - V_{0n})] - \nu \frac{\partial^2 V_X^p}{\partial z^2} \\ 0 &= i\omega [V_Y^p + \varepsilon_p(V_Y^n - V_Y^p)] + 2\beta\Omega \frac{\rho_n}{\rho_p} (V_Y^p - V_Y^n) - \nu \frac{\partial^2 V_Y^p}{\partial z^2} \\ 0 &= i\omega [V_Z^p + \varepsilon_p(V_Z^n - V_Z^p)] - \nu \frac{\partial^2 V_Z^p}{\partial z^2} \end{aligned} \quad (8.2.17)$$

Introducing the same boundary conditions as before

$$\begin{aligned} \lim_{z \rightarrow \infty} V_i^p &= (V_{0p}, 0, 0) \\ \lim_{z \rightarrow 0} V_i^p &= (0, 0, 0) \end{aligned} \quad (8.2.18)$$

the solutions are

$$\begin{aligned} V_X^n &= V_{0n} + V_{0p} \frac{i\omega\varepsilon_n - 2\Omega\beta}{i\omega(1 - \varepsilon_n) + 2\beta\Omega} \exp\left(- (1 + i)\sqrt{\frac{\omega\mathfrak{I}}{2\nu}}z\right) \\ V_X^p &= V_{0p} - V_{0p} \exp\left(- (1 + i)\sqrt{\frac{\omega\mathfrak{I}}{2\nu}}z\right) \end{aligned} \quad (8.2.19)$$

where the other components vanish and

$$\mathfrak{I} = \frac{\omega(1 - \varepsilon_n - \varepsilon_p) - 2i\beta\Omega\left(1 + \frac{\rho_n}{\rho_p}\right)}{\omega(1 - \varepsilon_n) - 2i\beta\Omega} \quad (8.2.20)$$

To find the velocity fields we need to multiply the above equations by  $e^{i\omega t}$  and take the real part. This is shown in several steps as the algebra is more complicated

than in previous cases. Firstly we split  $\mathfrak{I}$  into real and imaginary parts.

$$\mathfrak{I} = \frac{\omega^2(1 - \varepsilon_n - \varepsilon_p)(1 - \varepsilon_n) + 4\beta^2\Omega^2 \left(1 + \frac{\rho_n}{\rho_p}\right) - 2i\beta\Omega\omega\frac{\rho_n}{\rho_p}}{\omega^2(1 - \varepsilon_n)^2 + 4\beta^2\Omega^2} \quad (8.2.21)$$

Now we need to do the same for  $-(1+i)\sqrt{\frac{\omega\mathfrak{I}}{2\nu}}$ . To simplify the algebra we will use.

$$A = \omega^2(1 - \varepsilon_n - \varepsilon_p)(1 - \varepsilon_n) + 4\beta^2\Omega^2 \left(1 + \frac{\rho_n}{\rho_p}\right) \quad (8.2.22)$$

$$B = 2\beta\Omega\omega\frac{\rho_n}{\rho_p} \quad (8.2.23)$$

$$C = \omega^2(1 - \varepsilon_n)^2 + 4\beta^2\Omega^2 \quad (8.2.24)$$

so that

$$\begin{aligned} -(1+i)\sqrt{\frac{\omega\mathfrak{I}}{2\nu}} &= -(1+i)\sqrt{\frac{\omega}{2\nu}}\sqrt{\frac{A-iB}{C}} \\ &= -(1+i)\sqrt{\frac{\omega}{2\nu}}\left(\frac{A^2+B^2}{C^2}\right)^{1/4} e^{-\frac{i}{2}\tan^{-1}(A/B)} \\ &= \sqrt{\frac{\omega}{2\nu}}\left(\frac{A^2+B^2}{C^2}\right)^{1/4} \left\{ -\cos\left[\frac{1}{2}\tan^{-1}\left(\frac{A}{B}\right)\right] \right. \\ &\quad \left. -\sin\left[\frac{1}{2}\tan^{-1}\left(\frac{A}{B}\right)\right] - i\cos\left[\frac{1}{2}\tan^{-1}\left(\frac{A}{B}\right)\right] \right. \\ &\quad \left. + i\sin\left[\frac{1}{2}\tan^{-1}\left(\frac{A}{B}\right)\right] \right\} \end{aligned} \quad (8.2.25)$$

Using various trigonometric identities,

$$\begin{aligned} \cos\left[\frac{1}{2}\tan^{-1}\left(\frac{B}{A}\right)\right] &= \sqrt{\frac{1}{2} + \frac{1}{2}\cos\left(\tan^{-1}\left(\frac{B}{A}\right)\right)} \\ &= \frac{1}{2^{1/2}}\sqrt{1 + \frac{A}{\sqrt{A^2+B^2}}} = \frac{1}{2^{1/2}}\frac{\sqrt{\sqrt{A^2+B^2}+A}}{(A^2+B^2)^{1/4}} \end{aligned} \quad (8.2.26)$$

Similarly

$$\sin\left[\frac{1}{2}\tan^{-1}\left(\frac{B}{A}\right)\right] = \frac{1}{2^{1/2}}\frac{\sqrt{\sqrt{A^2+B^2}-A}}{(A^2+B^2)^{1/4}} \quad (8.2.27)$$

Leading to

$$\begin{aligned}
-(1+i)\sqrt{\frac{\omega}{2\nu}} &= -\sqrt{\frac{\omega}{4\nu C}} \left[ \sqrt{\sqrt{A^2 + B^2} + A} + \sqrt{\sqrt{A^2 + B^2} - A} \right] \\
&\quad + i\sqrt{\frac{\omega}{4\nu C}} \left[ -\sqrt{\sqrt{A^2 + B^2} + A} + \sqrt{\sqrt{A^2 + B^2} - A} \right] \\
&= -\sqrt{\frac{\omega}{2\nu C}} \left[ \sqrt{\sqrt{A^2 + B^2} + B} \right] \\
&\quad - i\sqrt{\frac{\omega}{2\nu C}} \left[ \sqrt{A - B} \right] \\
&= -D_+ - iD_-
\end{aligned} \tag{8.2.28}$$

Where,

$$\begin{aligned}
D_+ &= \sqrt{\frac{\omega}{2\nu C}} \left[ \sqrt{\sqrt{A^2 + B^2} + B} \right] \\
D_- &= \sqrt{\frac{\omega}{2\nu C}} \left[ \sqrt{A - B} \right]
\end{aligned} \tag{8.2.29}$$

Using this in the velocity fields we get

$$\begin{aligned}
v_X^n &= V_{0n} \cos(\omega t) + \frac{V_{0p}}{C} [\omega^2 \varepsilon_n (1 - \varepsilon_n) - 4\Omega^2 \beta^2] e^{-D_+ z} \cos(D_- z - \omega t) \\
&\quad + \frac{V_{0p}}{C} 2\beta\Omega\omega (1 - 2\varepsilon_n) e^{-D_+ z} \sin(D_- z - \omega t) \\
v_X^p &= V_{0p} \cos(\omega t) - V_{0p} e^{-D_+ z} \cos(D_- z - \omega t)
\end{aligned} \tag{8.2.30}$$

This gives us that the Ekman boundary layer size for both fluids is  $1/D_+$ .

## 8.3 Dissipation

What information can we extract from the velocity fields that we have calculated? We have been able to find the length scales over which the fluid is affected by the presence of a boundary. We can also say something about how the boundary dissipates energy from the system. We will consider the three cases previously discussed.

### 8.3.1 Single Fluid

Having already assumed incompressibility we find that a constant density gives us a very simple way of calculating the change in energy from the Euler equations.

Contracting the equation of motion with  $\rho v_i$  gives

$$\begin{aligned}\rho v^j \frac{\partial}{\partial t} v_j &= \rho v^j \nu \nabla^2 v_j + \rho v^j F_j \\ &= \frac{\partial}{\partial t} \left( \frac{\rho}{2} v^2 \right)\end{aligned}\quad (8.3.1)$$

As any solutions we found are periodic then we would expect that the kinetic energy averaged over an oscillation will be constant. Denoting averaging over an oscillation by  $\langle \rangle$ , equation (8.3.1) gives,

$$\left\langle \frac{\partial}{\partial t} \left( \frac{\rho}{2} v^2 \right) \right\rangle = \langle \rho v^j \nu \nabla^2 v_j \rangle + \langle \rho v^j F_j \rangle \quad (8.3.2)$$

The left hand side will vanish as it is the averaged change in kinetic energy and we are in a steady state. The right hand side contains two energy terms. The first is dissipation due to shear viscosity, while the second is due to the driving force. Any energy dissipated in the boundary layer must be balanced by energy given to the system by the driving force, giving,

$$\langle \dot{E}_D \rangle = - \langle \rho v^j F_j \rangle \quad (8.3.3)$$

where  $E_D$  is the energy dissipated per unit volume. Substituting  $F_i$  and  $v_i$  from (8.1.2) and (8.1.7) respectively, we find

$$\begin{aligned}\langle \dot{E}_D \rangle &= \rho \langle V_0^2 \omega \cos(\omega t) \sin(\omega t) \rangle \\ &\quad - \rho \left\langle \frac{V_0^2 \omega}{2} e^{-\sqrt{\frac{\omega_1}{2\nu}} z} \cos \left( \sqrt{\frac{\omega_1}{2\nu}} z - \omega t \right) \sin(\omega t) \right\rangle \\ &\quad - \rho \left\langle \frac{V_0^2 \omega}{2} e^{-\sqrt{\frac{\omega_2}{2\nu}} z} \cos \left( \sqrt{\frac{\omega_2}{2\nu}} z - \omega t \right) \sin(\omega t) \right\rangle \\ &\quad - \rho \left\langle \Omega V_0^2 e^{-\sqrt{\frac{\omega_1}{2\nu}} z} \sin \left( \sqrt{\frac{\omega_1}{2\nu}} z - \omega t \right) \cos(\omega t) \right\rangle \\ &\quad + \rho \left\langle \Omega V_0^2 e^{-\sqrt{\frac{\omega_2}{2\nu}} z} \sin \left( \sqrt{\frac{\omega_2}{2\nu}} z - \omega t \right) \cos(\omega t) \right\rangle\end{aligned}\quad (8.3.4)$$

Noting that  $\langle \sin(2\omega t) \rangle = 0$  and  $\langle \sin^2(\omega t) \rangle = \langle \cos^2(\omega t) \rangle = \frac{1}{2}$ ,

$$\langle \dot{E}_D \rangle = -\rho \frac{V_0^2 \omega_1}{4} e^{-\sqrt{\frac{\omega_1}{2\nu}} z} \sin \left( \sqrt{\frac{\omega_1}{2\nu}} z \right) - \rho \frac{V_0^2 \omega_2}{4} e^{-\sqrt{\frac{\omega_2}{2\nu}} z} \sin \left( \sqrt{\frac{\omega_2}{2\nu}} z \right) \quad (8.3.5)$$

When the frame rotation is set to zero the change in energy dissipation will be given by,

$$\langle \dot{E}_D \rangle = -\rho \frac{V_0^2 \omega}{2} e^{-\sqrt{\frac{\omega}{2\nu}} z} \sin \left( \sqrt{\frac{\omega}{2\nu}} z \right) \quad (8.3.6)$$

We can integrate this over all positive  $z$  to find the total energy dissipated per second per area of boundary. For a constant  $\delta$  we have the identity

$$\int_0^\infty e^{-z/\delta} \sin(z/\delta) dz = \frac{\delta}{2} \quad (8.3.7)$$

This gives that the change in energy dissipated by the boundary is

$$\dot{E} = \int_0^\infty \langle \dot{E}_D \rangle dz = -\rho \frac{V_0^2}{2} \sqrt{\frac{\omega\nu}{2}} \quad (8.3.8)$$

### 8.3.2 Two Fluids

We would like to do a similar calculation for the two fluid system. When entrainment is not included then finding the change in kinetic energy is a simple task as we can calculate

$$\rho_n v_n^j \frac{\partial}{\partial t} v_j^n + \rho_p v_p^j \frac{\partial}{\partial t} v_j^p \quad (8.3.9)$$

This is the change in total kinetic energy. When entrainment is included, the averaged quantity that should vanish is not so obvious as the momentum of each constituent is modified. There have been two approaches to this, though the conclusions are equivalent. The first is to define an internal energy due to the entrainment and add this to the kinetic energy [18]. It is this new quantity, the total energy dependent upon velocity, (when averaged) that can be assumed constant. On the other hand we could redefine the kinetic energy to include the effects of entrainment [57]. This may seem strange, but we have already accepted that entrainment modifies the separate fluid component momenta. It is no great leap to suggest we should also redefine the kinetic energy. Rewriting the modified energy in our notation we find

$$\dot{E}_T = \rho_n v_n^j \frac{\partial}{\partial t} \left[ v_j^n + \varepsilon_n (v_j^p - v_j^n) \right] + \rho_p v_p^j \frac{\partial}{\partial t} \left[ v_j^n + \varepsilon_n (v_j^p - v_j^n) \right] \quad (8.3.10)$$

where  $E_T$  is the energy dependent upon velocity. This is again fairly simple to calculate from the multi-fluid momentum equations.

### Entrainment

We will start by neglecting the mutual friction so that we can concentrate on the effect of entrainment in a multi-fluid system. Using the linearised equations of

motion gives

$$\begin{aligned} \rho_n v_n^j \frac{\partial}{\partial t} \left[ v_j^n + \varepsilon_n (v_j^p - v_j^n) \right] + \rho_p v_p^j \frac{\partial}{\partial t} \left[ v_j^n + \varepsilon_p (v_j^n - v_j^p) \right] \\ = \rho_p v_p^j \nu \nabla^2 v_j^p + \rho_n v_n^j F_i^n + \rho_p v_p^j F_i^p \end{aligned} \quad (8.3.11)$$

Averaging over an oscillation gives

$$\begin{aligned} 0 &= \left\langle \rho_n v_n^j \frac{\partial}{\partial t} \left[ v_j^n + \varepsilon_n (v_j^p - v_j^n) \right] + \rho_p v_p^j \frac{\partial}{\partial t} \left[ v_j^n + \varepsilon_p (v_j^n - v_j^p) \right] \right\rangle \\ &= \left\langle \rho_p v_p^j \nu \nabla^2 v_j^p \right\rangle + \left\langle \rho_n v_n^j F_j^n + \rho_p v_p^j F_j^p \right\rangle \end{aligned} \quad (8.3.12)$$

giving

$$\left\langle \dot{E}_D \right\rangle = - \left\langle \rho_n v_n^j F_j^n + \rho_p v_p^j F_j^p \right\rangle \quad (8.3.13)$$

Inserting the relevant quantities, (8.2.5) and (8.2.12), from earlier in this chapter and using  $\langle \sin(2\omega t) \rangle = 0$  and  $\langle \sin^2(\omega t) \rangle = \langle \cos^2(\omega t) \rangle = \frac{1}{2}$  we find that

$$\left\langle \dot{E}_D \right\rangle = -\frac{\rho_p}{2} V_{0p}^2 \omega \aleph e^{\left(-\sqrt{\frac{\omega \aleph}{2\nu}} z\right)} \sin\left(\sqrt{\frac{\omega \aleph}{2\nu}} z\right) \quad (8.3.14)$$

where  $\aleph$  was defined in equation (8.2.11) Using (8.3.7) we calculate the total dissipation per second per area of boundary as

$$\dot{E} = \int_0^\infty \left\langle \dot{E}_D \right\rangle dz = -\rho_p \frac{V_{0p}^2}{2} \sqrt{\frac{\nu \omega \aleph}{2}} \quad (8.3.15)$$

This result shows how the dissipated energy is affected by entrainment.

### Mutual Friction

Constructing a multi-fluid energy equation, including mutual friction, gives

$$\begin{aligned} \rho_n v_n^j \frac{\partial}{\partial t} \left[ v_j^n + \varepsilon_n (v_j^p - v_j^n) \right] + \rho_p v_p^j \frac{\partial}{\partial t} \left[ v_j^n + \varepsilon_p (v_j^n - v_j^p) \right] \\ = \rho_p v_p^j \nu \nabla^2 v_j^p + \rho_n v_n^i 2\beta \epsilon_{ijk} \Omega^j \epsilon^{klm} \hat{\Omega}_l (v_m^n - v_m^p) \\ + \rho_n v_p^i 2\beta \epsilon_{ijk} \Omega^j \epsilon^{klm} \hat{\Omega}_l (v_m^p - v_m^n) + \rho_n v_n^j F_j^n + \rho_p v_p^j F_j^p \end{aligned} \quad (8.3.16)$$

Which when averaged over an oscillation becomes

$$\left\langle \dot{E}_I \right\rangle = \left\langle \dot{E}_D \right\rangle + \left\langle \rho_n v_n^j F_j^n + \rho_p v_p^j F_j^p \right\rangle = 0 \quad (8.3.17)$$



where  $\dot{E}_D$  now includes the effect of mutual friction. We substitute  $F_i^X$  (8.2.16) and  $v_i^X$  (8.2.30) into this while remembering that  $\langle 2 \sin(\omega t) \cos(\omega t) \rangle = \langle \sin(2\omega t) \rangle = 0$  and  $\langle \sin^2(\omega t) \rangle = \langle \cos^2(\omega t) \rangle = \frac{1}{2}$  to get

$$\begin{aligned}
 \langle \dot{E}_D \rangle &= - \langle \rho_n v_n^j F_j^n + \rho_p v_p^j F_j^p \rangle \\
 &= - \rho_n \beta \Omega (V_{0n} - V_{0p})^2 \\
 &\quad + \rho_n \frac{V_{0p}}{2C} e^{-D_+ z} \sin(D_- z) \left\{ - 8\beta^2 \Omega^2 \omega V_{0n} (1 - \varepsilon_n) \right. \\
 &\quad \left. + 4\beta^2 \Omega^2 \omega V_{0p} \left( 1 - 2\varepsilon_n - \frac{\rho_p}{\rho_n} \right) - \frac{\rho_p}{\rho_n} \omega^3 V_{0p} (1 - \varepsilon_p - \varepsilon_n) (1 - \varepsilon_n) \right\} \\
 &\quad + \rho_n \frac{V_{0p}}{2C} e^{-D_+ z} \cos(D_- z) 2\beta \Omega \left\{ V_{0p} \omega^2 (1 - 2\varepsilon_n + 2\varepsilon_n^2) - 2V_{0n} \omega^2 (1 - \varepsilon_n)^2 \right\}
 \end{aligned} \tag{8.3.18}$$

The first term in this expression is due to the mutual friction between the two constituents throughout the fluid. It is due to the velocity difference set up in the background and is not an effect of having a boundary. So that we can concentrate on boundary effects we set  $V_{0n} = V_{0p} = V_0$ . We also neglect  $\beta^2$  terms as we have already neglected  $\beta'$  which is of the same order. Integrating this expression over  $z$  we find the dissipated energy per area of boundary as

$$\begin{aligned}
 \int_0^\infty \langle \dot{E}_D \rangle dz &= - \rho_p \omega^3 \frac{V_0^2}{2C} \frac{D_-}{D_+^2 + D_-^2} (1 - \varepsilon_p - \varepsilon_n) (1 - \varepsilon_n) \\
 &\quad - \rho_n \beta \Omega \frac{V_0^2 \omega^2}{C} \frac{D_+}{D_+^2 + D_-^2} (1 - 2\varepsilon_n)
 \end{aligned} \tag{8.3.19}$$

This is unfortunately still too complicated to substitute the expressions for  $C$ ,  $D_+$  and  $D_-$  back in to this solution without getting lost in algebra. Concentrating on the role of mutual friction we set  $\varepsilon_n = \varepsilon_p = 0$ . We then find that

$$A \approx \omega^2 \tag{8.3.20}$$

$$B = 2\beta \Omega \omega \frac{\rho_n}{\rho_p} \tag{8.3.21}$$

$$C \approx \omega^2 \tag{8.3.22}$$

$$D_+ \approx \sqrt{\frac{1}{2\nu\omega}} \left( \omega + \beta \Omega \frac{\rho_n}{\rho_p} \right) \tag{8.3.23}$$

$$D_- \approx \sqrt{\frac{1}{2\nu\omega}} \left( \omega - \beta \Omega \frac{\rho_n}{\rho_p} \right) \tag{8.3.24}$$

This gives us that (8.3.19) is approximately

$$\dot{E}_\beta = \int_0^\infty \langle \dot{E}_D \rangle dz = -\rho_p \omega \frac{V_0^2}{2} \sqrt{\frac{\nu}{2\omega}} \left( 1 + \beta \frac{\Omega}{\omega} \frac{\rho_n}{\rho_p} \right) \quad (8.3.25)$$

We can look at how large an effect we expect the mutual friction to have by taking the ratio of the energy dissipated in the mutual friction case  $\dot{E}_\beta$  to the single fluid case  $\dot{E}_0$ . In the absence of any coupling, the two-fluid case reduces to the single fluid problem where  $\rho$  is the proton density. We find that the ratio is

$$\frac{\dot{E}_\beta}{\dot{E}_0} = \left( 1 + \beta \frac{\Omega}{\omega} \frac{\rho_n}{\rho_p} \right) \quad (8.3.26)$$

For typical values,  $\beta = 4 \times 10^{-4}$ ,  $\Omega = 40$  s and  $\rho_p/\rho_n = 0.05$ , we find

$$\frac{\dot{E}_\beta}{\dot{E}_0} = \left( 1 + \frac{1.2 \times 10^{-1}}{\omega} \right) \quad (8.3.27)$$

This shows that  $\omega$  does not have to be very small for mutual friction to have a significant effect. On the other hand if we choose the oscillation is an inertial mode we know that  $\omega \approx 2\Omega$ . Substituting this into (8.3.26) and leaving  $\beta$  as a free parameter we find

$$\frac{\dot{E}_\beta}{\dot{E}_0} = (1 + 10\beta) \quad (8.3.28)$$

This shows that we need  $\beta \geq 0.1$  for the energy dissipated to be significantly modified by mutual friction. For expected values of  $\beta$  this is not the case. For inertial waves we would not expect mutual friction to be important in calculating the effect of Ekman layers on inertial modes. It is only for lower frequency waves that mutual friction will be important.

## 8.4 Summary

We have carried out an initial investigation into the significance of including a boundary when considering superfluid oscillation problems. This will be important when considering global oscillations of a neutron star (see for example or references [31]). In particular, we have set up a two constituent model with a boundary and calculated how the mutual friction affects the energy that is dissipated from the system by the boundary. We have shown that there are situations in which

the mutual friction has a significant effect on the solution. This is particularly important when considering the damping of global modes. For future work we would like to relax the  $\beta' = 0$  assumption so that the strong coupling case of the vortex lines to the proton fluid can be investigated. This may be particularly important in models of free precession [32]

## Chapter 9

# Glitches

So far we have only considered some of the local effects of a two constituent fluid. We need to apply these findings to the model of a neutron star and observed phenomena. To describe any neutron star phenomena in full will take a more complicated model than we will construct, but we can take the first few steps. In this chapter we concentrate on the glitch phenomenon in which the interaction between the internal constituents is thought to be important. A glitch is a global phenomenon and so we want to use our equations of motion to describe the star as a whole. In doing so we will focus on the bulk motion, neglecting the detailed fluid dynamics. The hope is that this will lead to a representation of the basic dynamics of the system [69].

### 9.1 Conservation of energy and angular momentum

If we consider the star as a closed system then the energy and angular momentum of the star will be conserved. As a starting point we will consider a star composed of a single fluid. This will give us a feel for how to approach the more complicated two-constituent problem.

### 9.1.1 Single fluid

For a single fluid we can write the Euler equations as

$$\mathcal{E}_i = \left( \frac{\partial}{\partial t} + v^j \nabla_j \right) v_i + \nabla_i (\tilde{\mu} + \phi) = 0 \quad (9.1.1)$$

where  $\phi$  is the gravitational potential and  $\tilde{\mu} = \mu/m$  is the chemical potential divided by the mass of a particle. We have assumed that the energy  $E$  depends only upon the number density  $n$ . From this the pressure  $P$  of the fluid is defined by

$$d\mu = \frac{1}{n} dP \quad (9.1.2)$$

For simplicity we will assume that the fluid in the whole star is rotating like a solid body around an axis, which we label  $z$ . We will now derive the conservation of angular momentum and energy from the Euler equations. The fluid velocity can be written as

$$v_i = \epsilon_{ijk} \Omega^j x^k = \Omega r \varphi_i \quad (9.1.3)$$

where we take  $\Omega = \Omega(t)$ ,  $r$  is the distance from the  $z$ -axis and  $\varphi_i$  is a unit vector in the direction of rotation. It follows that

$$v^j \nabla_j v_i = 0 \quad (9.1.4)$$

$$v^j \nabla_j (\tilde{\mu} + \phi) = 0 \quad (9.1.5)$$

Contracting (9.1.1) with  $\rho v_i$  and integrating over a fixed volume  $V$  gives

$$\frac{\partial E}{\partial t} = \int \rho v^j \frac{\partial v_j}{\partial t} dV = \frac{\partial}{\partial t} \left( \frac{1}{2} \int \rho v^2 dV \right) = 0 \quad (9.1.6)$$

This shows that the kinetic energy is conserved in the system. It was unnecessary to specify the shape of the volume so this holds when  $V$  is the volume of the neutron star. From the assumption that the fluid is in solid body rotation we have

$$v^2 = \Omega_j \Omega^k \left( \delta_k^j x^2 - x^j x_k \right) \quad (9.1.7)$$

where  $x^2 = x^j x_j$ . From this we define the moment of inertia as

$$I_l^i = \int \rho (\delta_l^i x^2 - x^i x_l) dV \quad (9.1.8)$$

We can use (9.1.7) and (9.1.8) to rewrite the change in kinetic energy equation (9.1.6) as

$$\frac{\partial E}{\partial t} = \frac{1}{2} \frac{\partial}{\partial t} \left( I_l^i \Omega_i \Omega^l \right) = 0 \quad (9.1.9)$$

We now consider the  $z$  component of the angular momentum. We need to assume

$$\epsilon_{ijk} x^j \nabla^k (\tilde{\mu} + \phi) = 0 \quad \text{for} \quad i = z \quad (9.1.10)$$

Contracting  $\mathcal{E}_i$  with  $\rho \epsilon_{ijk} x^j$  and integrating gives

$$\begin{aligned} \frac{\partial J_i}{\partial t} &= \int \rho \epsilon_{ijk} x^j \mathcal{E}^k dV \\ &= \frac{\partial}{\partial t} \left[ \int \rho \Omega^j (\delta_j^i x^2 - x^i x_j) dV \right] = \frac{\partial}{\partial t} (I_j^i \Omega^j) = 0 \quad \text{for} \quad i = z \end{aligned} \quad (9.1.11)$$

We can see that for cylindrical polar coordinates with  $\Omega^i = (0, 0, \Omega)$  and  $I_z^z = I$  we will get the standard results

$$E = \frac{1}{2} I \Omega^2 \quad \text{and} \quad J^z = I \Omega \quad (9.1.12)$$

### 9.1.2 Two constituents

We now consider a two constituent star. In order for this to be a simple step we ignore any mutual friction effects. The Euler equations can be written as

$$\mathcal{E}_i^X = \left( \frac{\partial}{\partial t} + v_X^j \nabla_j \right) (v_i^X + \varepsilon_X w_i^{YX}) + \nabla_i (\phi + \tilde{\mu}_X) + \varepsilon_X w_j^{YX} \nabla_i v_X^j = 0 \quad (9.1.13)$$

Following the analysis in the previous section, we take the velocity fields of the constituents to those of rotating solid bodies. We also assume that the two constituents are rotating around the same axis so that we can write

$$v_i^X = \Omega_X r \varphi^i \quad \text{and} \quad w_{YX}^i = v_Y^i - v_X^i = (\Omega_Y - \Omega_X) r \varphi^i \quad (9.1.14)$$

As we are assuming solid body rotation  $\Omega_X$  are constant. From these assumptions and the axial symmetry of the system we find that

$$v_X^j \nabla_j v_i^X = 0 \quad (9.1.15)$$

$$v_X^j \nabla_j (\phi + \tilde{\mu}_X) = 0 \quad (9.1.16)$$

We continue to follow the method used in the single fluid case and contract  $\mathcal{E}_i^X$  with  $\rho_X v_i^X$  and integrate over a fixed volume to find

$$\frac{\partial E_X}{\partial t} = \int \rho_X v_i^X \mathcal{E}_i^X dV = \frac{1}{2} \int \left[ (\rho_X - 2\alpha) \frac{\partial}{\partial t} v_X^2 + 4\alpha v_X^j \frac{\partial v_j^Y}{\partial t} \right] dV = 0 \quad (9.1.17)$$

Writing the constituent indices explicitly, we have

$$\frac{\partial E_n}{\partial t} = \frac{1}{2} \int \left[ (\rho_n - 2\alpha) \frac{\partial}{\partial t} v_n^2 + 4\alpha v_n^j \frac{\partial v_j^p}{\partial t} \right] dV = 0 \quad (9.1.18)$$

$$\frac{\partial E_p}{\partial t} = \frac{1}{2} \int \left[ (\rho_p - 2\alpha) \frac{\partial}{\partial t} v_p^2 + 4\alpha v_p^j \frac{\partial v_j^n}{\partial t} \right] dV = 0 \quad (9.1.19)$$

From this we can find the total change in energy by adding these two expressions to get

$$\frac{\partial E}{\partial t} = \frac{\partial E_n}{\partial t} + \frac{\partial E_p}{\partial t} = \frac{1}{2} \frac{\partial}{\partial t} \left\{ \int [\rho_n v_n^2 + \rho_p v_p^2 - 4\alpha w_{np}^2] dV \right\} = 0 \quad (9.1.20)$$

We know that this represents the conservation of energy of the system. It is clear that this equation contains more than the combined kinetic energies of the two constituents. The total energy also includes the internal energy due to entrainment. This was shown in section 8.3.2, equation (8.3.10). The constituent moment of inertia is defined by

$$I_{X_i}^j = \int \rho_X (\delta_i^j x^2 - x_i x^j) dV \quad (9.1.21)$$

so that for  $\Omega_i^X$  aligned along the  $z$ -axis

$$\frac{\partial E}{\partial t} = \frac{\partial}{\partial t} \left\{ \frac{1}{2} I_n \Omega_n [\Omega_n + \varepsilon_n (\Omega_p - \Omega_n)] + \frac{1}{2} I_p \Omega_p [\Omega_p + \varepsilon_p (\Omega_n - \Omega_p)] \right\} = 0 \quad (9.1.22)$$

where  $I_X = I_{X_z}$ . Similarly we can calculate the total change in angular momentum. We note that

$$\epsilon_{ijk} x^j v_X^l \nabla^k v_l^X = \epsilon_{ijk} x^j x^k \Omega_X^2 - \epsilon_{ijk} x^j \Omega_k^X x_l \Omega_X^l = 0 \quad \text{for } i = z \quad (9.1.23)$$

as  $\Omega_i^X$  is parallel to the  $z$ -axis. Contracting  $\mathcal{E}_i^X$  with  $\rho_x \epsilon_{ijk} x^j$  and integrating over a volume  $V$  gives,

$$\begin{aligned} \frac{\partial J_z^X}{\partial t} &= \int \rho_X \epsilon_{ijk} x^j \mathcal{E}^k dV \\ &= \int \rho_X \epsilon_{ijk} x^j \left[ (1 - \varepsilon_X) \frac{\partial v_X^k}{\partial t} + \varepsilon_X \frac{\partial v_Y^k}{\partial t} \right] dV = 0 \quad \text{for } i = z \end{aligned} \quad (9.1.24)$$

We can write this in terms of inertia to get

$$\frac{\partial J_i^X}{\partial t} = \frac{\partial}{\partial t} \left\{ I_{X_i}^j [\Omega_j^X + \varepsilon_X (\Omega_j^Y - \Omega_j^X)] \right\} = 0 \quad \text{for } i = z \quad (9.1.25)$$

Adding the two equations we find that

$$\frac{\partial J_z}{\partial t} = \frac{\partial}{\partial t} (I_n \Omega_n + I_p \Omega_p) = 0 \quad (9.1.26)$$

We have shown the unsurprising result that total angular momentum is conserved.

If one constituent spins down then the other must spin up.

## 9.2 Simple spin down model

We are not yet in a position to model a simple glitch as we have not included the mutual friction as a coupling mechanism. Before we do this it is useful to look at how we may use the conservation equations we have found to model the rotational evolution of a neutron star. We showed in (9.1.25) that the angular momentum of each separate constituent is conserved. In a neutron star we would expect the protons to be spun down due to a magnetic torque  $j_i^{em}$ . We include this in the equations by breaking the conservation of the proton angular momentum, so that

$$\frac{\partial J_i^p}{\partial t} = -j_i^{em} \quad (9.2.1)$$

We will assume that the magnetic torque is related to the angular velocity of the protons by

$$j_{em} = \mathcal{A} I_p \Omega_p^3 \quad (9.2.2)$$

This represents the standard magnetic dipole model. We will assume that the constituent moments of inertia are constant. Noting that  $I_n \varepsilon_n = I_p \varepsilon_p$  and defining  $\varepsilon = \varepsilon_p$  the equations (9.1.25) become

$$I_n \dot{\Omega}_n + I_p \varepsilon (\dot{\Omega}_p - \dot{\Omega}_n) = 0 \quad (9.2.3)$$

$$I_p \dot{\Omega}_p + I_p \varepsilon (\dot{\Omega}_n - \dot{\Omega}_p) = -\mathcal{A} I_p \Omega_p^3 \quad (9.2.4)$$

Defining  $\tilde{I} = I_p/I_n$  then (9.2.3) gives

$$\dot{\Omega}_n = -\frac{\varepsilon \tilde{I}}{1 - \varepsilon \tilde{I}} \dot{\Omega}_p \quad (9.2.5)$$



Substituting this into (9.2.4) gives

$$\left(1 - \varepsilon - \frac{\varepsilon^2 \tilde{I}}{1 - \varepsilon \tilde{I}}\right) \dot{\Omega}_p = -\mathcal{A} \Omega_p^3 \quad (9.2.6)$$

Rearranging this gives

$$\underbrace{\left(1 - \frac{\varepsilon}{1 - \varepsilon \tilde{I}}\right)}_{\equiv \bar{I}} \dot{\Omega}_p = -\mathcal{A} \Omega_p^3 \quad (9.2.7)$$

This is a separable equation and so we must solve the integral equation

$$\int_{\Omega_0}^{\Omega_p} \frac{d\Omega_p}{\Omega_p^3} = -\frac{\mathcal{A}}{\bar{I}} \int_{t_0}^t dt \quad (9.2.8)$$

where  $\Omega_0$  is  $\Omega_p$  at time  $t_0$ . Setting  $t_0 = 0$  we find the solution is

$$\frac{1}{\Omega_0^2} - \frac{1}{\Omega_p^2} = -\frac{2\mathcal{A}}{\bar{I}} t \quad (9.2.9)$$

or equivalently

$$\Omega_p = \Omega_0 \left(1 + \frac{2\mathcal{A}\Omega_0^2 t}{\bar{I}}\right)^{-1/2} \quad (9.2.10)$$

For  $\mathcal{A}\Omega_0^2 t / \bar{I} \ll 1$  we can expand to get

$$\Omega_p \approx \Omega_0 \left(1 - \frac{\mathcal{A}\Omega_0^2 t}{\bar{I}}\right) \quad (9.2.11)$$

From this we can find the characteristic timescale  $\tau$  for the protons to become static. Ignoring entrainment effects we have that

$$\tau = \frac{1}{\mathcal{A}\Omega_0^2} \quad (9.2.12)$$

$\mathcal{A}$  has been calculated from the standard dipole model of neutron stars [73]. Modifying the standard result so that the torque acts on the proton fluid rather than the whole star we find

$$\mathcal{A} = \frac{B_p^2 R^6 \sin^2 \theta}{6c^3 I_p} \quad (9.2.13)$$

where  $B_p$  is the magnetic strength of the dipole with axis at an angle  $\theta$  to the rotation axis.  $R$  is the radius of the star and  $c$  is the speed of light. As  $I_p \ll I_n \approx I$  we write

$$I_p \approx \frac{I_p}{I_n} I \approx \frac{I_p}{I_n} \frac{2MR^2}{5} \quad (9.2.14)$$

where  $M$  is the mass of the star. Typically accepted values for these parameters for a glitching neutron star are,  $B = 10^{12} \text{G}$ ,  $R = 10^6 \text{cm}$ ,  $I_p/I_n = 0.1$ ,  $\Omega_0 =$

$2\pi/0.15 \text{ s}^{-1}$  and  $M$  is 1.4 solar masses. We set  $\theta = \pi/2$  to find the timescale over which  $\Omega_p$  decays is

$$\tau \approx 4 \times 10^{12} \text{ s} \approx 10^5 \text{ years} \quad (9.2.15)$$

We can now use this to find the change in period  $\dot{P}$ . We know that

$$P = \frac{2\pi}{\Omega_p} \rightarrow \dot{P} = -\frac{2\pi}{\Omega_p^2} \dot{\Omega}_p \quad (9.2.16)$$

From (9.2.7) and (9.2.12) we have that

$$\dot{\Omega}_p \approx -\frac{\Omega_0}{\tau} \quad (9.2.17)$$

so that

$$\dot{P} \approx \left( \frac{\Omega_0}{\Omega_p} \right) \frac{P}{\tau} \approx 10^{-13} \quad (9.2.18)$$

From (9.2.5) we have that

$$\Omega_n - \Omega_{0n} = -\frac{\varepsilon \tilde{I}}{1 - \varepsilon \tilde{I}} (\Omega_p - \Omega_0) \quad (9.2.19)$$

where  $\Omega_{0n} = \Omega_n(0)$ . We substitute (9.2.11) into this, to get

$$\Omega_n \approx \Omega_{0n} + \frac{\varepsilon \tilde{I}}{1 - \varepsilon \tilde{I}} \frac{\Omega_0 t}{\tau} \quad (9.2.20)$$

We can use this to find how long it takes for a ‘reasonable’ lag to develop between the two constituents. Assuming that the two constituents are rotating together at time  $t = 0$  then  $\Omega_{0n} = \Omega_0$ . The lag is then given by

$$\begin{aligned} \Delta\Omega = \Omega_n - \Omega_p &= \frac{\varepsilon \tilde{I}}{1 - \varepsilon \tilde{I}} \frac{\Omega_0 t}{\tau} + \frac{\Omega_0 t}{\tau} \\ &= \left( 1 + \frac{\varepsilon \tilde{I}}{1 - \varepsilon \tilde{I}} \right) \frac{\Omega_0 t}{\tau} = \frac{1}{1 - \varepsilon \tilde{I}} \frac{\Omega_0 t}{\tau} \end{aligned} \quad (9.2.21)$$

or

$$\frac{\Delta\Omega}{\Omega_p} \approx \frac{1}{1 - \varepsilon \tilde{I}} \frac{t}{\tau} \quad (9.2.22)$$

It has been suggested [55] that the neutron star can sustain a relative lag  $\frac{\Delta\Omega}{\Omega_p}$  of  $\approx 10^{-4}$ . From (9.2.22) we find that

$$\frac{t}{\tau} \approx 10^{-4} \rightarrow t \approx 10 \text{ years} \quad (9.2.23)$$

Glitches have been observed to occur every few years in some neutron stars. The time that we have calculated is thus of the correct order.

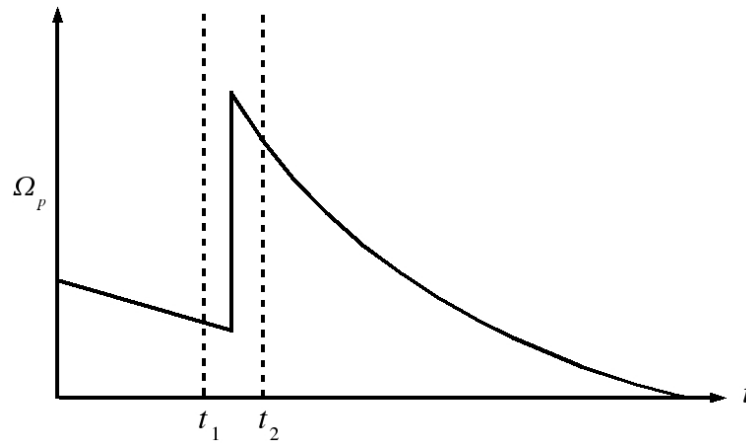


Figure 9.1: A typical glitch profile

### 9.3 Modelling a Glitch

Before incorporating the mutual friction into this global model, we will look at a possible mechanism for glitches. Figure 9.1 shows a typical glitch frequency profile. In our discussions of superfluids we have concentrated on the vortices that allow the superfluid to rotate. We know that these vortices must end on a boundary of the fluid, or form loops. For the neutrons in a neutron stars core to rotate there will be many vortices threading through the star. The usual assumption is that the vortices are in a straight array. This is because it is the simplest configuration of vortex lines that allows rotation in the superfluid. For our simple glitch model we will also use this assumption. It is worth noting that a polarized turbulent configuration of vortices also involves rotation. We will not consider turbulent flows as we have seen that we expect turbulence to be a localised effect. It would be difficult to apply this to a global model. We should also investigate the simpler case of straight vortices before complicating the problem. For either case there will be vortex lines that end on the boundary of the fluid. For a neutron star this boundary will be the crust. It has been suggested that there will be a force between the vortex core and the nucleons in the crust lattice. This will 'pin' the vortices in place. It is easy to see that in the case of a straight array this pinning will fix the vortex number density. This in turn fixes the neutron fluids angular momentum. If we assume that the charged fluid is locked to the crust via magnetic

effects then there will be no drag on the vortex lines from electron scattering. The vortices will be rotating with the charged fluid component. The crust, and hence the charged fluid and vortices, will be acted on by the magnetic torque and will be 'spun down'. The Magnus force will be acting on the vortices as there will be a velocity difference between the vortex lines and the neutron fluid. For the vortices to stay pinned this Magnus force must be balanced by the forces on the vortex from the crust. At some critical velocity difference we would expect the Magnus force to overcome the pinning force. This velocity difference is the lag  $\Delta\Omega$  that was discussed in the previous section. Assuming that all of the vortices unpin simultaneously then the mutual friction will act throughout the star. This becomes the mechanism by which the two fluid constituents couple and the lag decays. This is the glitch jump. There is an exchange of angular momentum from the neutron fluid to the protons. Now that the lag is smaller the vortices can begin to repin to the crust. This repinning is the relaxation part of the glitch. Finally the system is in a position for the lag to increase and eventually glitch again. To model this proposed mechanism we are going to need to split the model in several sections. Referring to figure 9.1 we look at the regions  $t < t_1$ ,  $t_1 < t < t_2$  and  $t > t_2$ . In the pre-glitch region  $t < t_1$  the vortices are completely pinned. For the glitch region where  $t_1 < t < t_2$  the most important force will be the mutual friction. This should be a short phase of the glitch and so the magnetic torque will be a small effect. In the relaxation region where  $t > t_2$  we need to find a way to repin the vortices and investigate the interaction of the mutual friction with the magnetic torque.

### 9.3.1 Pre-glitch

For this region we have already mentioned that there will be no friction between the two constituents due to electron scattering off the vortices. For a completely straight array we can assume that the Magnus force on the vortices will be balanced by pinning forces in the crust. This problem reduces to the one already studied in section 9.2. The evolution of the rotation of the proton and neutron fluids will be given by (9.2.11) and (9.2.20), respectively. As a comment on the effects of

entrainment, if we look at a small part of this region then  $\dot{J}_{em}$  will be approximately constant. Solving (9.1.25) we find

$$\dot{\Omega}_p = -\frac{1}{I_p} \left( 1 - \frac{\varepsilon I_n}{I_n - \varepsilon I_p} \right)^{-1} \dot{J}_{em} \quad (9.3.1)$$

This tells us that even though there is a spin down torque acting on the proton momentum the velocity of the protons can, in fact, increase when

$$\frac{I_n}{I_n + I_p} < \varepsilon < \frac{I_n}{I_p} \quad (9.3.2)$$

For  $\varepsilon$  of order unity and  $I_p/I_n \approx 0.1$  which are expected to be typical in the outer core [19] we find that the crust would be spun down as expected. On the other hand if we look at the neutron fluid we find the condition for spin up is

$$0 < \varepsilon < \frac{I_n}{I_n + I_p} \quad (9.3.3)$$

For the expected values of  $\varepsilon$  and  $I_p/I_n$  we find the neutron fluid spins up. As we do not observe the neutron fluid directly this does not help us to constrain the entrainment parameter, though it is a nice example of the drastic effect that entrainment can have on a system.

### 9.3.2 The glitch

To model the glitch we need to include the mutual friction into our model. As the glitch occurs over a short timescale we will ignore spin down effects due to the magnetic torque. As in section 9.2 we need to set up global evolution equations.

#### Evolution equations

The equations of motion for the two constituents are

$$\begin{aligned} \mathcal{E}_i^X &= \left( \frac{\partial}{\partial t} + v_X^j \nabla_j \right) (v_i^X + \varepsilon_X w_i^{YX}) + \nabla_i (\phi + \tilde{\mu}_X) + \varepsilon_X w_j^{YX} \nabla_i v_X^j \\ &= \frac{\rho_n}{\rho_X} \beta |\lambda| w_i^{YX} - \frac{\rho_n}{\rho_X} \beta' \epsilon_{ijk} \lambda^j w_{YX}^k \end{aligned} \quad (9.3.4)$$

where

$$\lambda_i = 2\Omega_i^n + \varepsilon_n (2\Omega_i^p - 2\Omega_i^n) \quad (9.3.5)$$

We will again assume that the two constituents are rotating around a common axis  $z$ . From this we can find the energy equations for each constituent as

$$\begin{aligned}\frac{\partial E_X}{\partial t} &= \int \rho_X v_X^j \mathcal{E}_j^X dV \\ &= \int \rho_X v_X^j \beta \frac{\rho_n}{\rho_X} |\lambda| w_j^{YX} - \rho_X v_X^j \beta' \frac{\rho_n}{\rho_X} \epsilon_{jkl} \lambda^k w_{YX}^l dV\end{aligned}\quad (9.3.6)$$

The second term on the right hand side will vanish as  $v_i^X$  is parallel to  $w_i^{YX}$ . Written in terms of inertia  $I_{X_i}^j$  (9.1.21) and setting  $\Omega_i^x = (0, 0, \Omega_x)$  the total change in energy is given by

$$\begin{aligned}\frac{\partial E_X}{\partial t} &= \frac{\partial}{\partial t} \left\{ \frac{1}{2} I_n \Omega_n [\Omega_n + \varepsilon_n (\Omega_p - \Omega_n)] + \frac{1}{2} I_p \Omega_p [\Omega_p + \varepsilon_p (\Omega_n - \Omega_p)] \right\} \\ &= -\beta |\lambda| (\Omega_p - \Omega_n)^2 I_n\end{aligned}\quad (9.3.7)$$

We can see that when mutual friction is included then there will be a loss of kinetic energy. The stable state will be when the two fluids are rotating together ( $\Omega_p = \Omega_n$ ). We can also calculate the global change in angular momentum for each constituent. Looking at the  $z$  component of the angular momentum we find

$$\begin{aligned}\frac{\partial J_i^X}{\partial t} &= \int \rho_X \epsilon_{ijk} x^j \mathcal{E}^k dV \\ &= \int \epsilon_{ijk} x_X^j \beta \rho_n |\lambda| w_{YX}^k - \epsilon_{ijk} x_X^j \beta' \rho_n \epsilon^{klm} \lambda_l w_m^{YX} dV\end{aligned}\quad (9.3.8)$$

Noting that

$$\epsilon_{ijk} x_X^j \epsilon^{klm} \lambda_l w_m^{YX} = x_X^j \lambda_i w_j^{YX} - x_X^j \lambda_j w_i^{YX} = 0 \quad \text{for } i = z \quad (9.3.9)$$

and

$$\epsilon_{ijk} x_X^j w_{YX}^k = \epsilon_{ijk} x_X^j \epsilon^{klm} \Omega_l^{YX} x_m^X = \Omega_i^{YX} x_X^j x_j^X - \Omega_j^{YX} x_X^j x_i^X \quad (9.3.10)$$

we can write the change in angular momentum in terms of the constituent moments of inertia to get

$$\frac{\partial J_i^X}{\partial t} = \beta |\lambda| (\Omega_j^Y - \Omega_j^X) I_{n_i}^j \quad (9.3.11)$$

The total angular momentum is given by

$$\frac{\partial J_i}{\partial t} = \frac{\partial J_i^n}{\partial t} + \frac{\partial J_i^p}{\partial t} = 0 \quad (9.3.12)$$

This shows that the angular momentum is conserved. This is exactly what we would expect as there are no external forces involved.

### Solving the evolution equations

To solve these equations we will rewrite them in terms of the lag and a quantity related to the total angular momentum. The conservation of angular momentum will make this variable a simple one to deal with, while the lag is an important quantity. For simplicity we will neglect the effect of entrainment. From (9.1.26), (9.3.12) and assuming that the moment of inertia of each constituent is constant we define  $V$  from the angular momentum such that

$$I_n \dot{\Omega}_n + I_p \dot{\Omega}_p = I \dot{V} = 0 \quad (9.3.13)$$

This will give us that  $V$  is a constant. From (9.1.26) and (9.3.11) we find that the rate of change of lag is given by

$$\dot{\Omega}_n - \dot{\Omega}_p = \dot{\mathcal{W}} = -2\Omega_n \beta \left(1 + \frac{I_n}{I_p}\right) \mathcal{W} \quad (9.3.14)$$

where  $\mathcal{W} = \Omega_n - \Omega_p$  is the lag. From (9.3.13) we can rewrite  $V$  as

$$\begin{aligned} V &= \frac{I_n}{I} \Omega_n + \frac{I_p}{I} \Omega_p = \frac{I_n}{I} \Omega_n + \frac{I_p}{I} (\Omega_n - \mathcal{W}) \\ &= \Omega_n - \frac{I_p}{I} \mathcal{W} \end{aligned} \quad (9.3.15)$$

Substituting this into (9.3.14) gives

$$\dot{\mathcal{W}} = -2\beta \left(V + \frac{I_p}{I} \mathcal{W}\right) \left(1 + \frac{I_n}{I_p}\right) \mathcal{W} \quad (9.3.16)$$

This is the stage at which the change of variables helps us. Because  $V$  is a constant (9.3.16) is a separable equation so we must solve the integral

$$\begin{aligned} \int_{\mathcal{W}_0}^{\mathcal{W}} \left(V + \frac{I_p}{I} \mathcal{W}\right)^{-1} \mathcal{W}^{-1} d\mathcal{W} \\ = \int_{\mathcal{W}_0}^{\mathcal{W}} \frac{I_p}{IV} \left(\frac{1}{\mathcal{W}} - \frac{1}{\mathcal{W} - IV/I_p}\right) d\mathcal{W} = -2\beta \frac{I}{I_p} \int_{t_0}^t dt \end{aligned} \quad (9.3.17)$$

where  $\mathcal{W}_0 = \mathcal{W}(t_0)$ . For simplicity we assume that the glitch occurs at time  $t_0 = 0$ . This means that the lag at the moment of unpinning is  $\mathcal{W}_0$ . Solving the integral we find

$$\ln(\mathcal{W}) - \ln(\mathcal{W}_0) - \ln\left(\mathcal{W} + \frac{IV}{I_p}\right) + \ln\left(\mathcal{W}_0 + \frac{IV}{I_p}\right) = -2\beta \frac{IV}{I_p} t \quad (9.3.18)$$

which rearranges to give

$$\frac{\mathcal{W}}{\mathcal{W} + \frac{IV}{I_p}} = \frac{\mathcal{W}_0 + \frac{IV}{I_p}}{\mathcal{W}_0} e^{-2\beta \frac{IV}{I_p} t} \quad (9.3.19)$$

Finally, the evolution of  $\mathcal{W}$  is given by

$$\mathcal{W} = \frac{IV}{I_p} \frac{\left(\mathcal{W}_0 + \frac{IV}{I_p}\right) e^{-2\beta \frac{IV}{I_p} t}}{\mathcal{W}_0 - \left(\mathcal{W}_0 + \frac{IV}{I_p}\right) e^{-2\beta \frac{IV}{I_p} t}} \quad (9.3.20)$$

It would be better if we could define  $V$  in terms of initial conditions. We would then be able to plot the function with realistic parameter values. Defining the initial rotation of the protons as  $\Omega_0$  we can find  $V$  at time  $t = t_0$ . From (9.3.13) we can show that

$$V = \frac{1}{I} (I_n \Omega_n + I_p \Omega_p) = \frac{I_n}{I} \left(V + \frac{I_p}{I} \mathcal{W}_0\right) + \frac{I_p}{I} \Omega_0 \quad (9.3.21)$$

This rearranges to give

$$V = \frac{I_n}{I} \mathcal{W}_0 + \Omega_0 \quad (9.3.22)$$

We can substitute this back in to the evolution equation for  $\mathcal{W}$  (9.3.20) to give

$$\mathcal{W} = \left(\frac{I_n}{I_p} \mathcal{W}_0 + \frac{I}{I_p} \Omega_0\right) \frac{\left(\frac{I}{I_p} \mathcal{W}_0 + \frac{I}{I_p} \Omega_0\right) e^{-2\beta \left(\frac{I_n}{I_p} \mathcal{W}_0 + \frac{I}{I_p} \Omega_0\right) t}}{\mathcal{W}_0 - \left(\frac{I}{I_p} \mathcal{W}_0 + \frac{I}{I_p} \Omega_0\right) e^{-2\beta \left(\frac{I_n}{I_p} \mathcal{W}_0 + \frac{I}{I_p} \Omega_0\right) t}} \quad (9.3.23)$$

or

$$\mathcal{W} = \left(\frac{I_n}{I_p} \mathcal{W}_0 + \frac{I}{I_p} \Omega_0\right) \left[ \frac{I (\mathcal{W}_0 + \Omega_0)}{I_p \mathcal{W}_0} e^{2\beta \left(\frac{I_n}{I_p} \mathcal{W}_0 + \frac{I}{I_p} \Omega_0\right) t} - 1 \right]^{-1} \quad (9.3.24)$$

This gives us that the relaxation timescale  $\tau_g$  is

$$\tau_g = \frac{1}{2\beta} \left(\frac{I_n}{I_p} \mathcal{W}_0 + \frac{I}{I_p} \Omega_0\right)^{-1} \quad (9.3.25)$$

For a neutron star we expect  $\mathcal{W}_0 \ll \Omega_0$  and so the quantity  $\mathcal{W}_0$  can be neglected in this equation. Considering expected parameters,  $\beta = 0.0005$ ,  $I/I_p = 10$  and  $\Omega_0 = 40 \text{ s}^{-1}$ , we find

$$\tau_g = 2.5 \text{ s} \approx 17P \quad (9.3.26)$$

For these parameters we have found a value of  $\tau_g < 40 \text{ s}$ . This coincides with the observation that the glitch jump is shorter than the time resolution of about 40 seconds [1].



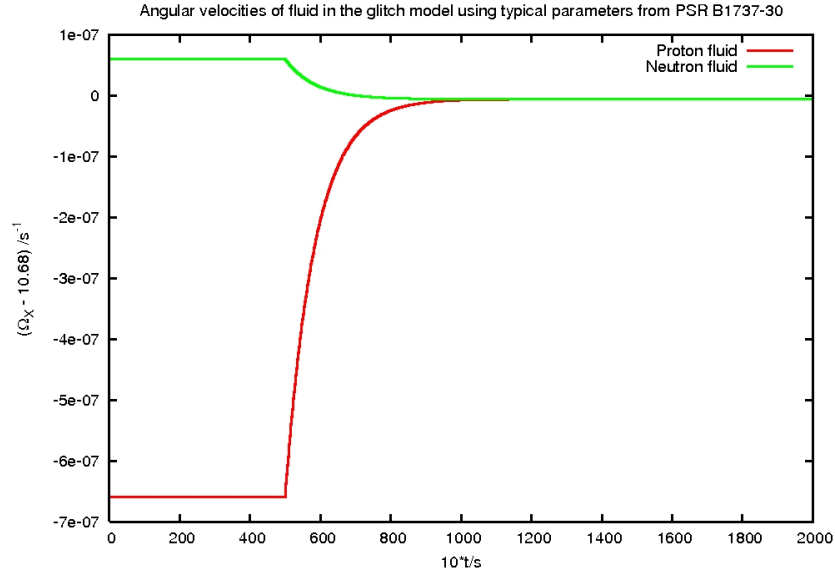


Figure 9.2: Simulated results for the pre-glitch and glitch regions using initial fluid rotations suggested by data from PSR B1737-30. The angular velocities of the two constituents in the first 50 seconds are not parallel but the effect of the magnetic spindown torque is smaller than the resolution of the graph.

To bring the results of the last two sections together, figure 9.2 shows the output of a simple script that models these two regions. We have taken  $\varepsilon = 0.01$ ,  $\beta = 0.0005$  and  $I_p/I_n = 0.1$ . Over this region the spin down torque has been assumed approximately constant and  $\mathcal{A} \approx 10^{-16}$ . The script evolves the initial rotations of the two constituents according to the pre-glitch model, with no mutual friction and a spin down torque. Once the lag reaches a critical point the model follows the evolution equation that includes mutual friction. The rest of the parameters have been chosen so that they fit with the observations of the pulsar PSR B1737-30.

### 9.3.3 Relaxation

To model the relaxation we need to include both the effect of mutual friction and the magnetic torque. We must also model the repinning of the vortex lines to the crust. If we don't then the model cannot explain multiple glitch events. We noted that the difference between the pinned and unpinned models was the

mutual friction. To simulate repinning we shall introduce a continuous function that ‘switches off’ the mutual friction. The quantity  $\beta$  will be replaced by  $\beta(t)$  where at time  $t = 0$  we set  $\beta(0) = \beta$ .  $\beta$  must decrease with time, simulating vortices repinning to the crust. Physically we would not expect this function to depend explicitly on time, but on quantities like the lag. The size of the lag sets the magnitude of the Magnus force on the vortex lines which must be overcome for the vortices to repin. In reality we have not modelled in detail the repinning mechanism and so we cannot be that accurate. Representing the ‘switching off’ function as a function of time allows us to see if repinning can recreate observed features of the relaxation. We will choose an exponential function so that

$$\beta(t) = \beta e^{-t/\tau_r} \quad (9.3.27)$$

where  $\tau_r$  is the characteristic timescale for repinning. We need to solve the change in angular momentum equations again. Including the repinning mutual friction and the magnetic torque we find

$$I_n \dot{\Omega}_n = 2\beta(t)\Omega_n (\Omega_p - \Omega_n) I_n \quad (9.3.28)$$

$$I_p \dot{\Omega}_p = 2\beta(t)\Omega_n (\Omega_n - \Omega_p) I_n - \mathcal{A}I_p\Omega^3 \quad (9.3.29)$$

This is not a simple system to solve analytically and so we solve it numerically..

In private communications with observers at Jodrell Bank Observatory we have been told that the glitch data shows an interesting feature in the frequency derivative of the pulses. The curve relating to the relaxation of a glitch seems to be split into two elements. There is some background spin down which is linear in the frequency derivative. We would assume that this is the effect of the magnetic torque. Closer to the glitch the frequency derivative has a smaller magnitude than the linear part. We might suggest that this is the effect of the torque acting on both fluid constituents, through the unpinned vortices. As the same force is effectively acting on a larger mass then the torque will not have as great an effect on the angular velocity as when the neutrons are decoupled from the proton fluid. By using some exaggerated numbers in our relaxation model and using MAPLE to solve the system numerically we can show this type of feature. Typical results are

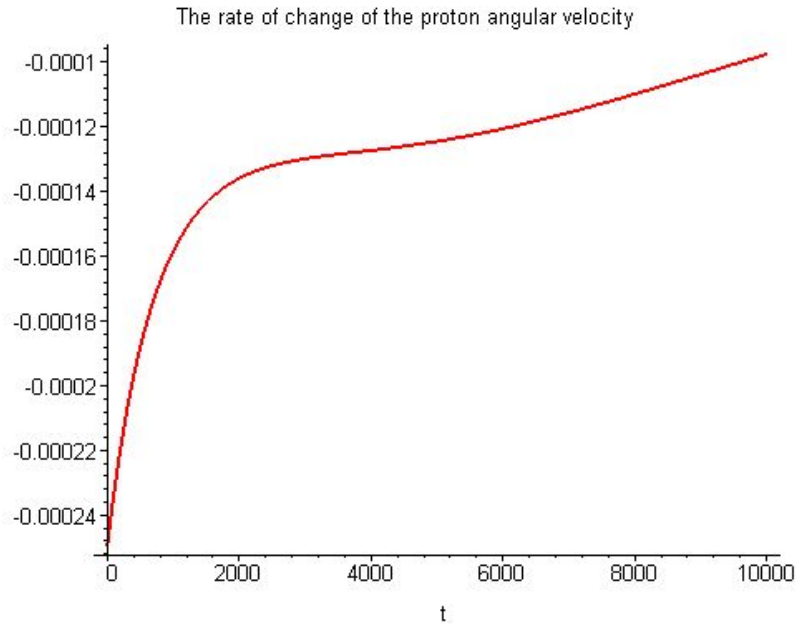


Figure 9.3: The rate of change in angular velocity ( $d\Omega_p/dt$ ) is plotted with respect to time. Note that parameters that were used to plot this graph were not realistic, but chosen to emphasise the overall features.

shown in figure 9.3. The main problem in using realistic parameters is that we found that the coefficient  $\beta$  needed to be of similar order to  $\mathcal{A}$  in order to avoid numerical difficulties. In nature we do not expect this as we have already shown that if  $\mathcal{A} \approx 10^{-15}$  then the timescales for the lag to reach an expected critical point is of the right order for glitching pulsars. We also need a large enough value of  $\beta$  so that the glitch jump occurs within  $\approx 40$  s. This just means that we have not guessed the correct form of  $\beta(t)$ , but we expected this. The important point is that a repinning model has the potential to deal with features associated with glitch relaxation.

## 9.4 Matching Data

Now that we have a simple model of the glitch phenomenon, we can start to consider what information the observations can give us. We shall again consider the three regions. In the pre-glitch region the data gives us the spin down rate of

the crust. Our model suggests that this in fact gives us the spin down of the proton fluid and hence the magnitude of  $\dot{J}_{em}$ . The glitch jump shows two things. Firstly the magnitude of the jump will be related to the largest supported lag and the ratio of fluid inertia. Equation (9.3.24) shows that at late times we expect the lag to go to zero. This will be modified if we include the pinning function, but should be approximately true for these timescales. From the definition of  $V$  (9.3.15) we are given that  $V$  is constant throughout the glitch. We have

$$V = \Omega_0 + \frac{I_n}{I_n + I_p} \mathcal{W}_0 = \Omega_1 \quad (9.4.1)$$

where  $\Omega_0$  and  $\Omega_1$  are the proton angular velocities before and after the glitch respectively.  $\mathcal{W}_0$  is the initial velocity difference between the two fluid constituents. From this we find the size of the glitch is given by

$$\Omega_1 - \Omega_0 = \Delta\Omega = \frac{I_n}{I_n + I_p} \mathcal{W}_0 \quad (9.4.2)$$

We have mentioned previously that observations limit the characteristic timescale of the glitch rise to  $< 40$  s. Equation (9.3.25) shows us that this timescale  $\tau_g$  is inversely proportional to  $\beta$ . This would give us a lower limit on the ‘average’ value of  $\beta$  over star. We should note that this quantity has a dependency on the neutron density, and hence varies with position. This timescale still gives us a handle on this quantity. The relaxation region will give us information on the form of the repinning function. Further study should give us a better idea of the form of this function. We can certainly match the timescales of the function  $\beta(t)$  and the region that we have associated with repinning in frequency derivative data. Finally we should note that we can match these parameters when including entrainment into the problem. To constrain entrainment we would need more information about the glitch. The entrainment modifies the constituent momenta and so even if we ‘turned off’ the mutual friction after the initial jump our model shows a different frequency derivative before and after the glitch. In the pre-glitch region there is a lag between the constituents and so the entrainment modifies the constituent momenta. The magnetic torque will be acting on a modified angular momentum. After the glitch there is no lag and so the proton fluid momentum is not modified by entrainment and hence the rate of spin down will change. We have even noted

that in the pre-glitch region the increase in lag can be faster than we expect from the crust rotation rate. For the range of  $\varepsilon$  given in (9.3.3) the neutron fluid spins up, hence increasing the lag. Extracting these effects from the data would be very difficult and may require a more sophisticated data analysis. The effect of entrainment will be hidden with a lot of other unknown physics. However as more of the processes are understood it is possible that glitches will help us to constrain the entrainment parameter.

## 9.5 Summary

We have constructed a simple model for the neutron star glitch phenomenon using the two fluid model and the mutual friction due to superfluid vortices. For typical values of the parameters our model has a glitch rise time shorter than the upper bound set by observation. We also have a way of getting a long relaxation time by using a ‘switching off’ function to simulate repinning. More work needs to be done on investigating the likely form of this function and whether repinning can fully explain the observations. It may be necessary to use numerical methods to carry this idea forwards if further complications are needed to properly simulate a glitch. This will certainly be the case if we try to make the repinning dependent upon quantities like the constituent velocity difference, which will be position dependent.

We also need to consider the role of superfluid turbulence in glitches. We have already stated in chapter 6 that there are cases in which the neutrons may be turbulent and other studies show it may be relevant in glitches [56]. We expect the force due to turbulence to be position dependent and so it is not clear that a ‘body averaged’ model, like the one we have discussed, will work.

# Chapter 10

## Summary

In this thesis we have investigated the role of superfluids in a multi-constituent model of neutron star cores. In particular we have considered the effect of entrainment and the mutual friction force. We have used different model scenarios to illustrate the complex dynamics associated with superfluid turbulence, wave propagation, pulsar glitches and viscous boundary layers. This study lays the foundation for future work in this area, and provides key insights into the modelling of realistic neutron stars.

In chapter 5 we set up the equations of motion for a two-constituent fluid with an array of vortices. This allowed us to investigate the consequences of the mutual friction that acts between the two constituents.

Chapter 6 provided the derivation of the forces on the fluid constituents when the neutron superfluid is turbulent. It was argued that we should consider the possibility of turbulence in neutron stars seriously. We extended the isotropic turbulence model to one in which the turbulence is polarised. We derived this force phenomenologically using results from experiments with superfluid Helium [75]. This force can now be applied to model neutron star phenomena, e.g. glitches and free precession. In the future it may be necessary to use numerical methods to simulate these phenomena. The fact that turbulence may be localised makes analytical work on global models very tough and so a numerical approach will be

---

more appropriate. Such work would extend existing studies of isotropic turbulence [60].

In chapter 7 we investigated the nature of the waves that are present in a two-constituent fluid with a mutual friction due to vortices. The role of various fluid properties was discussed, in particular the mutual friction force. We established that the presence of vortices, and hence mutual friction, can make the waves unstable. This instability is a mechanism that can create turbulence in the fluid. A further step in this work would be to find the relevance of the mutual friction coefficient  $\beta'$ . For a strong coupling between the proton fluid and the vortices this coefficient can no longer be neglected. Strong coupling may be important for a number of neutron star phenomena [32].

In chapter 8 we carried out an initial investigation into the significance of including a boundary when considering superfluid oscillation problems. This is important when considering global oscillations of a neutron star (see [31] for discussion and references ). We set up a two constituent model with a boundary and calculated how the mutual friction affects the energy that is dissipated from the system by the boundary. We showed that there are situations in which the mutual friction has a significant effect on the solution. This is particularly important when considering the damping of global modes. Future work should relax the  $\beta' = 0$  assumption so that the strong coupling case of the vortex lines to the proton fluid can be investigated. This may be particularly important in models of free precession [32].

In chapter 9 we constructed a simple model for the neutron star glitch phenomenon using the two fluid model and the mutual friction due to superfluid vortices. For typical values of the parameters our model has a glitch rise time shorter than the upper bound set by observation. We also have a way of getting a long relaxation time by using a ‘switching off’ function to simulate repinning. More work needs to be done on investigating the likely form of this function and whether repinning can fully explain the observations. Again, it may be necessary to use numerical methods to carry this idea forwards if further complications are needed to properly simulate a glitch. This will certainly be the case if we try to make the repinning

---

dependent upon quantities like the constituent velocity difference, which will be position dependent. We also ought to consider the role of superfluid turbulence in glitches. We have already stated in chapter 6 that there are cases in which the neutrons may be turbulent and other studies show it may be relevant in glitches [56]. However, we expect the force due to turbulence to be position dependent and so it is not clear that a ‘body averaged’ model, like the one we have discussed, will work.



# Bibliography

- [1] Abney, M., Epstein, R.I., Olinto, A.V., ApJ. **466** L91 (1996)
- [2] Alpar, A., Baykal, A., Mon.Not.Roy.Astron.Soc. **269** 849 (1994)
- [3] Alpar, M.A., Langer, S.A., Sauls, J.A., **282** 533 (1984)
- [4] Alpar, M.A., Sauls, J.A., ApJ. **327** 723 (1988)
- [5] Annett, J.F., *Superconductivity, Superfluids and Condensates* Oxford Univ. Press. (2004)
- [6] Anderson, P.W., Itoh, N., Nature **256** 25 (1975)
- [7] Andersson, N., Comer, G.L., Class. Quantum Grav. **23** 5505 (2006)
- [8] Andersson, N., Comer, G.L., Grosart, K., Mon.Not.Roy.Astron.Soc. **355** 918A (2004)
- [9] Andersson, N., Comer, G.L., Prix, R., Mon.Not.Roy.Astron.Soc. **354** 101 (2004)
- [10] Andersson, N., Sidery, T., Comer, G.L., Mon.Not.Roy.Astron.Soc. **368** 162 (2006)
- [11] Andersson, N., Sidery, T., Comer, G.L., Mon.Not.Roy.Astron.Soc. **381** 747 (2007)
- [12] Andreev, A.F., Bashkin, E.P., Sov.Phys.JETP **42** 1 164 (1975)
- [13] Arfken, G., *Mathematical Methods for Physicists* Academic Press, 2nd ed.(1970)

- [14] Arms, R.J., Hama, F.R., Phys. Fluids **8** 553 (1965)
- [15] Baym, G., Pines, D., Annals of Phys. vol.**66** issue.2 816 (1971)
- [16] Bekarevich, I.L., Khalatnikov, I.M., Sov.Phys.JETP, **13** 3 (1961)
- [17] Burrows, A., Lattimer, J.M., Ap.J. **307** 178 (1986)
- [18] Carter, B., Chamel, N., Int.J.Mod.Phys.D **13**(2) 291 (2004)
- [19] Chamel, N., Nucl.Phys.A **773** iss 3-4, 263 (2006)
- [20] Donnelly, R.J., *Quantised Vortices in HeII* Cambridge Univ. Press. (1991)
- [21] Feibelman, P.J., Phy.Rev.D **4** 1589 (1971)
- [22] Feynman, R.P., Prog. Low Temp. Phys., ed C.J. Gorter(North-Holland, Amsterdam), p. 17 (1955)
- [23] Finne, A.P., Araki, T., Blaauwgeers, R., Eltsov, V.B., Kopnin, N.B., Krusius, M., Skrbek, L., Tsubota, M., Volovik, G.E., Nature, **424** 1022 (2003)
- [24] Geurst, J.A., Physica B **153** 166 (1988)
- [25] Geurst, J.A., Physica B **154** 327 (1989)
- [26] Geurst, J.A., Physica A **183** 279 (1992)
- [27] Geurst, J.A., van Beelen, H., Physica A **206** 58 (1994)
- [28] Geurst, J.A., van Beelen, H., Physica B **205** 209 (1995)
- [29] Geurst, J.A., van Beelen, H., 1996, Phys. Rev. B **54** 6519 (1996)
- [30] Glaberson, W.I., Johnson, W.W., Ostermeier, R.M., Phys.Rev.Lett. **33** 1197 (1974)
- [31] Glampedakis, K., Andersson, N., Mon.Not.Roy.Astron.Soc **371** 1311 (2006)
- [32] Glampedakis, K., Andersson, N., Jones, D.I., arXiv0708.2693 (2007)
- [33] Glendenning, N.K., *Compact Stars* Springer (1996)

- [34] Goodstein, D.L., *States of Matter* Prentice-Hall Inc., New Jersey (1975)
- [35] Gorter, C.J., Mellink, J.H., *Physica* **15** 285 (1949)
- [36] Greenspan, H.P., *The Theory of Rotating Fluids* Breukelen Press, Brookline (1990)
- [37] Hall, H.E., *Proc.Roy.Soc., ser. A* **245** 546 (1958)
- [38] Hall, H.E., *Adv. in Phys.* **9** 89 (1960)
- [39] Hall, H.E., Vinen, W.F., *Proc.Roy.Soc.London A* **238** 215 (1956)
- [40] Haensel, P., Potekhin, A.Y., Yakovlev, D.G., *Neutron Stars 1* Springer (2007)
- [41] Henderson, K.L., Barengi, C.F., *Europhys.Lett.*, **67** pp. 56-62 (2004)
- [42] Ivanova, N., Taam, R.E., *Ap.J.* **601** 1058 (2004)
- [43] Jones, D.I., Andersson, N., *Mon.Not.Roy.Astron.Soc.* **324** 811 (2001)
- [44] Jou, D., Mongiovi, M.S., *Phys.Rev.B* **69** 094513 (2004)
- [45] Jou, D., Mongiovi, M.S., *Phys.Rev.B* **72** 144517 (2005)
- [46] Khalatnikov, I.M., *An Introduction to the Theory of Superfluidity* W. A. Benjamin, Inc., New York (1961)
- [47] Kim, E., Chan, M.H.W., *Nature* **427** 225 (2004)
- [48] Kopnin, N.B., *Phys.Rev.Lett* **92** 135301 (2004)
- [49] Krawczyk, A., Lyne, A.G., Gil, J.A., Joshi, B.C., *Mon.Not.Roy.Astron.Soc.* **340** 1087 (2003)
- [50] Landau, L.D., Lifshitz, E.M, *Mechanics* (1976)
- [51] Landau, L.D., Lifshitz, E.M, *The Classical Theory of Fields* Butterworth-Heinemann, 4th ed.(1983)
- [52] Landau, L.D., Lifshitz, E.M, *Fluid Mechanics* Pergamon Press, London, 2nd ed. (1982)

- [53] Link, B., Epstein, R.I., Lattimer, J.M., *Stellar Astrophysics proceedings* p117 (2000)
- [54] Lyne, A.G., Graham-Smith, F., *Pulsar Astronomy* Cambridge Univ. Press., 2nd ed. (1998)
- [55] Lyne, A.G., Shemar, S.L., Graham Smith, F., *Mon.Mot.Roy.Astron.Soc* **315** 534 (2000)
- [56] Melatos, A., Peralta, C., *ApJ.* **662** L99 (2007)
- [57] Mendell, G., *Ap.J.* **380** 530, (1991)
- [58] Mongiovi, M.S., Jou, D., *J.Phys: Condens.Matter* **17** 4423 (2005)
- [59] Onsager, L., *Nuovo Cimento Suppl.* **6** 249 (1949)
- [60] Peralta, C., Melatos, A., Giacobello, M., Ooi, A., *Ap.J.* **635** 1224 (2005)
- [61] Peralta, C., Melatos, A., Giacobello, M., Ooi, A., *Ap.J.* **651** 1079 (2006)
- [62] Prix, R., *Phys.Rev.D*, **69** 043001 (2004)
- [63] Prix, R., *Phys.Rev.D*, **71** 083006 (2005)
- [64] Prix, R., Comer, G.L., Andersson, N., *A&A* **381** 178 (2002)
- [65] Sauls, J.A., Stein, D.L., Serene, J.W., *Phys.Rev.D* **24** 4 (1982)
- [66] Schwarz, K.W., *Phys.Rev.Lett.* **49** 283 (1982)
- [67] Schwarz, K.W., *Phys.Rev.B* **38** 2398 (1988)
- [68] Sedrakian, A., *Phys.Rev.D* **71** 083003 (2005)
- [69] Sedrakian, A., Cordes, J.M., *Ap.J* **502** 378 (1998)
- [70] Sedrakian, A.D., Sedrakian, D.M., *Ap.J.* **442** 305s (1995)
- [71] Shabanova, T.V., *Mon.NotRoy.Astron.Soc* **356** 1435 (2005)
- [72] Shabanova, T.V., *Ap&SS* **308** 591 (2007)

- [73] Shapiro, S.L., Teukolsky, S.A., *Black Holes, White Dwarves, and Neutron Stars* Wiley Interscience (1983)
- [74] Sidery, T., Andersson, N., Comer, G.L., arXiv0706.0672 (2007)
- [75] Swanson, C.E., Barenghi, C.F., Donnelly, R.J., Phys.Rev.Lett. **50** 190 (1983)
- [76] Tsubota, M., Araki, T., Barenghi, C.F., Phys.Rev.Lett. **90** 205301 (2003)
- [77] Tsubota, M., Barenghi, C.F., Araki, T., Mitani, A., Phys.Rev.B **69** 134515 (2004)
- [78] Vinen, W.F., Proc. Roy. Soc. London A **240** 493 (1957)
- [79] Walmsley, P.M., Golov, A.I., Hall, H.E., Levchenko, A.A., Vinen, W.F., arXiv0710.1033 (2007)